Supplementary Material

Quantitative reversible one pot interconversion of three crystalline polymorphs by ball mill grinding

Ana M. Belenguer [1], Giulio I. Lampronti, *[1,2] Adam A. L. Michalchuk [3], Franziska Emmerling [3] and Jeremy K. M. Sanders*[1]

[1] Department of Chemistry, University of Cambridge, Lensfield Road, Cambridge CB2 1EW, UK

[2] Department of Earth Sciences, University of Cambridge, Downing Street, Cambridge, CB2 3EQ, UK.

[3] BAM Federal Institute for Materials Research and Testing, Richard-Willstätter Str. 11, 12489 Berlin, Germany

Abstract:

We demonstrate here using a disulfide system the first example of reversible, selective and quantitative transformation between three crystalline polymorphs by ball mill grinding. This includes the discovery of a previously unknown polymorph. Each polymorph is reproducibly obtained under well-defined neat or liquid assisted grinding conditions, revealing subtle control over the apparent thermodynamic stability. We discovered that presence of an impurity as low as 1.5% mol mol-1 acting as a template is required to enable these three polymorph transformations. The relative stabilities of the polymorphs are determined by the sizes of the nanocrystals produced under different conditions and by surface interactions with small amounts of added solvent. For the first time, we show evidence that each of the three polymorphs is obtained with a unique and reproducible crystalline size. This mechanochemical approach gives access to bulk quantities of metastable polymorphs that are inaccessible through recrystallisation.

Contents

Nomenclature and abbreviations used

DCC	Dynamic covalent chemistry (see section 2.1)
Solid state DCC	Solid state dynamic covalent chemistry (see section 2.2)
DCL	dynamic combinatorial library: library resulting from DCC
LAG	Refers to ball mill liquid assisted grinding. The term “LAG” is equivalent and assumes we are discussing ball mill LAG
NG	Refers to ball mill neat grinding. The term “NG” is equivalent and assumes we are discussing ball mill neat grinding
1-1	Refers to the homodimer $(2NO_2PhS)_2$ or bis(2-nitrophenyl) disulfide
1-1 Form I	$(2NO_2PhS)_2$ Form I
1-1 Form II	$(2NO_2PhS)_2$ Form II
2-2	Refers to the homodimer $(4ClPhS)_2$ or bis(4-chlorophenyl) disulfide
1-2	Refers to heterodimer $2NO_2PhSSPh4Cl$ regardless of the polymorphic form 1-2 = Form A + Form B
Form A	Refers to the polymorph of ($2NO_2PhSSPh4Cl$) obtained typically from NG: CSD refcode FUQLIM01.
Form B	Refers to the polymorph of($2NO_2PhSSPh4Cl$) obtained typically from LAG (50μL MeCN): CSD refcode FUQLIM.
Form C	Refers to the polymorph of($2NO_2PhSSPh4Cl$) obtained typically from LAG (50μL water):
dbu	1,8-Diazabicyclo[5.4.0]undec-7-ene (base catalyst)
MeCN	Acetonitrile
MeOH	Methanol
EtOH	Ethanol
IPA	2-propyl alcohol
TFA	Trifluoroacetic acid
FA	Formic acid
HPLC	High performance liquid chromatography
PXRD	Powder X-ray diffractometry
GC	Gas Chromatography
ID	Internal diameter
Hz	Hertz (frequency used to swing the grinding jars by the ball mill grinder)
h	hours
m	minutes

1 Experimental Section: Materials and Equipment

1.1 Materials

All solvents used for ball mill grinding experiments were obtained as follows: acetonitrile (MeCN), was HPLC grade from Fisher Scientific as well as Methanol (MeOH), Ethanol (EtOH), 2-propyl alcohol (IPA).

All disulfide starting materials and reagents used in the solids state DCC experiments were purchased from commercial suppliers: 1,8-Diazabicyclo[5.4.0]undec-7-ene (dbu) [6674-22-2] (>97.5 % by GC) was obtained from Acros Organics, bis(4-chlorophenyl) disulfide [1142-19-4] (98+%) referred here as **2-2** was purchased from TCI and bis(2-nitrophenyl) disulfide [1155-00-6] (98%) referred here as **1-1** was purchased from Sigma Aldrich.

The snap-closure grinding jars were made in house from 316 stainless steel grade. The screw closure grinding jars were machined in house from 440C stainless steel grade which required hardening and tempering. This was done at Wallwork Cambridge Ltd. All the ball bearings were sourced from Dejay Distribution Ltd.

The heating mantles (Non-Adhesive Wire Wound Silicone Heater, 12V, 20W) for the grinding jars were custom-built for our grinding jars by Holroyd Components Ltd in UK. The heating mantles controller and the feedback thermocouples were manufactured by the electronic workshop at the Department of Chemistry, University of Cambridge.

1.2 Equipment

1.2.1 Ball mill grinder

Preparation of multigram batches of **Form A** and **Form B** (Section 3.4 and 3.3) as well as general exploratory work (Section 6) were performed at the University of Cambridge, Department of Chemistry using a modified Retsch MM400 with an automated press-finger as shown in Figure 1a).

The polymorph transformation turnover experiments (Section 5) were all performed at BAM in Berlin using an unaltered Retsch MM400 Shaker Mill as shown in Figure 1b.

a) b)

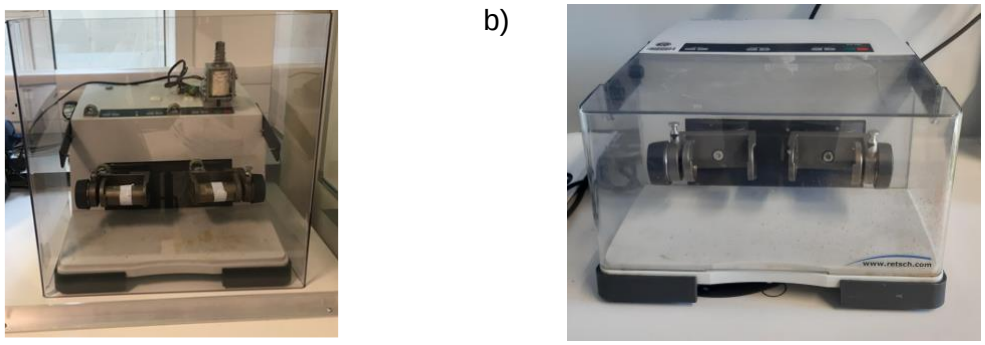

Figure S 1: a) Modified Retsch MM400 Shaker Mill (ball mill grinder) from Cambridge with protective cover removed and replace by external safety screen and with automation installed. b) Unmodified Retsch MM400 Shaker Mill from BAM in Berlin.

1.2.2 Grinding jars

1.2.2.1 14.5 mL Screw closure grinding jars with Teflon washer

The grinding jars were manufactured in-house from AISI440C stainless steel with the same internal dimensions and volume (14.5 mL internal volume: 19 mm ID x 54mm internal length) as the snap closure grinding jars prepared from 316 Stainless steel used in previous publications.[1-5] The screw closure was lined with a Teflon washer to ensure good sealing when the grinding jar is closed. 316 Stainless steel is relatively soft tested as -5 HRC (HRC stands for Rockwell Hardness measured on the C scale) and the thread is easily damaged on extensive grinding and requires continuous maintenance.[6] To avoid this damage, screw closure jars were machined in-house from AISI440C stainless steel and the clean machined jars were subjected to a hardening and tempering process to reach + 56HRC. This design should prevent the escape of the vapor phase of the solvent and also prevent powder and added solvent from being trapped in the junction of the closure while avoiding damage to the thread of the screw closure. These grinding jars were used for the solvent equilibrium experiments.[7-9]

Figure S 2 14.5mL stainless steel screw-closure grinding jars;

1.2.2.2 46 mL large scale snap closure grinding jars

Large-scale snap-closed grinding jars were manufactured in-house from 316 stainless steel with the same overall outside length as the normal grinding jars so as to fit the Retsch MM400 Shaker Mill. The internal diameter of the hemispheres was set to 38 mm ID, and the grinding jar had 54 mm internal length giving an internal volume 46 mL. These grinding jars were used to prepare multigram scale batches of **Form B** (Section 3.3) and **Form A** (Section 3.4) by dynamic covalent mechanochemistry (DCC) by grinding equimolar amounts of homodimers (**1-1** and **2-2**) in the presence of dbu.

Figure S 3 46 mL large scale stainless steel snap closure grinding jars with two ½ inch ID hardened stainless steel ball bearings (each ball 8.22g).

1.2.3 Equipment to control the heating of grinding jars while grinding

The grinding jar must be enveloped in a heating mantle (Figure S4a) and connected to the heating controller (Figure S4a). To protect the heating mantle from loss of heat to the environment, various layers of Velcron are fixed around the heating mantle.

a) b)

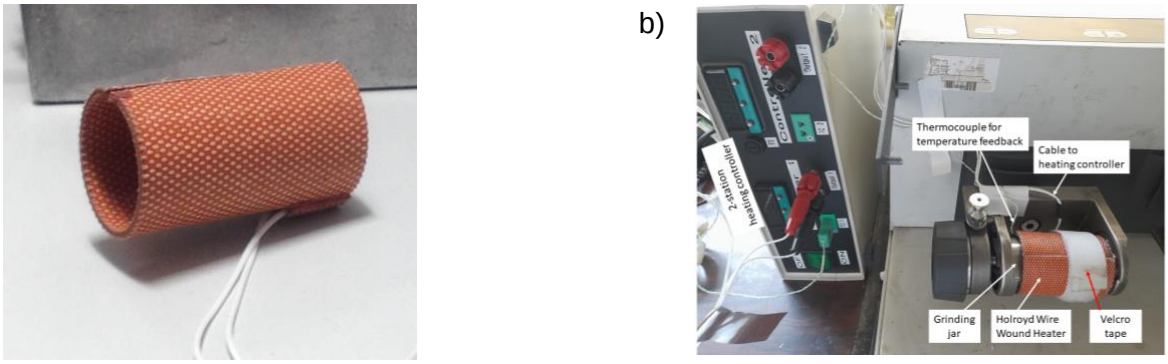

Figure S 4 a) Silicone heater mantle for grinding jar; b) Set up of the jar enveloped in the heating mantle.

1.3 HPLC equipment

HPLC analysis of the chemical composition of the powder were performed using both at Department of Cambridge, University of Cambridge and at BAM in Berlin using a very similar set up of a modular Agilent 1200 Series HPLC system composed of a HPLC high pressure binary pump, autosampler with injector programming capabilities, Peltier type column oven with 6 µL heat exchanger and a Diode Array Detector with a semi-micro flow cell (1.6µL, 6mm pathlength) to reduce peak dispersion when using short columns as in this case. The flow-path was connected using 0.12 mm ID stainless steel tubing to minimize peak dispersion.

For the analysis, an HPLC method described in Section 2.1 was used.

1.4 PXRD equipment

The PXRD scans of the samples obtained from the preparation of **Form B** and **Form A** by Dynamic Covalent Chemistry, large scale (Section 3.3 and 3.4), crystallization batches of **Form B** (Section 3.5) and the exploratory work on polymorph interconversion between **Form B**, **Form A** and **Form C** (Section 6) were run at the Department of Cambridge, University of Cambridge using the following equipment.

X-ray powder diffractograms in the 2θ range 5-45° (Cu Kα radiation, step size 0.03°, time/step 100 s, 0.04 rad soller, VxA 40x40) were collected with spinning setup.either (1) on an X-Pert PRO MPD powder X-ray diffractometer or (2) on a Panalytical X'Pert Pro diffractometer both equipped with an X'Celerator detector.

The PXRD scans of the polymorph interconversion studies between **Form B**, **Form A** and **Form C** (Section 5) were run at BAM in Berlin using the following equipment.

Powder X-ray diffractometry (PXRD) patterns were collected with Cu Kα radiation (λ = 1.50406 nm) on a D8 Advanced diffractometer (Bruker AXS, Germany) equipped with a LYNXEYE detector. Samples were measured in reflection geometry in a 2Θ range from 5° to 45° with a step size of 0.009° with spinning setup.

2 Experimental Section: Analysis of the solid-state samples

2.1 Analysis by HPLC

The chemical composition of the DCC experiments performed by grinding, were analysed by reverse phase HPLC using an Agilent 1200 Series composed of a HPLC high pressure binary pump, autosampler, column oven and a Diode Array Detector. 1.8μm Zorbax XDB C18, (4.6mm ID × 50 mm length) was used as the HPLC column. The conditions of the HPLC method are as follows:

Solvent A: Water +0.1% Formic acid;

Solvent B: Acetonitrile +0.1% Formic acid;

Gradient of 0-2 minutes 75% - 85%B with re-equilibration time of 1 minute.

Flowrate: 2 ml/min; Column temperature of 60°C;

Injection volume of 1 μL.

The signal was monitored at 259 nm (8 nm bandwidth) with reference at 550 nm (100 nm bandwidth). These wavelength parameters were selected as they gave the same peak area for **1-1** and **2-2** which are always added to the solid-state DCC preparation as equimolar, allowing to use the % peak area ratio (PAR) and refer the HPLC results for **1-1**, **2-2** and **1-2** as %mol/mol.

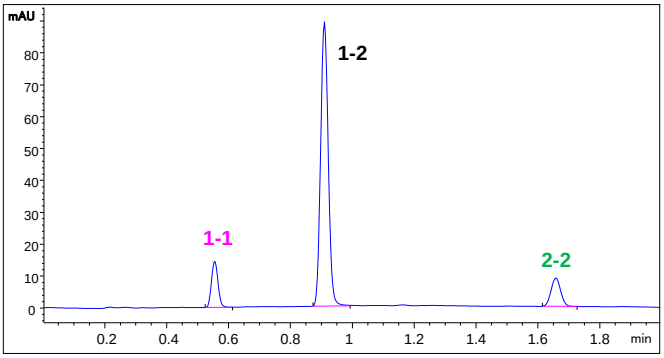

Figure S 5 Typical HPLC chromatogram of enriched heterodimer **1-2** (made up of **Form A** + **Form B** + **Form C**). HPLC run contains the two homodimers, **1-1** and **2-2**. The peak area as % peak area ration of **1-1** and **2-2** should give very similar Peak Area value when the UV signals are monitored at 259 nm (8 nm bandwidth) using a reference wavelength at 550 nm (100 nm bandwidth)

2.1.1 Preparation of HPLC samples from powder

HPLC samples were freshly prepared at a concentration of 1.0 mg/ml in acetonitrile containing 0.2%v/v of trifluoroacetic acid (TFA). The acid was added to quench dbu in the base catalysed DCC reaction. In this way, preventing the disulfide exchange reaction from taking place in solution. Otherwise, it would have resulted in the scrambling of the dynamic covalent chemistry library forming a statistical mixture of **1-1**, **2-2** and **1-2**, in a 1:1:2 proportion before the HPLC analysis.[5] The HPLC samples were then sonicated for a few minutes to bring them fully into solution before injecting them into the HPLC column.

2.2 Analysis by PXRD

2.2.1 Sample preparation for PXRD analysis

On completion of the grinding experiments for the preparation of large scale of **Form B** by **LAG** DCC (Section 3.3), and of **Form A** by **NG** DCC (Section 3.4) and the analytical samples from the exploratory work prepared as indicated in Sections 6, the grinding jar was immediately opened and the powder transferred to an agate mortar. The powder was gently ground with an agate pestle, and the powder transferred to the sample holder for Powder X-Ray diffractometry. After the collection of crystals of **Form B** (Sections 3.5), the crystals were transferred to an agate mortar. The crystals were well ground with an agate pestle, and the powder transferred to the sample holder for Powder X-Ray diffractometry.

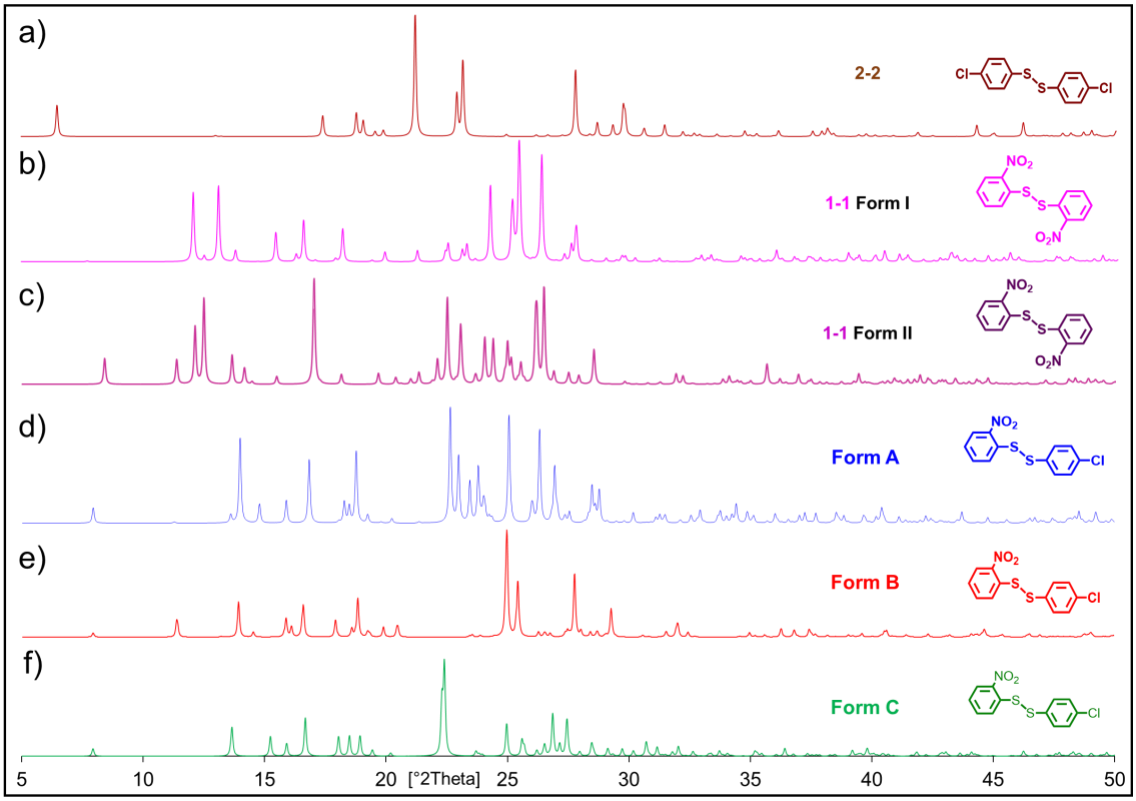

Figure S 6 Simulated PXRD scans of a) the starting materials **2-2** [CCDC code: DCPHDS02]; b) **1-1 Form I** [CCDC code: ODNPDS02] and c) **1-1 Form II** [CCDC code ODNPDS11]; and d) polymorphs **Form A** [CCDC code: FUQLIM01]**,** e) **Form B** [CCDC code: FUQLIM] and f) **Form C** [CCDC code awaiting assignment. See Section 2.2.3 for crystal structure solution] of the heterodimer **1-2**.

On completion of the final polymorph interconversion of **Form A**, **Form B** and **Form C** by ball mill grinding (Section 5), the powder was directly transferred to the sample holder for Powder X-Ray diffractometry to avoid loss of material during manual grinding with mortar and pestle.

The PXRD scans of the starting materials **1-1** (**Form I** and **Form II**) and **2-2,** and the three polymorphs of **1-2**, namely **Form A, Form B** and **Form C** are shown in Figure S6. **Form I** is the commercially available form of **1-1** while **Form II** is obtained by ball mill grinding[10] or as an impurity in the recrystallisation of **Form B**.

2.2.2 Rietveld quantitative analysis of solid state samples

The crystal structure of **Form A, Form B** and **Form C** is shown in Figure S7.

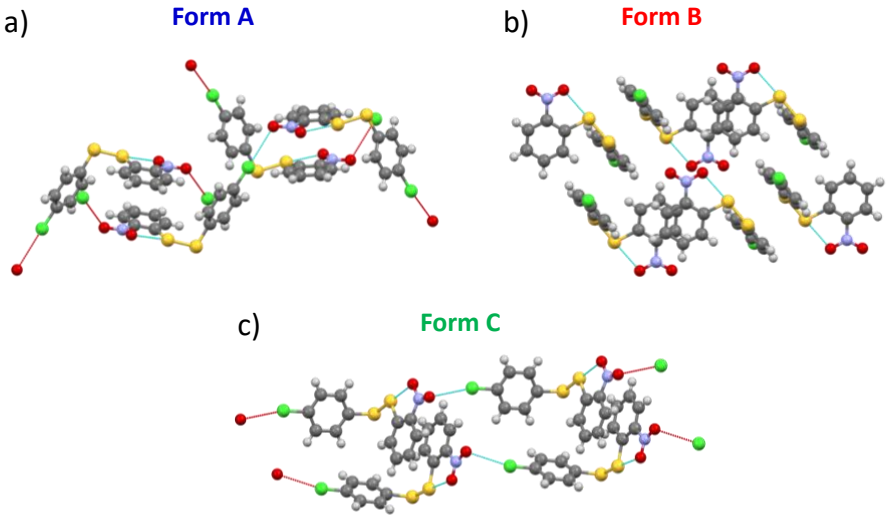

Figure S 7 Arrangement of the three polymorphs of **1-2** heterodimer molecule; **Form A**, **Form B** and **Form C** 1-D chains in (a) **Form A** [CCDC code: FUQLIM01] and (b) **Form B** [CCDC code: FUQLIM] and c) **Form C** [see Section 2.2.3 crystal structure solution] polymorphs respectively. Color codes: grey, carbon atoms; white, hydrogen atoms; yellow, sulfur atoms; red, oxygen atoms; blue, nitrogen atoms; green, chloride atoms.

2.2.3 Crystal structure solution of Form C

Powder diffraction data were analyzed with the software DASH.[11] 22 peaks were chosen in the 2θ range 5-40°, and a monoclinic cell was found with a volume of ~1268 Å^3 using the algorithm DICVOL.[12] Such volume is compatible with 4 product molecules. Space group determination with DASH resulted in space group nr. 14, $P2_1/c$, with multiplicity 4 and Z'=1. The crystal structure was solved by simulated annealing using one independent molecule with two torsion angles, and the best solution was chosen for Rietveld refinement. Rietveld refinement was performed with the software TOPAS V6.[13] A shifted Chebyshev function with 7 parameters and a Pseudo-Voigt function were used to fit background and peak shape, respectively. Spherical harmonics were used to model preferred orientation. Restraints were applied on bond distances and angles of oxamide molecule. An overall thermal parameter for each atomic species was adopted. Refinement converged with $\chi^2 = 1.294$, $R_{wp} = 6.926\%$, $R_B = 1.04$. Figure S8 shows experimental (black), calculated (red) and difference (grey) curves with peak position marks (green)

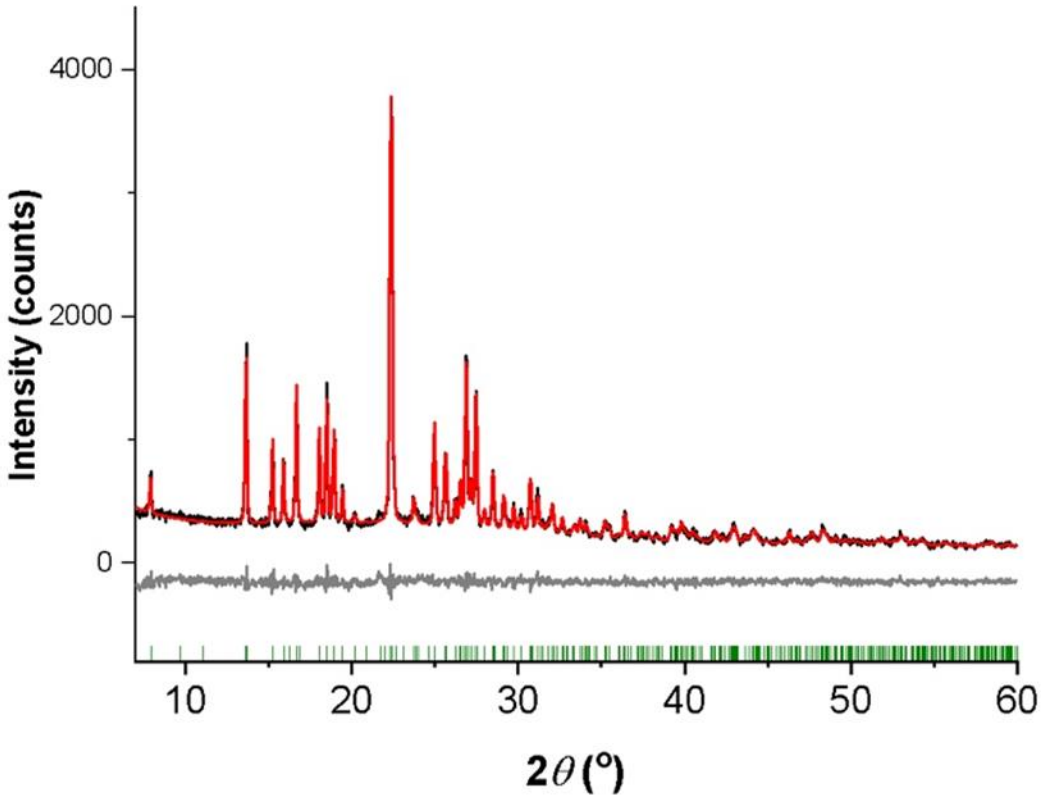

Figure S 8 Experimental (black dots), calculated (red line), and difference (grey line) patterns for the Rietveld refinement of Form C. Peak positions are indicated by green marks

2.2.4 Rietveld quantitative and crystal size analyses

Quantitative Rietveld refinements were performed with the software Topas V6.[13] 1-1 homodimer (**1-1**) was not included in the refinements as its concentration was found to be below the limit of detection by XRD. No structural parameter was refined. The March-Dollase model for preferred orientation[14] was applied on planes (0 1 0) for **Form A**, and (1 0 2) and (0 0 1) for **Form B** in the quantitative analysis. A shifted Chebyshev function with six parameters was used to fit the background. The peak shape and the parameters describing the diffractometer geometry were modeled with a fundamental parameters approach[15] using a LaB6 NIST standard.[16] The sample contribution to peak broadening was assumed to be crystal size related and isotropic (equivalent in all crystallographic directions), and was estimated by incorporating the Scherrer equation in the whole pattern refinement. A single Lorentzian Scherrer term (CS_L) for each phase was convoluted the Pseudo-Voigt function refined (see further for details). For quantification purposes, a minimum limit of 50 nm for the crystal size was defined to avoid correlations with the background. This limit was reduced to 10 nm instead for crystal size estimates. The extension of the peak overlap of **Form C** and **Form A** is such that it is hard to establish a limit of detection and quantification for **Form C** in **Form A** samples in particular. We believe the limit of detection of **Form C** in **Form A** samples could be as high as 15 wt%. We trust **Form C** is definitely present in **Form A** samples with more than 20 wt% of **Form C**. This means that in the first cycle of the clockwise turnover experiments the **Form C** to **Form A** conversion is not complete (see Table S8). It is however complete in the second cycle.

While the visual inspection of a Rietveld plot is the most reliable way to determine the quality of a fit, this is not practical for large datasets, such as those presented here. A global check of a

sequential refinement can be efficiently performed by comparing a couple of “goodness of fit” indices. One is the weighted profile R-factor (R_{wp}):

$$R_{wp}^2 = \frac{\sum_i w_i \left(y_{c,i} - y_{o,i}\right)^2}{\sum_i w_i \left(y_{o,i}\right)^2}$$

where y_c and y_o represent the calculated and observed intensity respectively for each point i. and the weight w_i is equal to $1/\sigma^2\left[y_{o,i}\right]$. The second index is “chi squared”:

$$\chi^2 = \left(\frac{R_{wp}}{R_{exp}}\right)^2$$

where (R_{exp}), the “expected R factor”, is:

$$R_{exp}^2 = \frac{\mathrm{N}}{\sum_i w_i \left(y_{o,i}\right)^2}$$

with N as the number of the data points. R_{wp} and χ^2 values ranged typically: from 10% to 12% and from 4 to 5 respectively for **Form B**; from 8% to 10% and from 3 to 4 respectively for **Form A** and **Form C**. The full list of goodness of fit indices is reported in Tables S8 and S10, together with the wt% values. Representative Rietveld plots are shown in Figure S9 to S11.

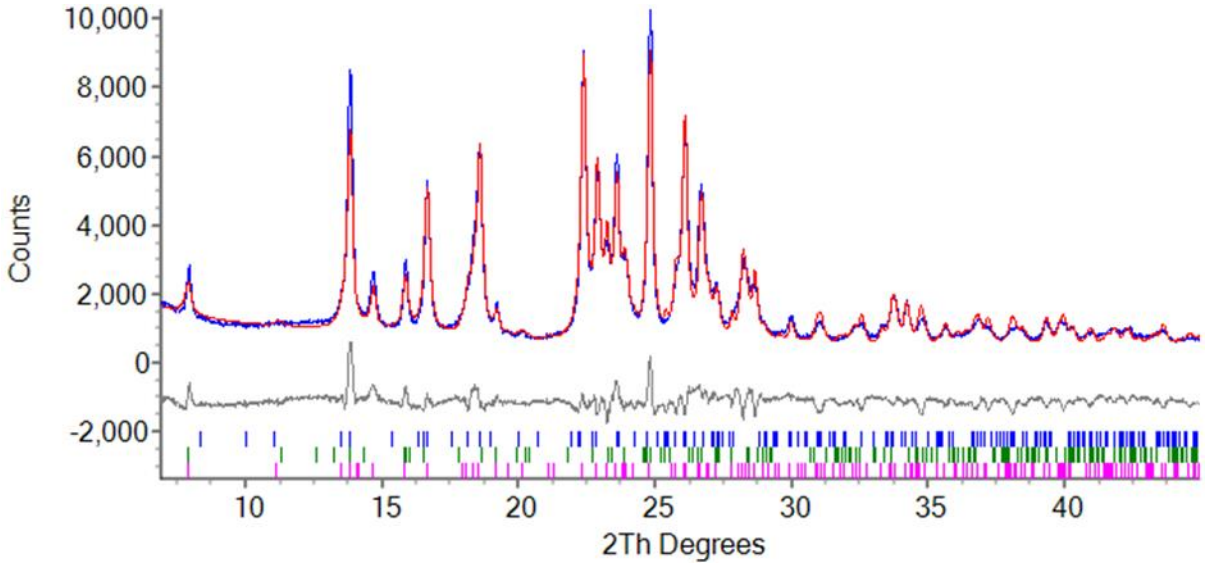

Figure S 9 Experimental (blue line), calculated (red line) and difference (grey line) patterns for a **Form A** sample. Peak positions are marked in pink, green, blue and yellow for **Form A**, **Form B**, **Form C** respectively. The χ^2 and R_{wp} are 3.56 and 9.56% respectively.

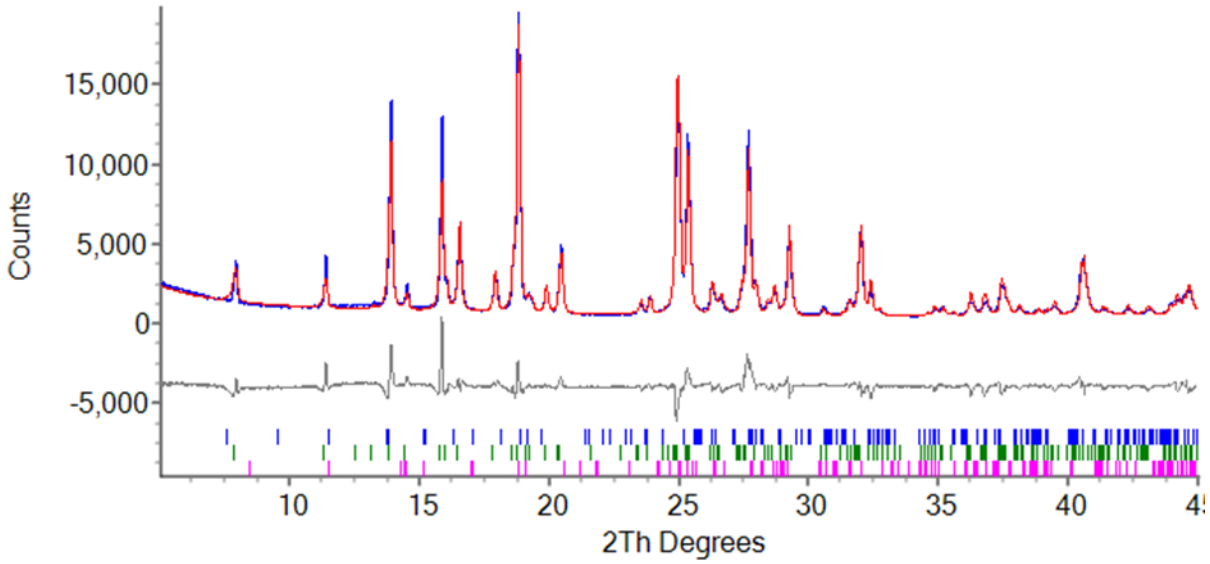

Figure S 10 Experimental (blue line), calculated (red line) and difference (grey line) patterns for a **Form B** sample. Peak positions are marked in pink, green, blue and yellow for **Form A**, **Form B**, **Form C** respectively. The χ^2 and R_{wp} are 4.80 and 12.27% respectively.

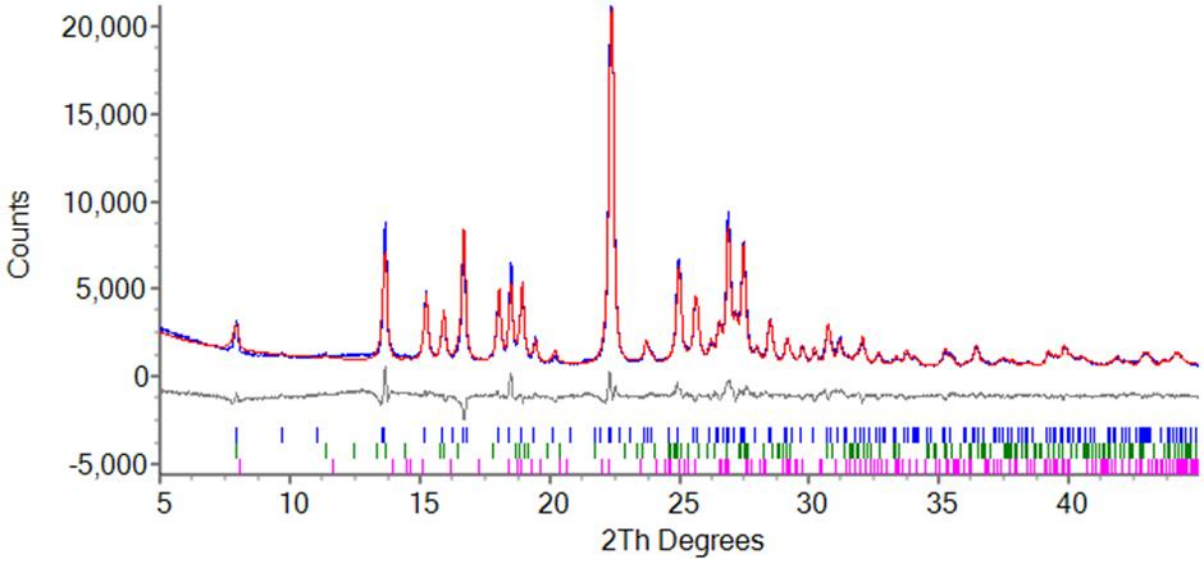

Figure S 11 Experimental (blue line), calculated (red line) and difference (grey line) patterns for a **Form C** sample. Peak positions are marked in pink, green, blue and yellow for **Form A**, **Form B**, **Form C** respectively. The χ^2 and R_{wp} are 3.60 and 8.81% respectively.

2.2.5 Crystal size determination from powder diffraction data

The crystal size was estimated including the Sherrer equation in the whole pattern Rietveld refinements. A Lorentzian function was convoluted for each phase, with a single isotropic Crystal Size (CS) parameter related to the Lorentzian full width half maximum (FWHM) Γ_L as in the Scherrer equation:[17]

$$L(nm) = \frac{K_s \lambda}{(cos\theta) * 10 * \tau}$$

$$\Gamma_L = \frac{57.32 * \lambda}{cos\theta * CS}$$

in which, L is the mean size of the ordered (crystalline) domains, K_s is a shape factor constant in the range (typically 0.9), λ is the X-ray wavelength, τ is the peak width in radians at FWHM. We here remind that the e.s.d. from the Rietveld calculation has no bearing on the precision or accuracy, being merely related to the mathematical fit of the model.[18] In other words, absolute numbers have a degree of uncertainty that cannot really be measured. On the other hand, so long as the same approach is used for all scans within a dataset, trends are reliable. For what concerns the accuracy of the size determination, it is known that for a typical laboratory X-ray diffraction instrument the Scherrer analysis provides sensitivity to crystallite size in the 1–100 nm range, the upper limit being set by the instrumental broadening.[19] Because of the nanocrystalline nature of the analysed powders and the absence of peaks above 45º in 2θ, the sample contribution to the peak broadening was assumed to be related to size only. In our experience related to the present case, a Scherrer crystal size of 100nm can vary by up to 30% relative of its value depending on the way the fundamental parameters are used to fit the LaB6 660b NIST standard - e.g., depending on whether the size and microstrain contribution for the NIST standard are assumed to be zero or are allowed to give a contribution to the LaB6 peak shape. However, if the crystal size is 60nm, this variation is no more than 10% relative. In other words, the smaller the crystal size, and the more reliable the number is. It is also important to point out that the peak shape tends to be dominated by the larger crystallites rather than the smaller ones, so the calculated size tends to be overestimated.[19]

2.2.6 Accurate cell determination with internal standard

At least three samples per polymorph with different content of **1-1** contaminant, were analysed with X-ray diffraction with an internal silicon standard. Data were collected in Bragg-Brentano geometry on a Bruker D8 diffractometer using MoKα radiation and a Lynxeye XE-T linear position sensitive detector, and analysed via Rietveld refinement as previously described. A gaussian peak at ~5.6 degrees was added to the background to fit a broad peak from the sample holder. In these refinements, the standard unit cell was kept fixed and used to refine the specimen displacement, in order to make the unit cell parameters as accurate and comparable as possible. Table S1 reports the so refined unit cell parameters and their relative e.s.d. There is no clear dependence of the cell volumes or any other cell parameters with the **1-1** content as determined by HPLC analyses. A representative Rietveld plot is shown in Figure S12.

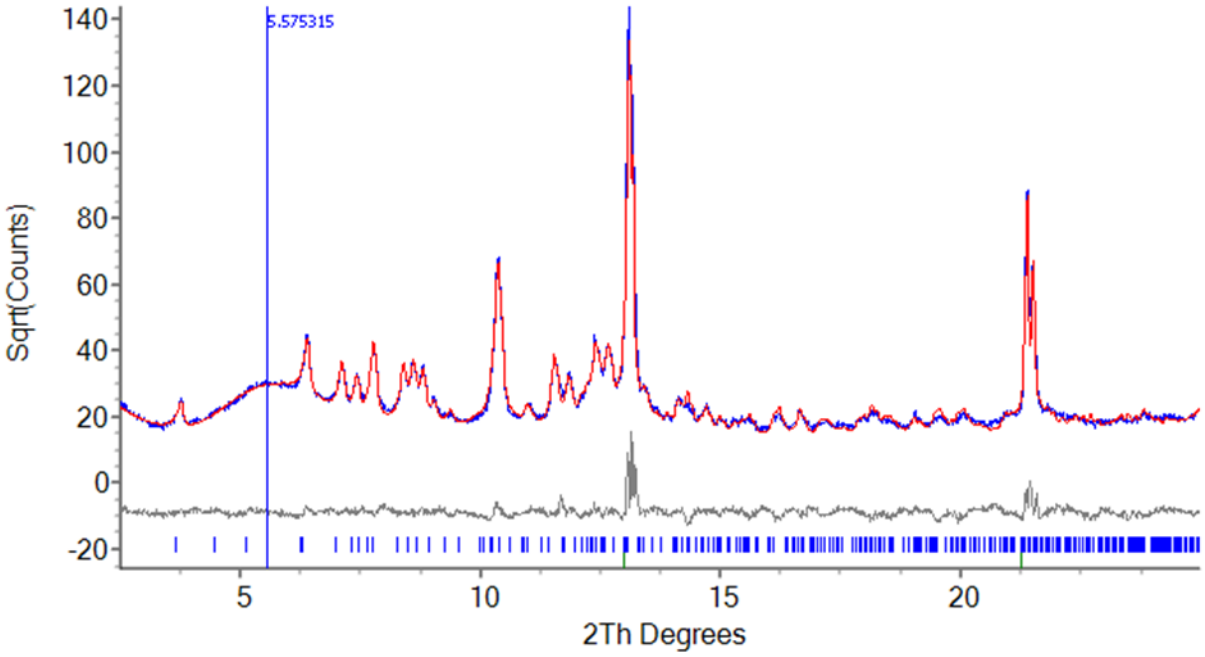

Figure S 12 Experimental (blue line), calculated (red line) and difference (grey line) patterns for a Form A sample. Peak positions are marked in blue and green for Form A and silicon respectively. The χ^2 and R_{wp} are 4.22 and 13.95% respectively.

Table S 1 a) unit cell parameters and relative e.s.d. as obtained from the Rietveld refienements with internal silicon standard; b) experiment code, polymorph transformation, R_{wp}, Goodness of Fit (GoF), unit cell volume and relative e.s.d. as obtained from the Rietveld refinements with internal silicon standard, % mol/mol of **1-1** in sample

a)

#	a A^3	**a (e.s.d.)**	**b** A^3	**b (e.s.d.)**	**c** A^3	**c (e.s.d.)**	**α**	**α (e.s.d.)**	**β**	**β (e.s.d.)**	**γ °**	**γ (e.s.d.)**
1	13.54	0.007	7.14	0.003	13.855	0.008	90	0	109.36	0.04	90	0
2	13.56	0.009	7.147	0.003	13.86	0.01	90	0	109.3	0.05	90	0
3	13.58	0.01	7.16	0.004	13.88	0.01	90	0	109.36	0.05	90	0
4	7.18	0.002	7.888	0.003	11.37	0.005	83.31452	0.034903	81.08	0.04	82.63	0.03
5	7.17	0.002	7.877	0.001	11.379	0.003	83.41907	0.025043	80.98	0.02	82.76	0.02
6	7.17	0.001	7.874	0.001	11.376	0.003	83.32158	0.025796	80.94	0.02	82.74	0.02
7	7.18	0.002	7.894	0.002	11.38	0.004	83.22831	0.024906	81	0.03	82.72	0.03
8	7.16	0.002	7.876	0.003	11.373	0.005	83.25787	0.038578	81.09	0.03	82.74	0.04
9	11.16	0.002	15.926	0.004	7.148	0.001	90	0	94.76	0.02	90	0
10	11.15	0.004	15.899	0.006	7.147	0.001	90	0	94.9	0.03	90	0
11	11.18	0.003	15.941	0.004	7.156	0.001	90	0	94.73	0.02	90	0

Continue on next page

b)

#	Experiment code + Si	Polymorph transformation	Rwp	Goodness of fit	Polymorph	Volume A^3	Volume (e.s.d.)	1-1 %mol mol^{-1}
1	AB26-012-H	**Form B** $_{crystal}$ -> **Form A**	13.95	4.22	**Form A**	1264	1	0.5
2	AB26-020-E	**Form B**-> **Form A**	10.63	3.25	**Form A**	1268	1	1.6
3	AB26-020-F	**Form B** $_{crystal}$ -> **Form A**	13.44	3.96	**Form A**	1274	2	1.7
4	AB25-179-D	**Form B** $_{crystal}$ -> **Form B** $_{powder}$	11.56	3.39	**Form B**	627.6	0.4	1.2
5	AB26-016-E	**Form C** -> **Form B**	13.11	4.26	**Form B**	626.6	0.3	2.2
6	AB26-018-C	**Form A** -> **Form B**	11.7	3.62	**Form B**	625.8	0.3	1.7
7	AB27-002-C	**Form B** $_{crystal}$ -> **Form B** $_{powder}$	14.19	4.6	**Form B**	628.5	0.3	0.5
8	AB27-002-D	**Form B** $_{crystal}$ -> **Form B** $_{powder}$	14.04	3.82	**Form B**	625.5	0.4	0.5
9	AB25-179-A	**Form B** $_{crystal}$ -> **Form C**	12.36	3.37	**Form C**	1266.4	0.5	0.2
10	AB25-179-C	**Form B** $_{crystal}$ -> **Form C**	10.26	3.06	**Form C**	1262.7	0.7	2.2
11	AB25-186-C	**Form B** $_{crystal}$ -> **Form C**	12.58	3.18	**Form C**	1270.7	0.5	2.1

3 Experimental Section

3.1 Introduction

We perform here reversible polymorph transformations between three polymorphs of **1-2**. For crystals structures see Figure S7.

- **Form A** can be typically obtained by ball mill NG from **Form B** (Section 4.2.1, 4.2.4 & 6.7.1) or from **Form C** (Section 4.1.2 & 6.5.2). It can also be prepared by another way from **Form B;**
  - by ball mill LAG with insufficient polar solvent (e.g. MeCN, Section 6.3.2) to solvate the surface of the crystals of **Form B**.[6]

  Form A is too bulk-metastable to be obtained by recrystallisation.
- **Form B** (bulk thermodynamic product). Can be obtained by recrystallisation (Section 3.5). It can also be obtained by ball mill LAG with MeCN from **Form A** (Section 4.1.3 & 6.7.2) or **Form C** (Section 4.2.3 & 6.6.2).
- **Form C** can be obtained by LAG with water from **Form B** (Section 4.1.1, 4.1.4 & 6.6.1) or **Form A** (Section 4.2.2 & 6.5.1).
  Form C is too bulk metastable to be obtained by recrsytallisation.

These polymorph transformations do not involve bond breaking and bond reforming expected from dynamic covalent mechanochemistry.

Important Note: As these transformations do not involve bond breaking and bond forming, the chemical composition of the starting polymorph is maintained throughout all subsequent transformations unless more **1-1** is added as described in the case of turnover polymorphs transformation in Section 5.

In order to investigate these polymorph transformations, we need first to obtain gram quantities of **1-2** in quantitative yield. **1-2** can only be quantitatively prepared by disulfide-exchange dynamic covalent mechanochemistry starting from equimolar amounts of the corresponding homodimers (**1-1** and **2-2**).[6] These mechanochemical reactions are base catalysed, and therefore require the use of **dbu**, acting as a nucleophile.[5] Under **LAG** (MeCN) conditions, **Form B** is obtained typically as 97% mol/mol (Table S2), while under **NG** conditions, **Form A** can be obtained as pure as 99 %mol/mol (Table S3). The remaining 1-5%mol/mol is composed of the homodimers (**1-1** and **2-2**) in equimolar ratios. We published that the commercially available **1-1** is **Form I** polymorph, which is quickly transformed to **Form II** polymorph on grinding.[4, 10]

In contrast, solution DCC in the presence of dbu will always result, given time, in at statistical mixture: 50% of **1-2** and 50% of an equimolar mixture of **1-1** and **2-2**.[5]

This project relies on having **1-2** heterodimer “free of dbu”, so as to avoid disulfide exchange through the dynamic covalent mechanochemistry (DCC) mechanism.

The best strategy to prepare quantitative **1-2** “free of dbu”, is to recrystallize **1-2** as **Form B** from the large-scale solid-state DCC batches of **1-2**.[6] Theoretically, it should make no difference if we recrystallize **1-2** from batches of **Form A** or **Form B** obtained by solid state DCC**,** as once in solution, the polymorphic information of **1-2** is lost. Only crystals of **Form B**, the bulk thermodynamic polymorph of **1-2**, has been obtained to date from recrystallisation experiments from various solvents such as MeCN, MeOH, EtOH and IPA. **Form A** and **Form C** are much too bulk metastable to recrystallize from solution.

We always found that **Form B** crystallises with some residual amount of **1-1**. This implies that **1-1** in the mother liquor recrystallises during the recrystallisation of **Form B**. Due to the high solubility of **2-2** in all solvents used for the recrystallisation of **1-2**, **2-2** is always absent in all crystal samples of **Form B** (See Table S4, S5 and S6).

Strategies to obtain high purity crystals of **Form B**

Initially we prepared all the "free of dbu" batches of **Form B** crystals, by recrystallizing **Form B** batches obtained by **LAG** DCC (Table S6, A) to G). At equilibrium, **Form B** prepared by **LAG** DCC (Section 3.3) has typically 1.5%mol/mol of each of **1-1** and **2-2**, and **1-2** being only around 97%mol/mol (See example on Table S2). Recrystallisation from these batches of **Form B** (Section 3.5) resulted in the 1st crop of **Form B** crystals containing around 1% mol/mol of **1-1**, 2nd and 3rd crop of **Form B** crystals had a higher content of **1-1** (See example on Table S4 and a list of all **Form B** crystal batches obtained this way on Table S6, A) to G).

Later on, we found that preparative batches of **Form A** by **NG** DCC resulted in over 98.5% mol/mol of **1-2** and less than 0.7%mol/mol of both **1-1** and **2-2,** as documented in the example on Table S3. Using **Form A** DCC batches for the recrystallisation experiments, resulted in high purity crystals: the 1st batch of **Form B**, often with just ≤ 0.2%mol/mol of **1-1** (See Table S6, batches H, J, N, O and P). An example of the chemical composition of these batches of **Form B** crystals can be seen on Table S5 and a list of all **Form B** crystal batches obtained this way on Table S6, H) to Q).

3.2 Design of experiments

Initially, the greatest challenge with this project was to find a reproducible procedure to transform crystals of **Form B** to **Form A** (Section 4.2.1) and from powder of **Form B** to **Form A** (4.2.4 and 6.3). Also, from crystals of **Form B** to **Form C** (Section 4.1.1) and from powder of **Form B** to **Form C** (Section 4.1.4 and 6.4). Once these two hurdles were resolved, development of the transformation of **Form A** to **Form C** and vice versa (Section 6.5), **Form B** powder to **Form C** and vice versa (Section 6.6) and **Form B** powder to **Form A** and vice versa (Section 6.7) were easily achieved.

To demonstrate that the polymorph transformation could be done either starting from crystals of **Form B** to be transformed into **Form C**, and from here into **Form A**, and then **Form B**, we run 2 polymorph transformation cycles in what we named "clockwise direction" described in Section 5.1.

In a similar way, starting from crystals of **Form B** to be transformed into **Form A**, from here into **Form C**, and then **Form B**, we run 2 polymorph transformation cycles in what we named "anti-clockwise direction" described in Section 5.2.

3.3 Preparation of gram batches of quantitative Form B

Typically, 1.6 g scale batches of **Form B** were prepared by grinding 1.36 mmol of $(2NO_2PhS)_2$ crystals (836.66mg, **1-1**) and 1.36 mmol of $(4ClPhS)_2$ crystals (781.27mg, **2-2**) in a large-scale snap closured grinding jar (See Section 1.2.2.2). Around of 2 %mol mol^{-1} of **Form B** seeds were added to speed up the reaction.[2] Two ½ inch stainless steel ball bearings and 200 μL MeCN were added. Finally, 10μL **dbu** were dispensed on top of a ball bearings. The grinding jar was snap-closed and secured with tape, and the solid was milled in a Retsch MM400 Shaker Mill for 15 minutes at 30 Hz. A quantitative conversion of the homodimers was achieved with

over 96% mol mol^{-1} conversion to **Form B** heterodimer as per HPLC analysis. An example of the chemical composition of 4 such batches is shown on Table S2, these batches were used for the recrystallisation to **Form B**, batch E (Table S4).

Table S 2 Tabulation of the experimental details and the chemical composition of the outcome of the ball mill LAG with MeCN preparation of four, gram-scale batches of **Form B** starting from equimolar ratios of the corresponding homodimers (**1-1** and **2-2**) in the presence of the base catalyst, **dbu**. The HPLC method is also listed. The PXRD scans of these four batches are consistent with **Form B** and were used in the preparation of batch E crystals of **Form B** (see Table S4)..

Preparation of Form B at preparative scale used for Batch E recrystallisation

[1-1]+[2-2]+2%M dbu (LAG/MeCN)

	Reagents:	$(2NO_2PhS)_2$	$(4ClPhS)_2$	Form B	Solvent	dbu	Powder removed from jar
	MW:	308.33	287.23	296.97	MeCN	152.24	
	%mol/mol:	49%	49%	2%M		2%M	
	mmol:	1.36 mmol	1.36 mmol	0.067 mmol		0.28 mmol	
	mgs/μL :	838.66	781.27	20 mg		10μL	
Batch #	grinding time @ 30 Hz	$(2NO_2PhS)_2$ weighed	$(4ClPhS)_2$ weighed	Form B weighed		dbu	material recovered
	2x1/2" balls	mg	mg	mg		μL	g
Batch 1	15 min	838.66 mg	781.38 mg	19.10 mg	200μL	10μL	1.6 g
Batch 2	15 min	838.67 mg	781.41 mg	20.53 mg	200μL	10μL	1.6 g
Batch 3	15 min	838.66 mg	781.36 mg	20.63 mg	200μL	10μL	1.6 g
Batch 4	15 min	838.65 mg	781.29 mg	19.80 mg	200μL	10μL	1.6 g
				Total		**40μL**	**6.4 g**

LC conditions [λ=259(8nm) ref 550(100		
Zorbax SB C18, 1.8 μm; 4.6mm ID x50 mm		
H_2O+0.1% HCOOH; **B**: MeCN+0.1%HCO		
min 75-85%B; 2ml/min; 60°C; run time=2.0		
HPLC results		
$(2NO_2PhS)_2$ (1-1)	Product (1-2)	$(4ClPhS)_2$ (2-2)
%M	%M	%M
1.3	**97.2**	**1.5**
1.4	**97.6**	**1.1**
2.3	**96.1**	**1.6**
2.4	**96.0**	**1.6**

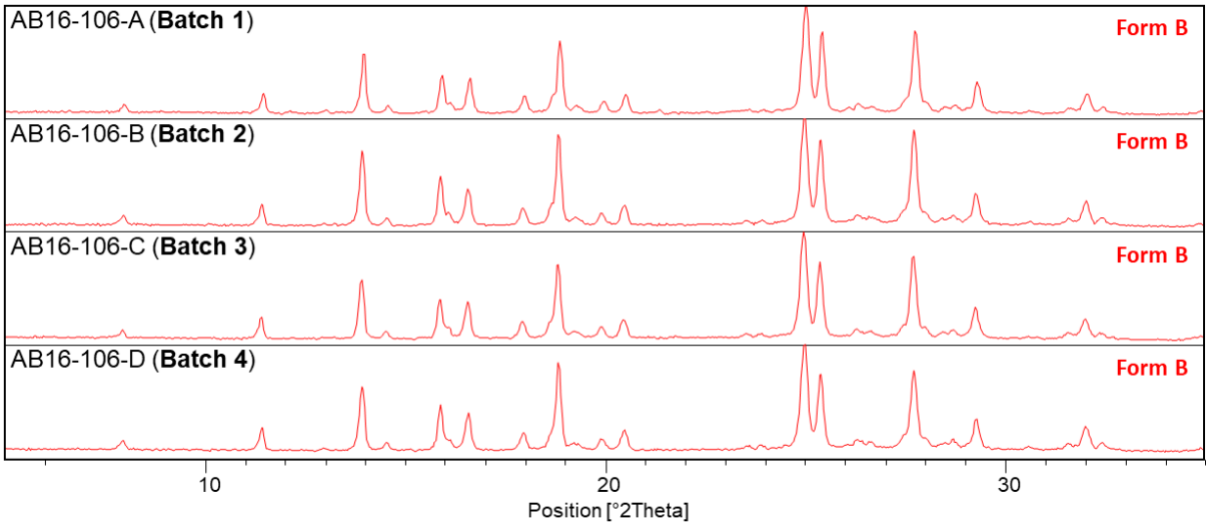

Figure S 13: PXRD of **Form B** batches (#1to #4) prepared by **LAG** DCC as listed in Table S2. Through the HPLC analysis we know that these batches contain **1-1** at 1.3-2.4% mol mol^{-1} levels (See Table S2). (See Figure S6 for comparison of simulated PXRDs).

3.4 Preparation of gram batches of quantitative Form A

Typically, 2.4 g scale batches of Form A were prepared by **NG**. 4.0 mmol of $(2NO_2PhS)_2$ crystals (1233.4 mg, **1-1**) and 4.0 mmol of $(4ClPhS)_2$ crystals (1148.9 mg, **2-2**) were added to a large-scale snap closured grinding jar as in Section 1.2.2.2. Around of 2 %mol mol^{-1} of **Form A** seeds were added to speed up the reaction.[2] Two ½ inch stainless steel ball bearings were

added and 12 μL dbu were pipetted on top of a ball bearing. The grinding jar was snap-closed and secured with tape, and the solid was milled in a Retsch MM400 Shaker Mill for 3x(16-20) minutes at 30 Hz. A conversion of the homodimers to **Form A** was achieved with over 98.5% mol mol^{-1} to the heterodimer as per HPLC analysis. An example of the chemical composition of 3 such batches is shown on Table S3, these batches were used for the recrystallisation to **Form B**, batch N (Table S5).

Table S 3 Tabulation of the experimental details and the chemical composition of the outcome of the ball mill neat grinding preparation of three, gram-scale batches of **Form A** starting from equimolar ratios of the corresponding homodimers (**1-1** and **2-2**) in the presence of the base catalyst, **dbu**. The HPLC method is also listed. The PXRD of these three batches are consistent with **Form A** and were used in the preparation of batch N crystals of **Form B** (see Table S5).

Preparation of Form A at prep. scale used for Batch N recrystallisation

[1-1]+[2-2]+2%M dbu (NG)

	Reagents:	$(2NO_2PhS)_2$	$(4ClPhS)_2$	Form A	dbu	Powder removed from jar
	MW:	308.33	287.23	296.97	152.24	
	%M:	47.96%M	47.96%M	4.08%M	2%M	
	mmol:	4 mmol	4 mmol	0.17 mmol	0.28 mmol	
	mgs/μL :	1233.4 mg	1148.9 mg	50 mg	12μL	
Batch #	grinding time @ 30 Hz	$(2NO_2PhS)_2$ weighed	$(4ClPhS)_2$ weighed	Form A weighed	dbu	material recovered
		mg	mg	mg	μL	g
Batch 1	3 x 16 min 5 min rest	1,233.5 mg	1148.4 mg	53.7 mg	12μL	2.3 g
Batch 2	3 x 20 min 5 min rest	1,233.1 mg	1148.3 mg	50.7 mg	12μL	2.5 g
Batch 3	3 x 20 min 5 min rest	1,233.0 mg	1149.3 mg	51.5 mg	12μL	2.4 g
				Total	**36μL**	**7.3 g**

HPLC conditions [λ=259(8nm) ref 550(100nm)]
Zorbax SB C18, 1.8 μm; 4.6mm ID x50 mm
A: H_2O+0.1% HCOOH; **B**: MeCN+0.1%HCOOH
0-2 min 75-85%B; 2ml/min; 60°C; run time=2.0 min

HPLC results		
$(2NO_2PhS)_2$ (1-1)	Product (1-2)	$(4ClPhS)_2$ (2-2)
%M	%M	%M
0.8	98.5	0.7
0.4	99.2	0.4
0.3	99.4	0.3

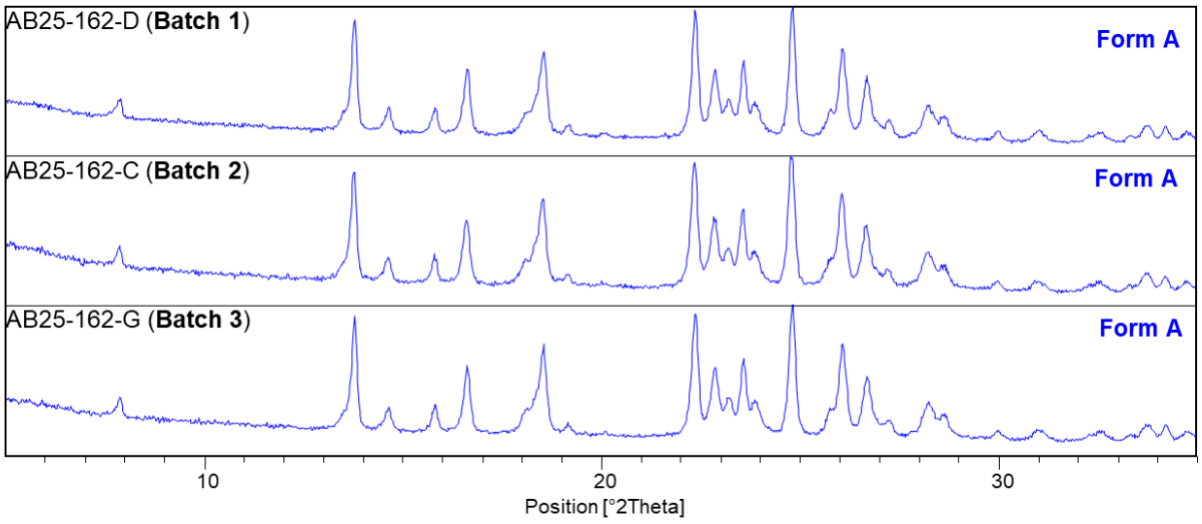

Figure S 14 PXRD of the batches (#1to #3) of **Form A** prepared by **NG** DCC as listed in Table S3. Through the HPLC analysis we know that these batches contain **1-1** at 0.3-0.8% mol mol^{-1} levels (See Table S3). (See Figure S6 for comparison of simulated PXRDs).

3.5 Preparation of Crystals of Form B

We can obtain crystals of Form B (CSD refcode FUQLIM and bulk thermodynamic product) by recrystallisation from acetonitrile, methanol, ethanol or isopropanol from either **Form B** (Section 3.3) or **Form A** (Section 3.4), these having been prepared by ball mill grinding and therefore contain **dbu**.

Warning: Both **Form A** and **Form B** of **1-2** prepared by solid state DCC contain **dbu**. It is important to account for the total concentration of **dbu** contained in the batches of **1-2** to be recrystallized. One to two equivalents of **TFA** must be added to the solvents to be used in the recrystallisation procedure in order to neutralise or even acidify the resulting solution of **1-2**. Disulfides have a reversible S-S bond which in the presence of unquenched **dbu** will undergo a disulfide exchange reaction in solution, giving place to a statistical mixture (1:1:2 of **1-1**:**2-2**:**1-2**). It is also important to monitor the mother liquors by HPLC to ensure that the recrystallisation solution has not scrambled.

Rescuing scrambled disulfide material. If by mistake, the TFA had not been added to neutralise the dbu, the mother liquor or the solid obtained will be found to contain a mixture of equimolar concentration of **1-1** and **2-2**, the rest being **1-2**. After evaporating the solvent, a known amount of dbu is added again to the scrambled mixture of disulfides. **LAG** DCC is performed if we want to obtain quantitative **Form B** (Section 3.3) or **NG** DCC is performed if we want to obtain quantitative **Form A** (Section 3.4). This reversibility is only possible because equilibrium in DCC reactions is the same regardless of the starting point as far as it contains reacted or unreacted equimolar concentration of **1-1** and **2-2,** as in this case.

Procedure

A batch of **Form B** (or **Form A**) is added to a large round-bottom flask, and the solvent (IPA, EtOH or MeOH) containing **TFA** (1-2 equivalent) to neutralise dbu is added under stirring, to form a solution of **1-2**. When using IPA, the solution was heated between 65-75 ^{o}C while when using MeOH the solution was heated around 60 ^{o}C and around 70 ^{o}C when using EtOH. This solution is filtered through a folded Whatman No 1 filter paper; the conical funnel and the receiving container had been heated with a heat gun to avoid **Form B** from precipitating in the cold glassware. This solution was left for **Form B** to crystallise overnight or even for a few days.

The 1st crop of **Form B** crystals was filtered through a Buchner sintered funnel under house vacuum. The filtrate was reserved to later obtain the 2nd crop and even the 3rd crop of **Form B** crystals. As the filtered crystals were suspected to contain **dbu** and **TFA**, they were washed with cold solvent and filtered under vacuum.

Table S 4 Crops of crystal batches of **Form B** prepared from **Form B** solid state DCC batches listed in Table S2. The amount of **1-1** impurity is relatively high as compare to crystal batches of **Form B** prepared from **Form A** solid state DCC batches as shown in Table S5.

Preparation of Crystal of Form B from DCC batches of Form B

Refluxed from MeOH at 60°C

Batch E	Reagents:	Form B	dbu	TFA	HPLC conditions [λ=259(8nm) ref 550(100nm)] Zorbax SB C18, 1.8 μm; 4.6mm ID x50 mm **A**: H_2O+0.1% HCOOH; **B**: MeCN+0.1%HCOOH 0-2 min 75-85%B; 2ml/min; 60°C; run time=2.0 min		
	MW:	296.97	152.24	114.02			
	density (g/mL)		1.018	1.49			
	mmol:	21.6 mmol	0.27 mmol	0.54 mmol			
	μL		40μL	41μL	HPLC results		
Crop #	Crop material	Form B weighed	dbu to be quenched	TFA used to quench	$(2NO_2PhS)_2$ (**1-1**)	Product (**1-2**)	$(4ClPhS)_2$ (**2-2**)
		g	μL	μL	%M	%M	%M
		6.4	40μL	41μL			
Crop 1	4.9 g				**0.9**	**99.1**	**0.0**
Crop 2	1.0 g				**1.9**	**98.1**	**0.0**

Table S 5 Crops of crystal batches of **Form B** prepared from **Form A** solid state DCC batches listed in Table S3. The amount of **1-1** impurity is relatively low as compare to crystal batches of **Form B** prepared from **Form B** solid state DCC batches as shown in Table S4.

Preparation of Crystals of Form B from Form A (DCC batches)

Refluxed from MeOH at 60°C

Batch N	Reagents:	Form A	dbu	TFA	HPLC conditions [λ=259(8nm) ref 550(100nm)] Zorbax SB C18, 1.8 μm; 4.6mm ID x50 mm **A**: H_2O+0.1% HCOOH; **B**: MeCN+0.1%HCOOH 0-2 min 75-85%B; 2ml/min; 60°C; run time=2.0 min		
	MW:	296.97	152.24	114.02			
	density (g/mL)		1.018	1.49			
	mmol:	24.6 mmol	0.24 mmol	0.24 mmol			
	μL		36μL	47μL	HPLC results		
Crop #	Crop material	Form A weighed	dbu to be quenched	TFA used to quench	$(2NO_2PhS)_2$ (**1-1**)	Product (**1-2**)	$(4ClPhS)_2$ (**2-2**)
		g	μL	μL	%M	%M	%M
		7.3	36μL	47μL			
Crop 1	4.6g				**0.2**	**99.8**	**0.0**
Crop 2	1.2 g				**0.5**	**99.5**	**0.0**
Crop 3	0.3 g				**1.4**	**98.6**	**0.0**

Table S6 give a list of the crystallization conditions used (load of **1-2**, solvent type and volume, recrystallisation temperature, polymorph used (**Form A** or **Form B** from solid state DCC), concentration of **dbu**, and concentration of **TFA** added to avoid scrambling. Table S6 list the relevant information on the preparation and analysis by HPLC of the batches of **Form B** crystals later used for the development of ball mill grinding procedures for polymorph transformation.

Table S 6 Experimentals details of recrystallised batches of **Form B** used in this project including the chemical composition of each of the crops obtained. The less pure batches A) to G) were obtained by recrystallisation using **Form B** batches obtained by prep DCC ball mill grinding. Batch E (Table S4) is an example obtained from **Form B** DCC batches (Table S2). The purer batches H) to Q) were obtained by recrystallisation using **Form A** batches obtained by prep DCC ball mill NG. Batch N (Table S5) is an example obtained from **Form A** batches (Table S3).

Batch	Solvent crystallised from	Polyrmoph used for crystallisation	Heated to °C	Load of Form A or Form B	Volume of solvent (mL)	dbu in **1-2**		**TFA**		Crop of crystals	Chemical composition HPLC % mol/mol		
						µL	mmol	µL added	mmol				
A	IPA	**Form B**	60 °C	6.4g	800 mL	32	0.21	16	0.21		**1-1**	**1-2**	**2-2**
										1st crop	1.0	99.0	0.0
										2nd crop	2.1	97.0	0.0
B	MeOH	**Form B**	64 °C	2.3g	500 mL	12	0.08	8	0.10		**1-1**	**1-2**	**2-2**
										1st crop	0.3	99.4	0.2
										2nd crop	0.9	99.1	0
C	IPA	**Form B**	60 °C	8.0g	780 mL	40	0.27	48	0.63		**1-1**	**1-2**	**2-2**
										1st crop	1.1	98.9	0
										2nd crop	2.5	97.5	0
D	IPA	**Form B**	60 °C	6.7g	800 mL	32	0.214	33	0.43		**1-1**	**1-2**	**2-2**
										1st crop	1.0	99.0	0
										2nd crop	2.1	97.9	0
E	MeOH	**Form B**	60 °C	6.4g	800 mL	40	0.27	41	0.54		**1-1**	**1-2**	**2-2**
										1st crop	0.9	99.1	0
										2nd crop	1.9	98.1	0
F	IPA	**Form B**	70 °C	7.8 g	500 mL	20	0.13	20	0.26		**1-1**	**1-2**	**2-2**
										1st crop	0.7	99.3	0
										2nd crop	1.5	98.5	0
										3rd crop	4.5	95.5	0
G	IPA	**Form B**	74 °C	13.7 g	1010 mL	50	0.33	50	0.65		**1-1**	**1-2**	**2-2**
										1st crop	1.3	98.7	0
										2nd crop	3.6	96.2	0.1
H	MeOH	**Form A**	62 °C	18.7 g	1300 mL	104	0.70	100	1.31		1-1	1-2	2-2
	Divided into 2 batches				800 mL					1st cropA	0.2	99.8	0.0
					500 mL					1st cropB	0.3	99.7	0.0
I	MeOH	**Form A**	60 °C	8.1 g	700 mL	20	0.13	20	0.26		**1-1**	**1-2**	**2-2**
										1st crop	0.3	99.7	0.0
										2nd crop	0.9	99.1	0.0
J	EtOH	**Form A**	70 °C	7.2 g	800 mL	45	0.30	55	0.72		**1-1**	**1-2**	**2-2**
										1st crop	0.2	99.8	0.0
										2nd crop	0.6	99.4	0.0
K	IPA	**Form A**	70 °C	7.3 g	800 mL	45	0.30	55	0.72		**1-1**	**1-2**	**2-2**
										1st crop	0.9	99.1	0.0
										2nd crop	2.8	97.2	0.0
L	EtOH	**Form A**	70 °C	7.2 g	800 mL	45	0.30	55	0.72		**1-1**	**1-2**	**2-2**
										1st crop	0.4	99.6	0.0
										2nd crop	1.4	98.5	0.0
M	MeOH	**Form A**	60 °C	7.1 g	700 mL	45	0.30	55	0.72		**1-1**	**1-2**	**2-2**
										1st crop	0.4	99.6	0.0
										2nd crop	1.8	98.0	0.0
N	MeOH	**Form A**	60 °C	7.1 g	800 mL	36	0.24	45	0.59		**1-1**	**1-2**	**2-2**
										1st crop	0.2	99.8	0.0
										2nd crop	0.5	99.5	0.0
										3rd crop	1.4	98.6	0.0
O	MeOH	**Form A**	60 °C	7.3 g	800 mL	36	0.24	45	0.59		**1-1**	**1-2**	**2-2**
										1st crop	0.1	99.9	0.0
										2nd crop	0.3	99.7	0.0
										3rd crop	1.1	98.9	0.0
P	MeOH	**Form A**	60 °C	7.4 g	800 mL	36	0.24	45	0.59		**1-1**	**1-2**	**2-2**
										1st crop	0.2	99.8	0.0
										2nd crop	0.4	99.6	0.0
										3rd crop	1.1	98.9	0.0
Q	MeOH	**Form A**	60 °C	7.1 g	800 mL	36	0.24	45	0.59		**1-1**	**1-2**	**2-2**
										1st crop	0.9	99.1	0.0
										2nd crop	1.7	98.3	0.0

4 Experimental procedures for the quantitative polymorph transformation between Form A, Form B and Form C

We have designed 6 procedures to transform each of the 3 polymorphs to each other and vice versa. The starting point are crystals of **Form B**.

To make sure that we had enough material to perform HPLC and PXRD analysis at each stage of the polymorph transformation, we decided to start from 300 mg of **Form B** crystals, instead of the typical loading of 200 mg. We decided to run 2 turnover cycles of the 3 polymorph transformations:

- one set in the clockwise direction (**Form B→ C→ A→ B→ C→ A→B**) described in Section 4.1,
- the other, in the anticlockwise direction (**Form B→ A→ C→ B→ A→ C→ B**) described in Section 4.2.

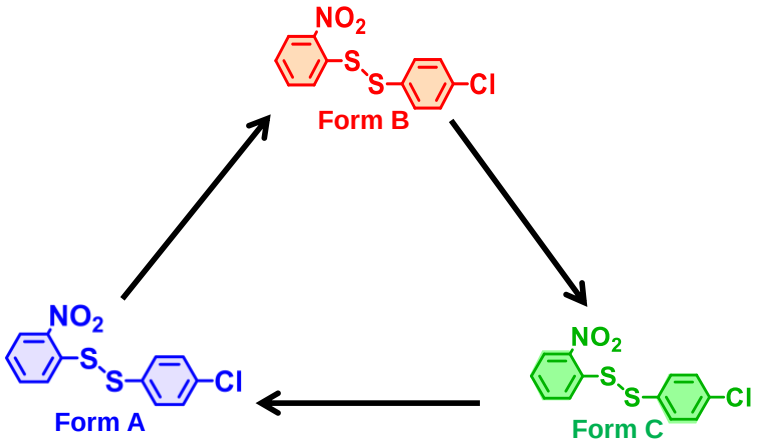

Scheme S 1: Clockwise transformation of **Form B** to **Form C** to **Form A** and further to **Form B**.

4.1 Experimental ball mill grinding procedures for polymorph transformation: clockwise Form B → Form C→ Form A

4.1.1 Procedure: clockwise Form B $_{crystals}$→Form C

This procedure is illustrated in Scheme S2.

Select a batch of **Form B** crystals that either contains 1.5%mol mol^{-1} of **1-1** (see Table S6) or alternatively, use a purer batch with <0.5%mol/mol of **1-1** and add enough **1-1** to make **Form B** crystals to contain ≥1.5%mol/mol of **1-1**.

a) In these experiments we transferred 1 mmol **Form B** crystals (297mg containing 0.2% mol mol^{-1} of **1-1**) to a 14.5mL screw-closure grinding jar manufactured from 440C stainless steel. Add 4.6 mg of **1-1** (1.5% mol mol^{-1}) on top of the crystals of **Form B**, and mix with a microspatula. Add now two 7 mm ID 440C stainless steel ball bearings on top of the crystals.

Note: It is very important that the hardness of the grinding jar matches the hardness of the ball bearings.

Close the jar and secure the junction with tape (Step a). Pre-mill the crystals for 5 minutes in a Retsch MM400 Shaker Mill to increase the surface area of the crushed crystals (Step b). Open grinding jar. Add 75 μL water (Step c). Close jar and tape junction and grind sample for 90 min at 30 Hz, allowing the grinder to rest for 5 minutes after 45 min grinding to avoid the grinding motor from overheating as well as the grinding jar. **Form C** should be obtained quantitatively (Step d) except for containing **1-1** at the required ≥1.5% mol mol^{-1}. Open and analyse the powder by HPLC and PXRD.

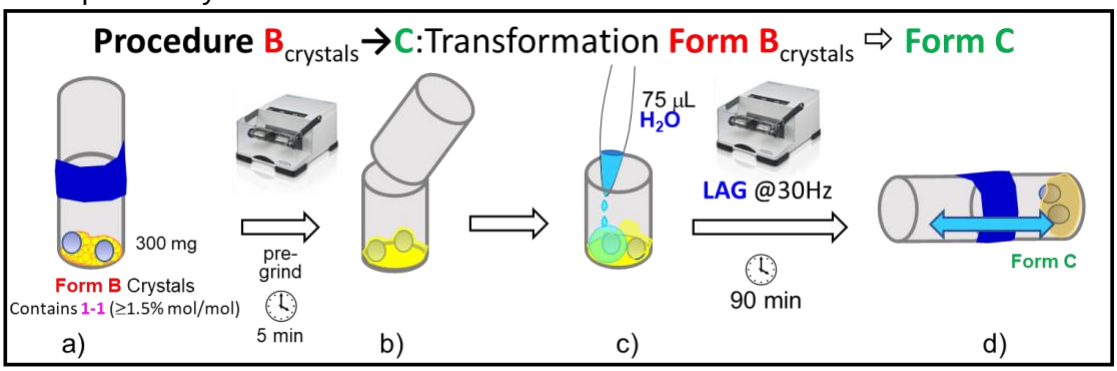

Scheme S 2 **Procedure $B_{crystals}$→C** explaining schematically and stepwise, the reproducible polymorphic transformation of **Form B** crystals to **Form C**; a) add around 300 mg of **Form B** crystals; this will typically contain ≥ 0.2% mol mol^{-1} of **1-1**. It must contain ≥ 1.5% mol mol^{-1} of **1-1** to enable this polymorph transformation. Add 2x7mm ball bearings, close jar and secure junction with tape. b) pre-NG at 30 Hz for 5 min. c) open jar. Add 75 μL water to the powder. A large globule of water will form, typically engulfing a ball; c) close and secure jar. d) LAG at 30 Hz for 90 min to obtain quantitative **Form C**.

4.1.2 Procedure: clockwise Form C→Form A

Allow the *in situ* powder of **Form C** from procedure 4.1.1, to dry in the fumehood. **Form C** must contain ≥1.5% mol mol^{-1} of **1-1**, if not, previous polymorph conversion from **Form B** would not have been possible.

This procedure is illustrated in Scheme S3. a) The grinding jar with this *in-situ* powder of **Form C** has already two 7 mm ID 440C stainless steel ball bearings. Allow water to dry. b) Close the grinding jar and secured the junction with tape. c) Grind the powder for 1.5 h at 30 Hz, allowing the grinder to rest for 5 minutes after each 45 min grinding to avoid the grinding motor from overheating as well as the grinding jar. **Form A** should be obtained quantitatively except for containing **1-1** at the required ≥1.5% mol mol^{-1}. Open and analyse the powder by HPLC and PXRD.

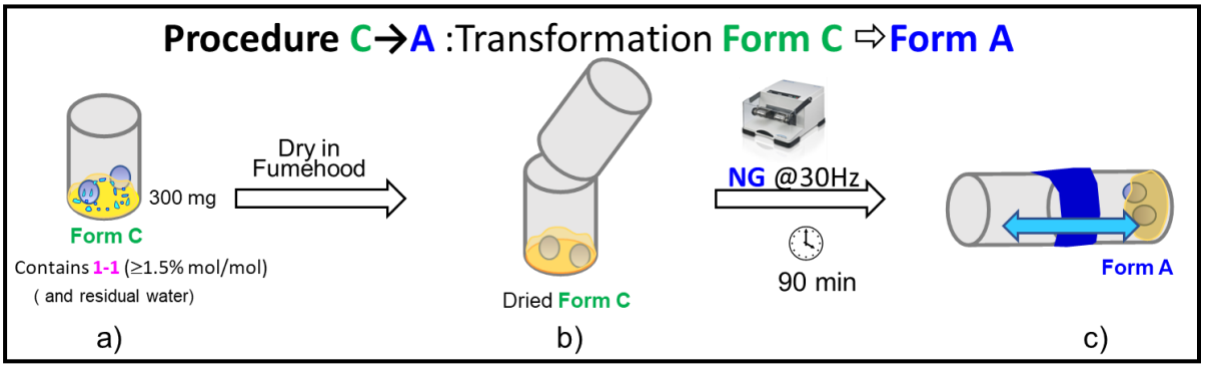

Scheme S 3 **Procedure C→A** explaining schematically and stepwise, the reproducible polymorphic transformation of **Form C** to **Form A**. a) grinding jar should contain around 300 mg of **Form C**, typically containing ≥ 1.5% mol mol^{-1} of **1-1** and 2x7mm ball bearings, b)close jar and secure with tape; c) NG at 30 Hz for 1.5 h to obtain quantitative **Form A**.

4.1.3 Procedure: clockwise Form A→Form B

In situ powder of **Form A** must contain ≥1.5% mol mol^{-1} of **1-1**, which was obtained following procedure 4.1.2.

This procedure is illustrated in Scheme S4. The grinding jar with this *in-situ* powder already has two 7 mm ID 440C stainless steel ball bearings. Add 75 μL MeCN (Step b). Close the grinding jar and secured the junction with tape (Step c). Grind the powder for 45 min at 30 Hz. **Form B** should be obtained quantitatively (Step d) except for containing **1-1** at the required ≥1.5% mol mol^{-1}. Open and analyse the powder by HPLC and PXRD.

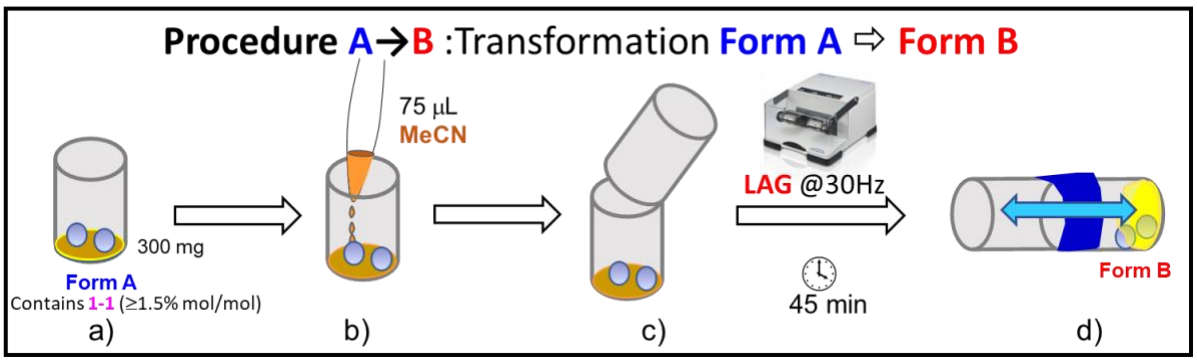

Scheme S 4 **Procedure A→B** explaining schematically and stepwise, the reproducible polymorphic transformation of **Form A** to **Form B**; **a)** Contains around 300 mg of **Form A** powder; this will typically contain ≥ 0.9% mol mol^{-1} of **1-1**; however it should contain ≥ 1.5% mol mol^{-1} of **1-1**, if later we want to do an *in situ* polymorph transformation from **Form B to Form C;** It already contains 2x7mm ball bearings; **b)** Add 75 μL MeCN. MeCN soaks quickly into powder. **c)** close jar and secure junction with tape; **d) LAG** at 30 Hz for 45 min to obtain quantitative **Form B**

4.1.4 Procedure: clockwise Form B_{powder}→Form C

This procedure is similar to Section 4.1.1 without the need for pregrinding the crystals. **Form C** should be obtained quantitatively (Step d) except for containing **1-1** at the required ≥1.5% mol mol^{-1}. Open and analyse the powder by HPLC and PXRD.

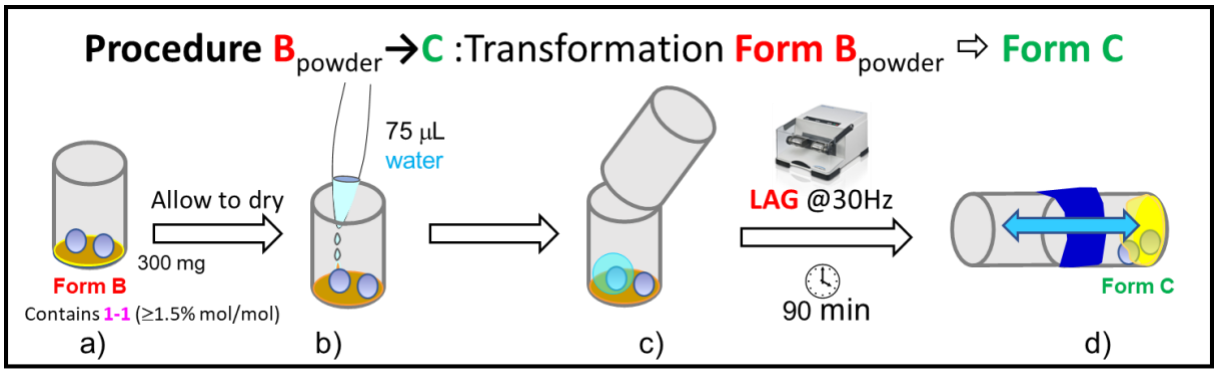

Scheme S 5 **Procedure B_{powder}→C** explaining schematically and stepwise, the reproducible polymorphic transformation of **Form B_{powder}** to **Form C**; This procedure is similar to Scheme S2. a) Contains around 300 mg of **Form B** powder; it should contain ≥ 1.5% mol mol^{-1} of **1-1** to enable this transformation**;** it should contain 2x7mm ball bearings; b) Add 75 μL water. A large globule of water will form, typically engulfing a ball. c) close jar and secure junction with tape; d) LAG at 30 Hz for 90 min to obtain quantitative **Form C**

4.2 Experimental ball mill grinding procedures for polymorph transformation: anticlockwise Form B → Form A→ Form C

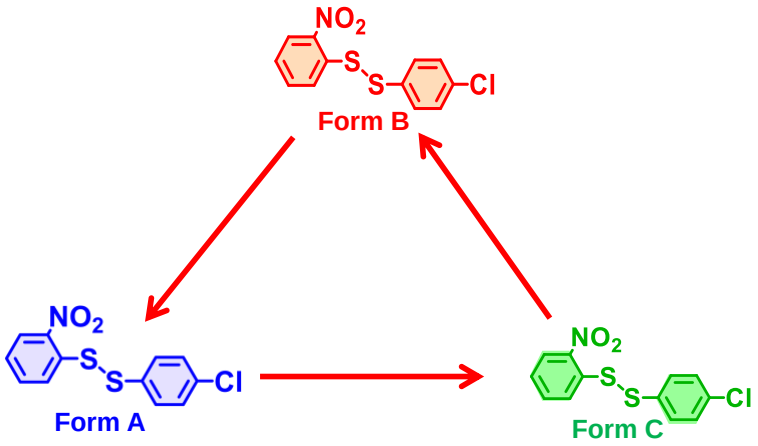

Scheme S 6 : Anticlockwise transformation of **Form B** to **Form A** to **Form C** and further to **Form B**.

4.2.1 Procedure: anticlockwise Form B $_{crystals}$→Form A

Select a batch of **Form B** crystals that either contains 1.5% mol mol^{-1} of **1-1** (see Table S6) or use a purer batch with <0.5% mol mol^{-1} of **1-1** and add **1-1** to make the **Form B** crystals to contain ≥1.5% mol mol^{-1} of **1-1**. In these experiments we transferred 1mmol **Form B** crystals (297mg containing 0.2% mol mol^{-1} of **1-1**) to a 14.5mL screw closure grinding jar manufactured from 440C stainless steel. On top of the crystals of **Form B**, add 4.6 mg of **1-1** (1.5% mol mol^{-1}) and mix with a microspatula. Add two 7 mm ID 440C stainless steel ball bearings on top of the crystals.

Note: It is important that the hardness of the grinding jar matches that of the ball bearings.

Step b: Close jar and secure the junction with tape and Step c grind sample for 3h 30 min (3x70 min) at 30 Hz, allowing the grinder to rest for 5 minutes after every 70 min grinding to avoid the grinding motor from overheating as well as the grinding jar. **Form A** should be obtained quantitatively (Step c) except for containing **1-1** at the required ≥1.5% mol mol^{-1}. Open and analyse the powder by HPLC and PXRD.

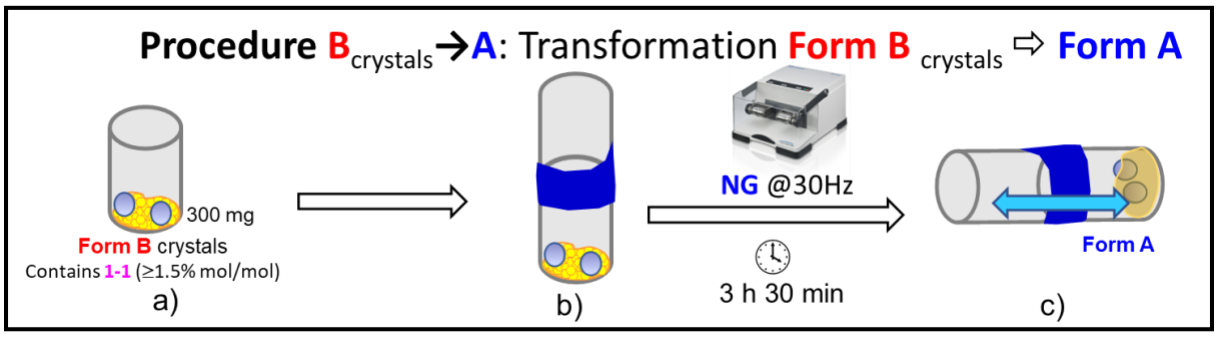

Scheme S 7 **Procedure B$_{crystals}$→A** explaining schematically and stepwise, the reproducible polymorphic transformation **Form B$_{crystals}$** to **Form A**. a) add around 300 mg of **Form B** crystals, typically containing ≥ 0.2% mol mol^{-1} of **1-1**; it should however contain ≥ 0.9% mol mol^{-1} of **1-1** to enable this transformation and even 1.5% mol mol^{-1} to enable future *in-situ* transformation of **Form B** to **Form C**. Add 2x7mm ball bearings, b) close jar and secure junction with tape; c) **NG** at 30 Hz for 3 h 30 min to obtain quantitative **Form A**.

4.2.2 Procedure: anticlockwise Form A→Form C

Starting from *in situ* powder of **Form A** (Step a) obtained following procedure 4.2.1. This must contain ≥1.5% mol mol^{-1} of **1-1**, later required for the polymorph conversion from **Form B** to **Form C**. However, **Form A** could have been formed by polymorph interconversion from **Form B** containing just ≥0.9% mol mol^{-1} of **1-1**. The grinding jar with this *in-situ* powder has already two 7 mm ID 440C stainless steel ball bearings. Add 75 μL water (Step b). Close jar and secured the junction with tape (Step c). Grind sample for 1h 30 min (2x45 min) at 30 Hz. **Form C** should be obtained quantitatively (Step d) except for containing **1-1** at the required ≥1.5% mol mol^{-1}. Open and analyse the powder by HPLC and PXRD.

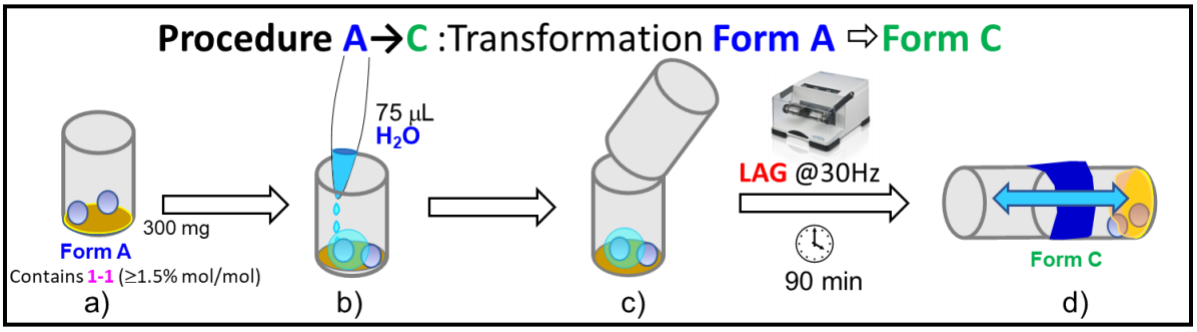

Scheme S 8 **Procedure A→C** explaining schematically and stepwise, the reproducible polymorphic transformation of **Form A** to **Form C**. a) the jar should contain around 300 mg of **Form A** powder; this will typically contain ≥ 0.9% mol mol^{-1} of **1-1**; it should however contain ≥ 1.5% mol mol^{-1} of **1-1** to enable future in-situ transformation of **Form B** to **Form C.** The jar should contain 2x7mm ball bearings; b) Add 75 μL water. A large globule of water will form, typically engulfing a ball. c) close jar and secure with tape; d) **LAG** at 30 Hz for 90 min to obtain quantitative **Form C**

4.2.3 Procedure: anticlockwise Form C→Form B

Allow the *in situ* powder of **Form C** (Step a) obtained following procedure 4.2.2. to dry overnight in the fumehood (Step a). This must contain ≥1.5% mol mol^{-1} of **1-1**. The grinding jar with this *in-situ* powder has already two 7 mm ID 440C stainless steel ball bearings. (Step b) Add 75 μL MeCN. (Step c) Close the grinding jar and secured the junction with tape. d) Grind the powder for 45 min at 30 Hz. **Form B** should be obtained quantitatively except for containing **1-1** at the required ≥1.5% mol mol^{-1}. Open and analyse the powder by HPLC and PXRD.

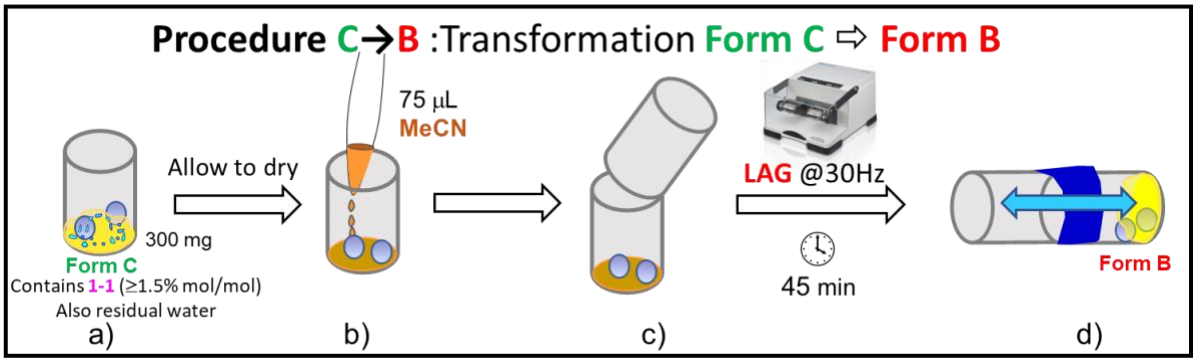

Scheme S 9 **Procedure C→B** explaining schematically and stepwise, the reproducible polymorphic transformation of **Form C** to **Form B**; (Step a) contains around 300 mg of **Form C** powder; this will typically contain ≥1.5% mol mol^{-1} of **1-1**; allow to dry residual water. Jar contains 2x7mm ball bearings; (Step b) Add 75 μL MeCN. MeCN soaks quickly into powder. (Step c) close jar and secure junction with tape; (Step d) **LAG** at 30 Hz for 45 min to obtain quantitative **Form B.**

4.2.4 Procedure: anticlockwise Form B $_{powder}$→Form A

This procedure is similar to Section 4.2.1, but starting from powder instead of crystals of **Form B**. **Form A** should be obtained quantitatively (Step c) except for containing **1-1** at the required ≥1.5% mol mol^{-1}. Open and analyse the powder by HPLC and PXRD.

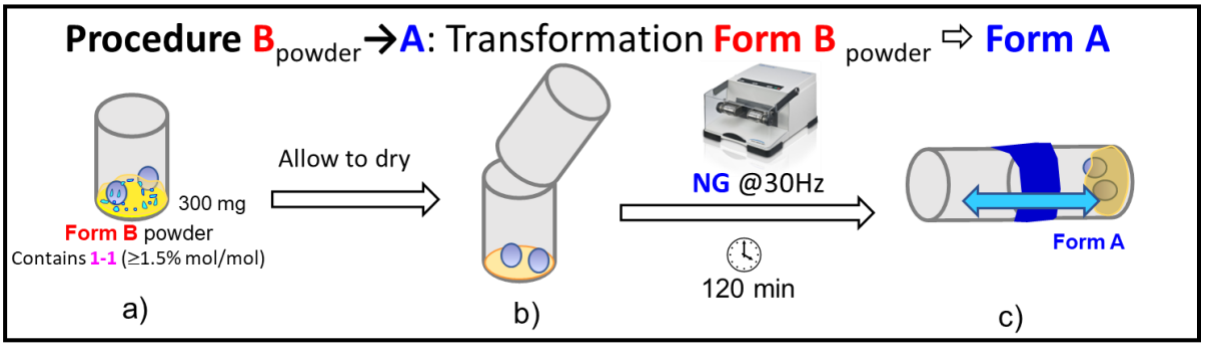

Scheme S 10 **Procedure B→A** explaining schematically and stepwise, the reproducible polymorphic transformation of powder of **Form B** to **Form A**. a) contains around 300 mg of **Form B** powder; this will typically contain ≥ 1.5% mol mol^{-1} of **1-1**; allow to dry residual MeCN. Contains 2x7mm ball bearings; b) close jar and secure junction with tape; c) NG at 30 Hz for 2h to obtain quantitative **Form A.**

5 Experimental data for the reversible polymorph transformation between Form A, Form B and Form C

All data was performed in duplicate, running 2 turnover cycles in the clockwise direction (Section 5.1) with the procedures discussed in Section 4.1 and also the anticlockwise direction (Section 5.2) with the procedures discussed in Section 4.2.

5.1 Clockwise polymorph conversion from Form B →C →A

the experimental and chemical composition while Table S8 presents the phase composition and the Scherrer size. The PXRD scans are presented in Figure S15.

Table S 7 Experimental details of the sample preparation of 2 polymorph turnover cycles between 3 polymorphs in clockwise directions (**Form B→C→A→B→C→A→B**) and chemical composition by HPLC analysis obtained for starting polymorph and the transformed polymorphs. a) replicate 1; b) replicate 2; Both replicate experiments were performed independent of each other. Typically, ball mill grinding times are executed in excess to what is absolutely necessary for a quantitative polymorph transformation, to ensure equilibrium is reached.

Polymorph transformation: Clockwise: **Form B→Form C→Form A→Form B**

Polymorph transformation	Starting polymorph				Experimental conditions			Final polymorph			
	Sample preparation				Grinding conditions			Chemical composition-			PXRD
Turnover (TO)	Starting Polymorph (300 mg = 1.01mmol)	Starting Polymorph Chemical Composition 1-1 : 1-2 : 2-2	1-1 added mg	1-1 added % mol 1-1 /mol 1-2	pre-grind time @ 30 Hz	solvent added	grinding time @ 30 Hz	$(2NO_2PhS)_2$ (1-1) %mol/mol	Product (1-2) %mol/mol	$(4ClPhS)_2$ (2-2) %mol/mol	Polymorph obtained (quantitative) except for 1-1
a)					**Replicate 1**						
cycle_1 Form B → Form C	Form $B_{crystal}$	0.12 : **99.9** : 0	4.66	1.50	5 min	75µL H_2O	90 min	1.7	**98.3**	0	Form C
cycle_1 Form C → Form A	Form C *in situ*	1.7 : **98.3** : 0	-	-	-	NG	90 min	1.6	**98.4**	0	Form A
cycle_1 Form A → Form B	Form A *in situ*	1.6 : **98.4** : 0	-	-	-	75µL MeCN	45 min	1.6	**98.4**	0	Form B
cycle_2 Form B → Form C	Form B *in situ*	1.6 : **98.4** : 0	-	-	-	75µL H_2O	120 min	1.7	**98.3**	0	Form C
cycle_2 Form C → Form A	Form C *in situ*	1.7 : **98.3** : 0	-	-	-	NG	90 min	1.7	**98.3**	0	Form A
cycle_2 Form A → Form B	Form A *in situ*	1.7 : **98.3** : 0	-	-	-	75µL MeCN	45 min	1.6	**98.4**	0	Form B
b)					**Replicate 2**						
cycle_1 Form B → Form C	Form $B_{crystal}$	0.12 : **99.9** : 0	4.62	1.50	5 min	75µL H_2O	90 min	1.8	**98.2**	0	Form C
cycle_1 Form C → Form A	Form C *in situ*	1.8 : **98.2** : 0	-	-	-	NG	90 min	1.6	**98.4**	0	Form A
cycle_1 Form A → Form B	Form A *in situ*	1.6 : **98.4** : 0	-	-	-	75µL MeCN	45 min	1.6	**98.4**	0	Form B
cycle_2 Form B → Form C	Form B *in situ*	1.6 : **98.4** : 0	-	-	-	75µL H_2O	120 min	1.7	**98.3**	0	Form C
cycle_2 Form C → Form A	Form C *in situ*	1.7 : **98.3** : 0	-	-	-	NG	90 min	1.7	**98.3**	0	Form A
cycle_2 Form A → Form B	Form A *in situ*	1.7 : **98.3** : 0	-	-	-	75µL MeCN	45 min	1.7	**98.3**	0	Form B

Table S 8: Polymorph transformation between 3 polymorphs. in clockwise directions (**Form B→C→A→B→C→A →B**). Experimental conditions, phase composition expressed as % mol mol^{-1} with respect to total polymorph and Scherrer size expressed in nm of the products of polymorph transformation including statistics. The values of the chemical composition by HPLC analysis (see Table S 7) have been added for comparison. a) replicate 1; b) replicate 2; Both replicate experiments were performed independent of each other. Typically, ball mill grinding times are executed in excess to what is absolutely necessary for a quantitative polymorph transformation, to ensure equilibrium is reached.

Polymorph transformation Clockwise: Form B→Form C→Form A→

Experimental conditions				Reaction product of ball mill reaction																
cycle steps	Starting polymorph	Ball mill grinding at 30 Hz 14.5 mL ss jars and 2 x 7mm diameter ss balls		Phase composition						Scherrer size						Statistics		HPLC		
				Form B		Form A		Form C		Form B		Form A		Form C						
		Solvent µL	grinding time @30Hz	% mol/ mol	e.s.d. mol%	% mol/ mol	e.s.d. mol%	% mol/ mol	e.s.d. mol%	nm	e.s.d. nm	nm	e.s.d. nm	nm	e.s.d. nm	Rwp Rietveld refinement Goodness	chisq Rietveld refinement Fit Index	1-1	1-2	2-2
a)	**Replicate 1**																			
1-1	Form B_{crys}	75µL H_2O	90 min	4.1	0.5	1.3	0.4	**94.5**	0.6					**86**	1.2	9.0	3.7	**1.7**	**98.3**	0
1-2	Form C	NG	90 min	2.2	0.4	**77.8**	0.6	20.0	0.5			**50**	0.7			8.2	3.2	**1.6**	**98.4**	0
1-3	Form A	75µL MeCN	45 min	**99.5**	0.3	0.2	0.2	0.3	0.2	**125**	2.2					13.0	5.1	**1.6**	**98.4**	0
2-1	Form B	75µL H_2O	120 min	2.1	0.6	1.0	0.3	**96.9**	0.6					**83**	1.2	9.0	3.6	**1.7**	**98.3**	0
2-2	Form C	NG	90 min	2.7	0.4	**87.2**	0.6	10.0	0.5			**54**	0.7			9.5	3.8	**1.7**	**98.3**	0
2-3	Form A	75µL MeCN	45 min	**99.2**	0.3	0.6	0.3	0.2	0.2	**131**	2.4					11.9	4.7	**1.6**	**98.4**	0
b)	**Replicate 2**																			
1-1	Form B_{crys}	75µL H_2O	90 min	7.9	0.5	1.2	0.3	**91.0**	0.5					**88**	1.3	9.2	3.7	**1.8**	**98.2**	0
1-2	Form C	NG	90 min	1.8	0.3	**62.5**	0.5	35.6	0.4			**54**	1.0			8.0	3.2	**1.6**	**98.4**	0
1-3	Form A	75µL MeCN	45 min	**99.6**	0.3	0.3	0.2	0.1	0.2	**128**	2.4					12.3	4.9	**1.6**	**98.4**	0
2-1	Form B	75µL H_2O	120 min	0.8	0.6	1.4	0.4	**97.8**	0.7					**92**	1.4	9.0	3.6	**1.7**	**98.3**	0
2-2	Form C	NG	90 min	3.0	0.4	**92.4**	0.6	4.5	0.5			**56**	0.7			9.6	3.9	**1.7**	**98.3**	0
2-3	Form A	75µL MeCN	45 min	**98.5**	0.5	1.2	0.4	0.3	0.2	**140**	2.6					12.1	4.8	**1.7**	**98.3**	0

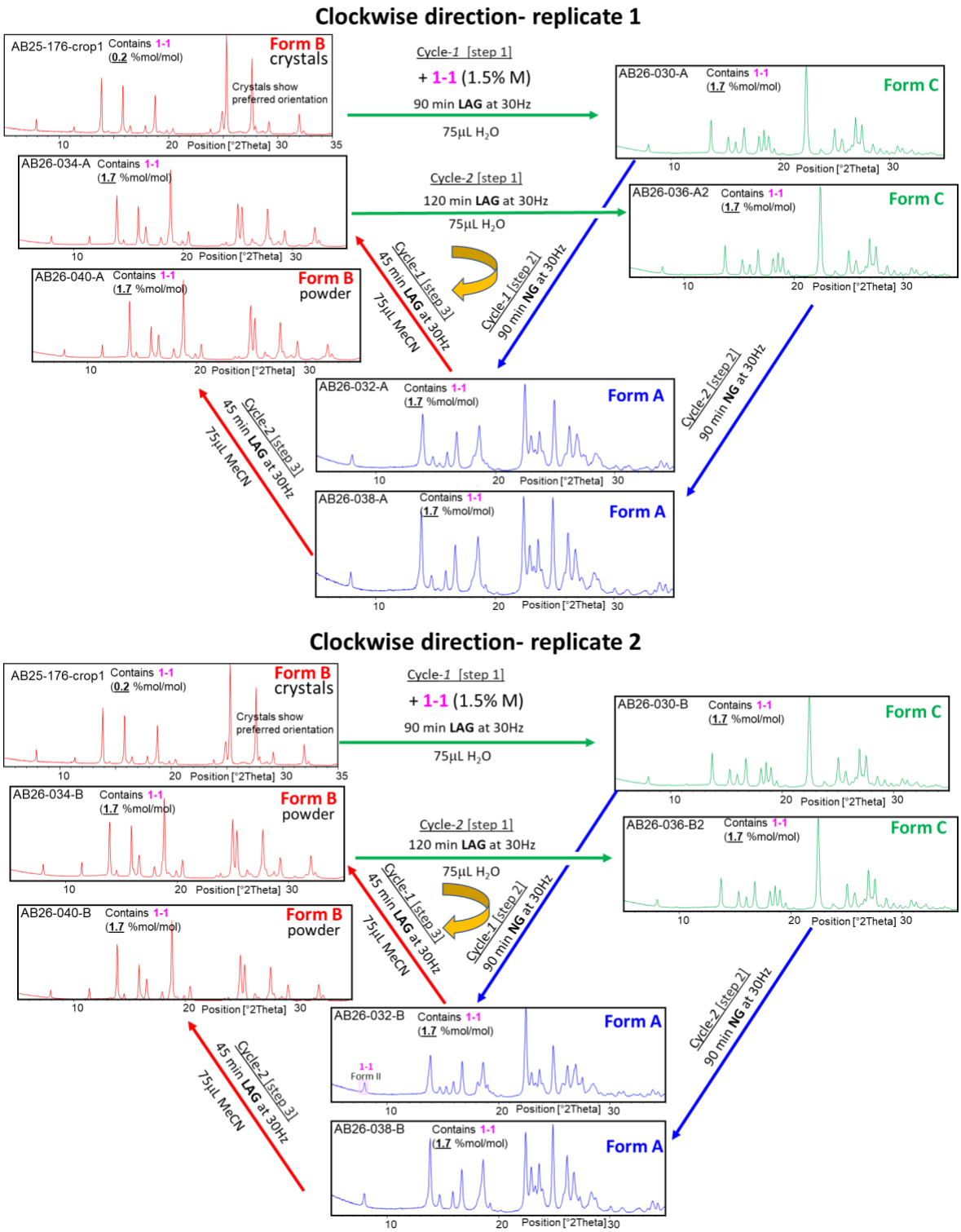

Figure S 15: Polymorph transformation between 3 polymorphs in clockwise directions (**Form B→C→A→B→C→A→B**) Top: Replicate 1; Bottom: Replicate 2. The polymorph transformation has been started from the crystalline form of **Form B** containing ≥ 1.5% mol mol^{-1} of **1-1**. This polymorph transforms **Form B** to **Form C** by **LAG** with water. On drying **Form C**, it transforms to **Form A** by **neat** grinding. **LAG** with acetonitrile transforms **Form A** to **Form B**. We performed 2 polymorph turnover cycles of these experiments. Addition of at least 1.5% mol mol^{-1} of **1-1** is required to obtain the polymorph transformations presented here.

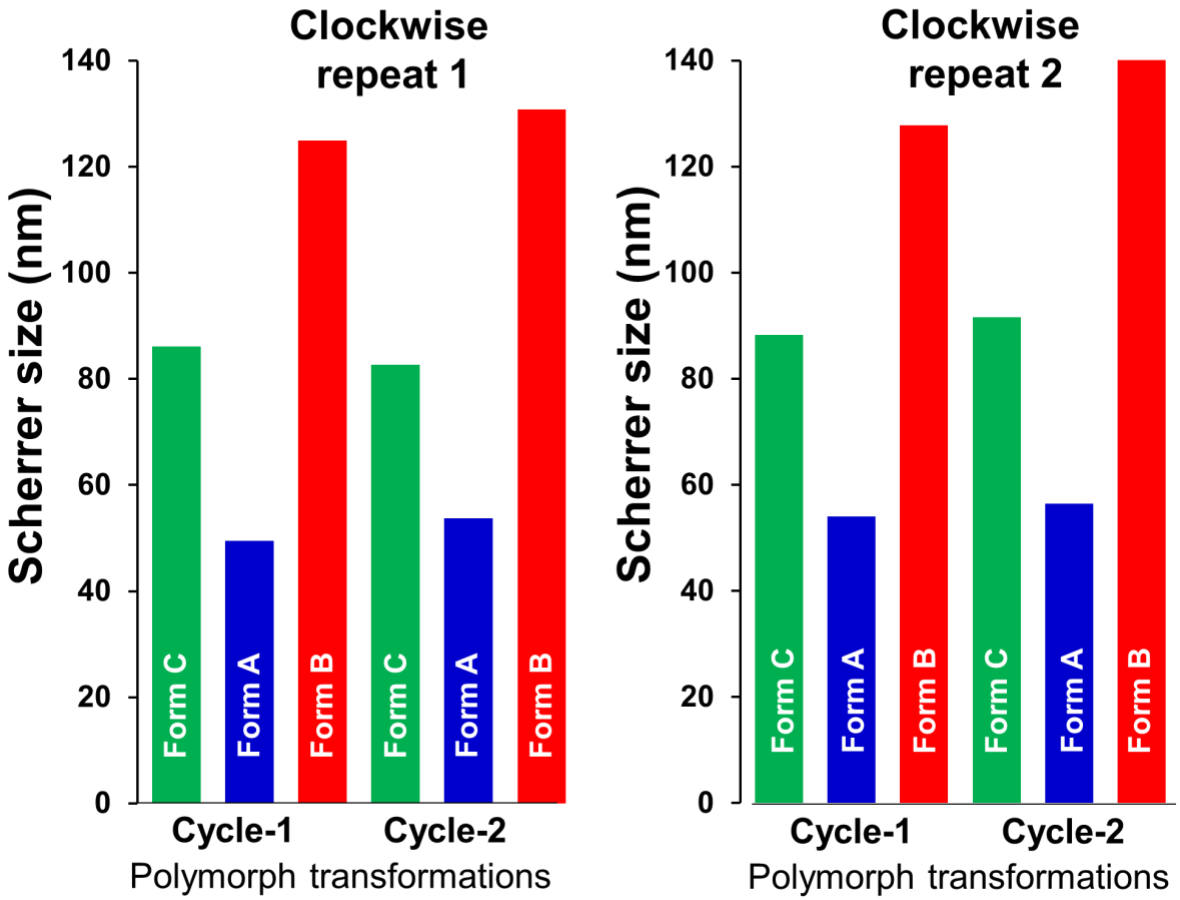

Figure S 16 Scherrer size for **Form C**, **Form A** and **Form B** obtained by the *in-situ* polymorph transformation in clockwise direction (**Form B→C→A→B→C→A→B**) as in Figure S15 with repeat 1 and repeat 2.

5.2 Anti-clockwise polymorph conversion from Form B →A →C

Table S9 presents the experimental and chemical composition while TableS10 presents the phase composition and the Scherrer size. The PXRD scans are presented in Figure S17.

Table S 9 Experimental details of the sample preparation of 2 polymorph turnover cycles between 3 polymorphs in anti-clockwise directions (**Form B→A→C→B→A→C→B**) and the chemical composition from HPLC analysis obtained for starting polymorph and the transformed polymorphs. a) replicate1; b) replicate 2; Both replicate experiments were performed independent of each other. Typically, ball mill grinding times are executed in excess to what is absolutely required for a quantitative polymorph transformation, to ensure equilibrium is reached.

Polymorph transformation Anti-clockwise: **Form B→Form A→Form C→Form B**

Polymorph transformation	Starting polymorph				Experimental conditions			Final polymorph			
	Sample preparation				Grinding conditions			Chemical composition-			PXRD
Turnover (TO)	Starting Polymorph (300 mg = 1.01mmol)	Starting Polymorph Chemical Composition 1-1 : 1-2 : 2-2	1-1 added mg	1-1 added % mol 1-1 /mol 1-2	pre-grind time @ 30 Hz	solvent added	grinding time @ 30 Hz	$(2NO_2PhS)_2$ (1-1) %M	Product (1-2) %M	$(4ClPhS)_2$ (2-2) %M	Polymorph obtained (quantitative) except for 1-1
a)				**Replicate 1**							
TO_1 Form B → Form A	Form $B_{crystal}$	0.12 : **99.9** : 0	4.68	1.50	5 min	75µL H_2O	3 h	1.7	**98.3**	0	Form A
TO_1 Form A → Form C	Form A *in situ*	1.7 : **98.3** : 0	-	-	-	NG	90 min	1.7	**98.3**	0	Form C
TO_1 Form C → Form B	Form C *in situ*	1.7 : **98.3** : 0	-	-	-	75µL MeCN	45 min	1.6	**98.4**	0	Form B
TO_2 Form B → Form A	Form B *in situ*	1.6 : **98.4** : 0	-	-	-	75µL H_2O	3 h	1.7	**98.3**	0	Form A
TO_2 Form A → Form C	Form A *in situ*	1.7 : **98.3** : 0	-	-	-	NG	90 min	1.6	**98.4**	0	Form C
TO_2 Form C → Form B	Form C *in situ*	1.6 : **98.4** : 0	-	-	-	75µL MeCN	45 min	1.6	**98.4**	0	Form B
b)				**Replicate 2**							
TO_1 Form B → Form A	Form $B_{crystal}$	0.12 : **99.9** : 0	4.68	1.50	5 min	75µL H_2O	3 h	1.7	**98.3**	0	Form A
TO_1 Form A → Form C	Form A *in situ*	1.7 : **98.3** : 0	-	-	-	NG	90 min	1.6	**98.4**	0	Form C
TO_1 Form C → Form B	Form C *in situ*	1.6 : **98.4** : 0	-	-	-	75µL MeCN	45 min	1.6	**98.4**	0	Form B
TO_2 Form B → Form A	Form B *in situ*	1.6 : **98.4** : 0	-	-	-	75µL H_2O	3 h	1.7	**98.3**	0	Form A
TO_2 Form A → Form C	Form A *in situ*	1.7 : **98.3** : 0	-	-	-	NG	90 min	1.7	**98.3**	0	Form C
TO_2 Form C → Form B	Form C *in situ*	1.7 : **98.3** : 0	-	-	-	75µL MeCN	45 min	1.7	**98.3**	0	Form B

Table S 10: Experimental details of the sample preparation of 2 cycles of polymorph transformation between 3 polymorphs. in anti-clockwise directions (**Form B→A→C→B→A→C→B**) and the chemical composition from HPLC analysis obtained for starting polymorph and the transformed polymorphs. a) replicate1; b) replicate 2; Both replicate experiments were performed independent of each other. Typically, ball mill grinding times are executed in excess to what is absolutely required for a quantitative polymorph transformation, to ensure equilibrium is reached.

Polymorph transformation Anti-clockwise: Form B→Form A→Form C→

Experimental conditions				Reaction product of ball mill NG & LAG reaction																
		Ball mill grinding at 30 Hz 14.5 mL ss jars and 2 x 7mm diameter ss balls		Phase composition						Scherrer size						Statistics		HPLC		
turn-overs steps	Starting polymorph			Form B		Form A		Form C		Form B		Form A		Form C		Rwp Rietveld refinement Goodness	chisq Rietveld refinement Fit Index	1-1	1-2	2-2
		Solvent µL	grinding time @30Hz	%M	e.s.d. mol%	%M	e.s.d. mol%	%M	e.s.d. mol%	nm	e.s.d. nm	nm	e.s.d. nm	nm	e.s.d. nm					
a)	**Replicate 1**																			
1-1	Form B_{crys}	NG	3 h	3.0	0.3	**92.6**	0.7	4.4	0.6			**55**	0.8			9.3	3.7	**1.7**	**98.3**	0
1-2	**Form A**	75µL H_2O	90 min	1.7	0.5	5.9	0.5	**92.4**	0.7					**85**	1.3	8.8	3.5	**1.7**	**98.3**	0
1-3	**Form C**	75µL MeCN	45 min	**99.0**	0.3	0.7	0.3	0.3	0.2	**126**	2.2					11.6	4.6	**1.6**	**98.4**	0
2-1	**Form B**	NG	3 h	3.0	0.4	**94.5**	0.6	2.5	0.5			**61**	0.9			9.2	3.7	**1.7**	**98.3**	0
2-2	**Form A**	75µL H_2O	90 min	1.4	0.5	6.6	0.5	**91.9**	0.7					**75**	1.2	8.1	3.3	**1.6**	**98.4**	0
2-3	**Form C**	75µL MeCN	45 min	**99.0**	0.3	0.8	0.3	0.2	0.2	**130**	2.5					11.4	4.5	**1.6**	**98.4**	0
b)	**Replicate 2**																			
1-1	Form B_{crys}	NG	3 h	2.7	0.3	94.1	0.6	3.2	0.5			56	0.8			9.3	3.7	**1.7**	**98.3**	0
1-2	**Form A**	75µL H_2O	90 min	2.0	0.5	10.0	0.5	88.0	0.6					78	1.2	8.9	3.5	**1.7**	**98.3**	0
1-3	**Form C**	75µL MeCN	45 min	98.8	0.3	0.9	0.3	0.3	0.2	131	2.4					11.7	4.6	**1.6**	**98.4**	0
2-1	**Form B**	NG	3 h	2.9	0.4	94.7	0.6	2.5	0.5			61	0.9			9.1	3.7	**1.6**	**98.4**	0
2-2	**Form A**	75µL H_2O	90 min	1.8	0.5	10.2	0.5	88.0	0.6					72	1.1	8.4	3.3	**1.7**	**98.3**	0
2-3	**Form C**	75µL MeCN	45 min	99.3	0.3	0.6	0.3	0.0	0.2	132	2.6					10.7	4.2	**1.7**	**98.3**	0

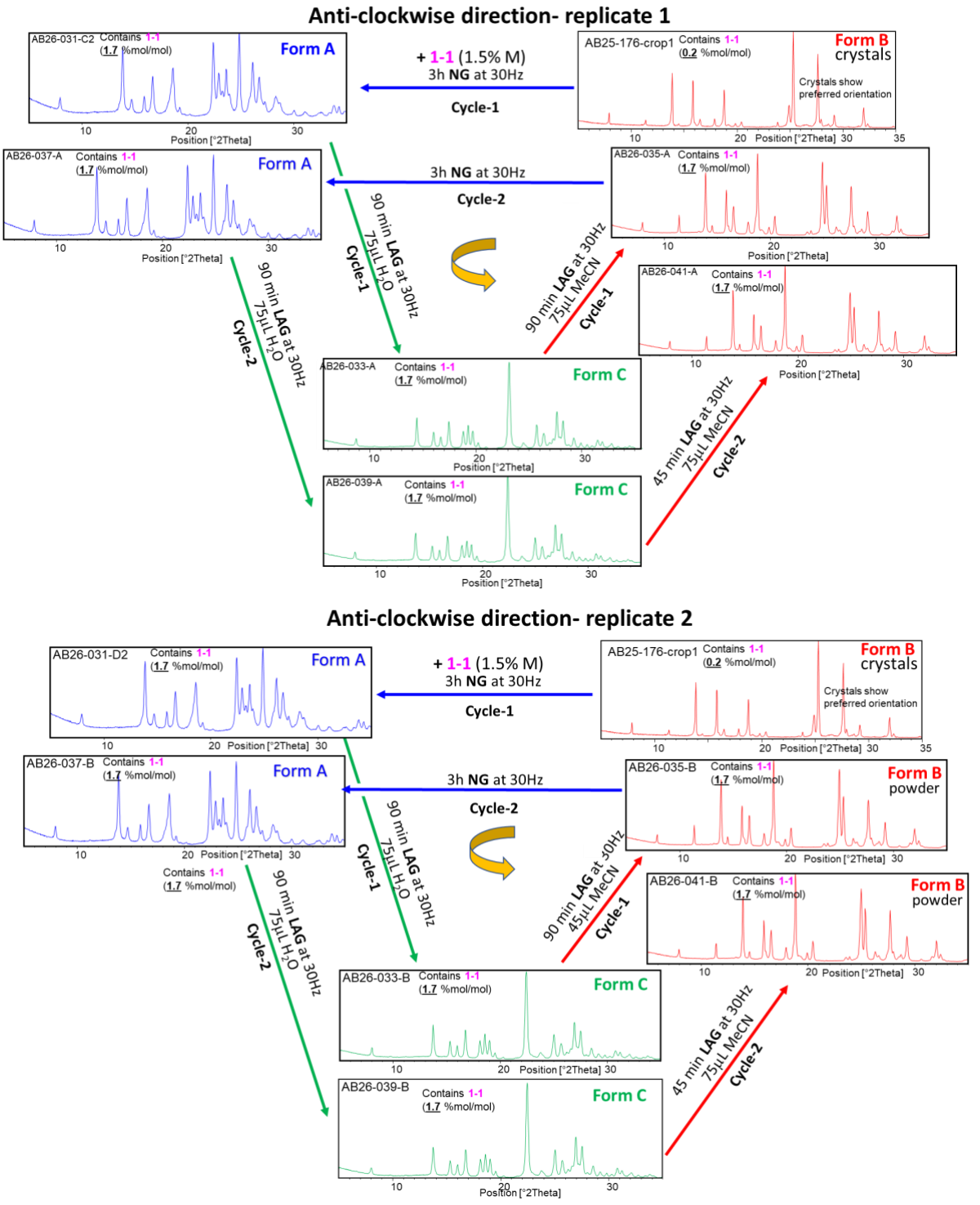

Figure S 17 Polymorph transformation between 3 polymorphs of **1-2** in anti-clockwise direction (**Form B→A→C→B→A→C→B**) Top: Replicate 1; Bottom: Replicate 2. The polymorph transformation is started from the crystalline form of **Form B**. This polymorph transforms **Form B** to **Form A** by **neat** grinding; then to **Form C** by **LAG** with water. On drying **Form C**, transforms back to **Form B** by **LAG** with acetonitrile. We performed 2 polymorph turnover cycles. Addition of ≥ 1.5% mol mol^{-1} of **1-1** is required to obtain the polymorph transformations presented here.

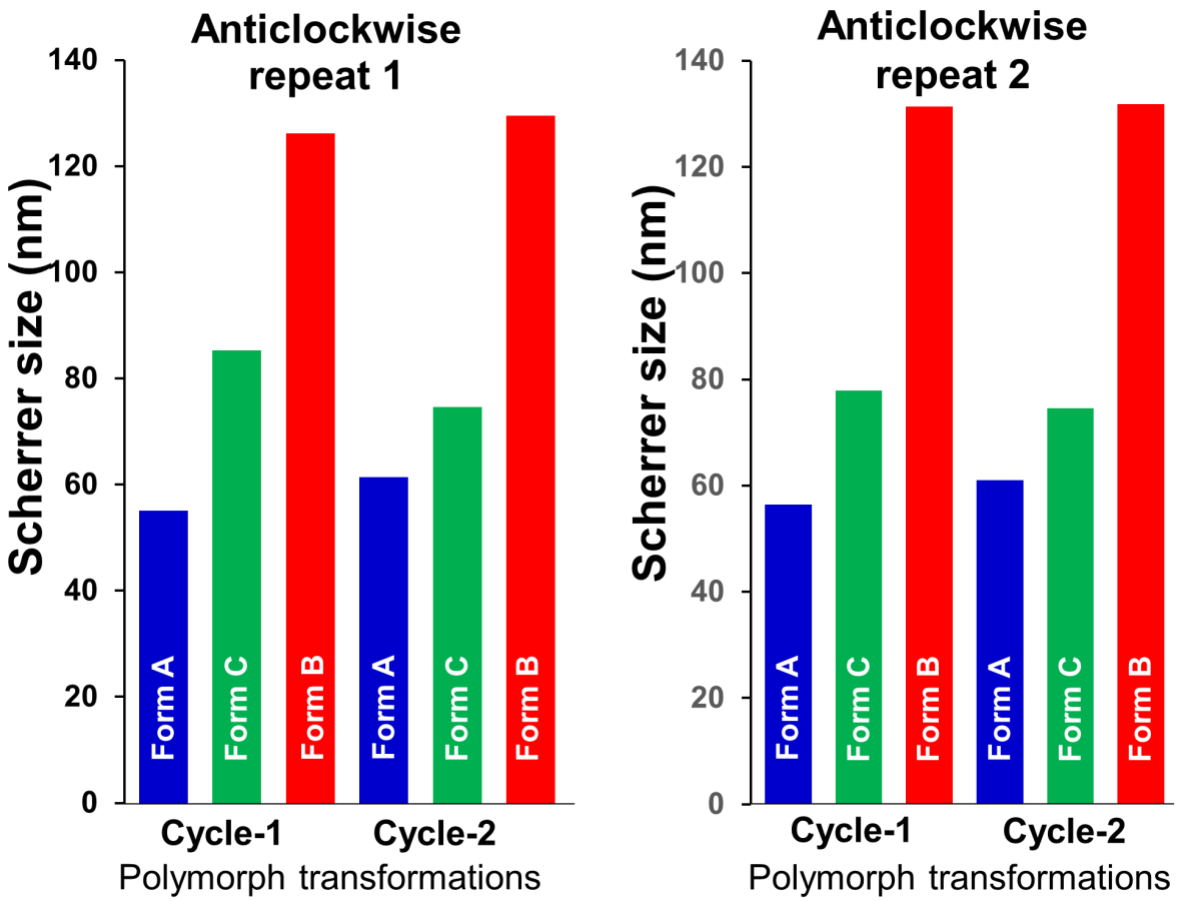

Figure S 18 Scherrer size for **Form A**, **Form C** and **Form B** obtained by the in-situ polymorph transformation. Polymorph transformation in anti-clockwise direction (**Form B→A→C→B→A→C→B**) as in Figure S17. Here we show the 2 repeats.

6 Exploratory studies to achieve reproducible transformation of Form B crystals to Form A or Form C

6.1 Introduction:

Starting from equimolar amounts of homodimers (**1-1** and **2-2**) in the presence of a base catalyst (**dbu)**, disulfide exchange reaction by ball mill grinding takes place, forming 2-nitrophenyl,4-chlorophenyl disulfide heterodimer (referred here as **1-2**) in quantitative yield. The formation of the polymorph **Form A** by **NG** and **Form B** by **LAG** with acetonitrile has been previously published.[1-3, 6, 8]

Form A is also obtained when using any polar organic solvent (e.g. MeCN, acetone) at volumes below the threshold value necessary to affect the surface of the nanocrystals (Section 6.3.2).[6]

Form B can be formed with most organic polar solvent (MeCN, acetone, ethyl acetate) as far as their added volume is above the threshold value necessary to affect the surface of the nanocrystals.[6]

All initial batches of **Form B** prepared by mechanochemistry DCC are typically around 97%mol/mol, at equilibrium, the remaining material being **1-1** at 1.5% mol/mol and **2-2** at 1.5% mol/mol. Recrystallisation of these batches from MeCN, MeOH, EtOH or IPA, formed crystals of **Form B** (thermodynamic product). All the crops of **Form B** crystals have been found to always contain **1-1** but never **2-2**, as **2-2** is extremely soluble in all solvents used for crystallisation.

During our initial work, the 1st crop obtained by recrystallisation of **Form B** (prepared from solid state DCC **Form B**) always contained **1-1** around1.5%mol/mol, as reported in the ESI (Table S16 taken from reference[6]). We have pursued different procedures to improve the purity of the batches of **Form B** crystals.

We found that we could prepare very pure preparative **Form A** DCC batches with yields > 98.5%mol/mol and < 1% mol/mol of **1-1**. Recrystallisation of these batches resulted in very pure (> 99.5% mol/mol) of **Form B** crystals, in some cases with just 0.1% mol/mol of **1-1**.

We have proven that crystals of **Form B** can be transformed by direct polymorph transformation (3-6 h **NG** at 30 Hz) in the absence of dbu to **Form A** and back to **Form B** with 30 min **LAG** with MeCN. We have demonstrated that this polymorph transformation is reversible and can be performed *in situ*, over and over again.[6]

6.2 Results and Discussion

As a picture tells more than one thousand words, we will give here a tour through the development of the procedures designed to perform polymorph transformation between **Form B**, **Form A** and **Form C.** We will present the procedures used as a scheme illustrating the steps required and the experiments in an illustrative form: on the left of the figures, the PXRD of the starting crystal or powder to be transformed with details of the batch of **Form B** crystals used and the level of **1-1**; on the right of the figures, the PXRD of the outcome of the ball mill grinding experiment.

We will here discuss the most difficult transformations in this project.

- Transformation of crystals of **Form B** to **Form A** (Section 6. 3)
- Transformation of crystals of **Form B** to **Form C** (Section 6. 4)

The outcome of these experiments proved to be very erratic and batch dependent, requiring a very extensive program of work:

Our first hypothesis was that failure or success in the polymorph transformation must be kinetic and not a thermodynamic issue. The transformation of one polymorph to another must have a high transition barrier.

We hypothesised that the problem here must lie in the lack of reproductivity of the dryness or moisture and even content of residual solvent on the surface of the different batches and crops of **Form B** crystals. **Form B** crystals being filtered from the mother liquor and subsequently washed with cold solvent to remove all traces of dbu and TFA before being allowed to dry.

The following procedures and experiments were performed to investigate this hypothesis.

6.3 Transformation of crystals of Form B to Form A

We investigated this polymorph transformation using 3 strategies previously reported.[1-2, 5-6]

At this stage we did not know if the crystals of **Form B** would behave differently from powder of **Form B**. Therefore, the development of this procedure is focused on always starting from crystals of **Form B**.

The later development starting from powder of **Form B** is reported in Section 6.7.1.

The strategies use for this transformation are:

- Section 6.3.1: covers all the different procedures which could result in the **NG** transformation of crystals of **Form B** to **Form A**
- Section 6.3.2: covers the procedures which resulted in the **LAG** transformation with insufficient volume of MeCN of crystals of **Form B** to **Form A**

Good lessons could be equally be learned from failed as from successful experiments.

6.3.1 Transformation of crystals of Form B to Form A by ball mill NG

NG can be seen as the typical procedure to transform **Form B** to **Form A**

The simplest procedure depicted in Scheme S11 to transform **Form B** crystals to **Form A** proved to be batch and crop dependent on the crystals of **Form B** used. (Figure S19 and S20).

We hypothesised at this stage, that the crystal batch dependency could be due to differences on the surface of the crystals from their collection from the mother liquor, washing step and implemented drying procedures.

1. We first checked if the reluctancy for some batches of **Form B** crystals (Figure S19 and S20), to transform to **Form A** could be due a high energy barrier. We proposed to grind the jar with a heating mantle up to 60^{o}C, (Scheme S 12). Despite the extensive grinding even under heat, no polymorph transformation occurred (Figure S21).
2. We then considered if the batches of crystals of **Form B** may not be dry enough, We proposed to dry them under vacuum. (Scheme S13). This clearly appears to make this transformation from **Form B** to **Form A** much worse (Figure S 22)
3. Next idea was to subject the overdried crystals of **Form B**, to high humidity before performing NG (Scheme S14) to check if humid crystals were more likely to transform. No transformation was obtained (Figure S 23)
4. We then consider if it may be better to transform the vacuum dried crystals of **Form B** to powder of **Form B** by **LAG** with MeCN before performing **NG** (Scheme S 15). The thinking was that the dry powder of **Form B** may transform better. Figure S20 shows a conversion to **Form A**, so it may help.
5. We here considered if the step of vacuum drying the crystals of **Form B** could be avoided. Scheme S16 depicts how crystals of Form B are subjected to 100% relative humidity before **NG**. Figure S25 make it look promising but not yet reproducible. c) did not convert despite using the same experimental conditions as b).
6. We here considered if we should increase the surface area of the crystal of **Form B** by pre-grinding before subjecting them to 100% humidity chamber as depicted in Scheme S17. The result from Figure S26 was good, as it fully transformed to **Form A**.
7. Similar to Scheme S17 in point 6, we performed the pre-milling manually using mortar and pestle leaving the crushed crystals in the high humidity chamber as shown in Scheme S18. The results from Figure S27 shows that only 2 out of 5 experiments transformed to **Form A**.

   In summary: it is only clear that humid crystals of Form B may enable the polymorph transformation to **Form A**, while overdried crystals will not. It is not clear if pre-griding crystals of **Form B** will help. However, there is no reliable procedure for the transformation of crystals of **Form B** to **Form A**.

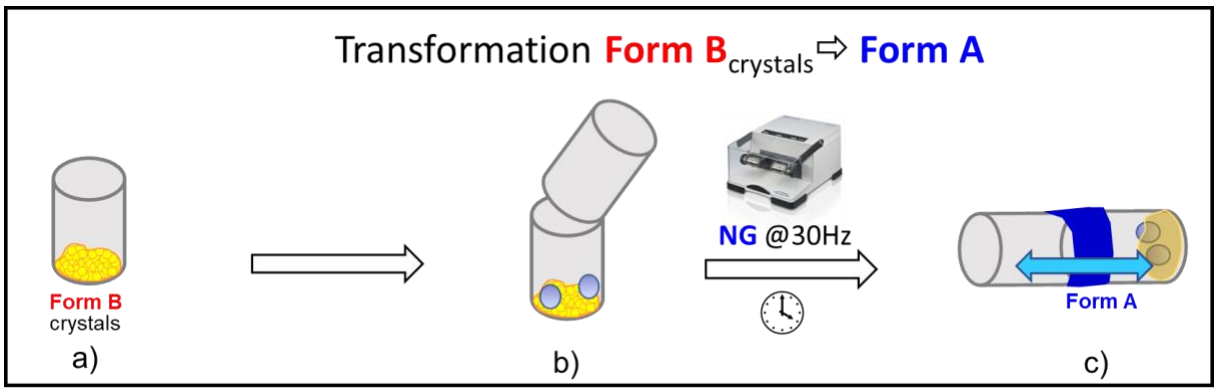

Scheme S 11 Schematic diagram of the NG procedure to transform crystals of **Form B** to **Form A** used in to the grinding experiments in Fig. S19 and S20. This scheme is based on Scheme S7. Step a) add crystals of Form B to jar. b) add 2x 7 mm ball bearings. Close jar and seal. c) **NG** at 30 Hz with the objective to transform crystals of **Form B** to **Form A**.

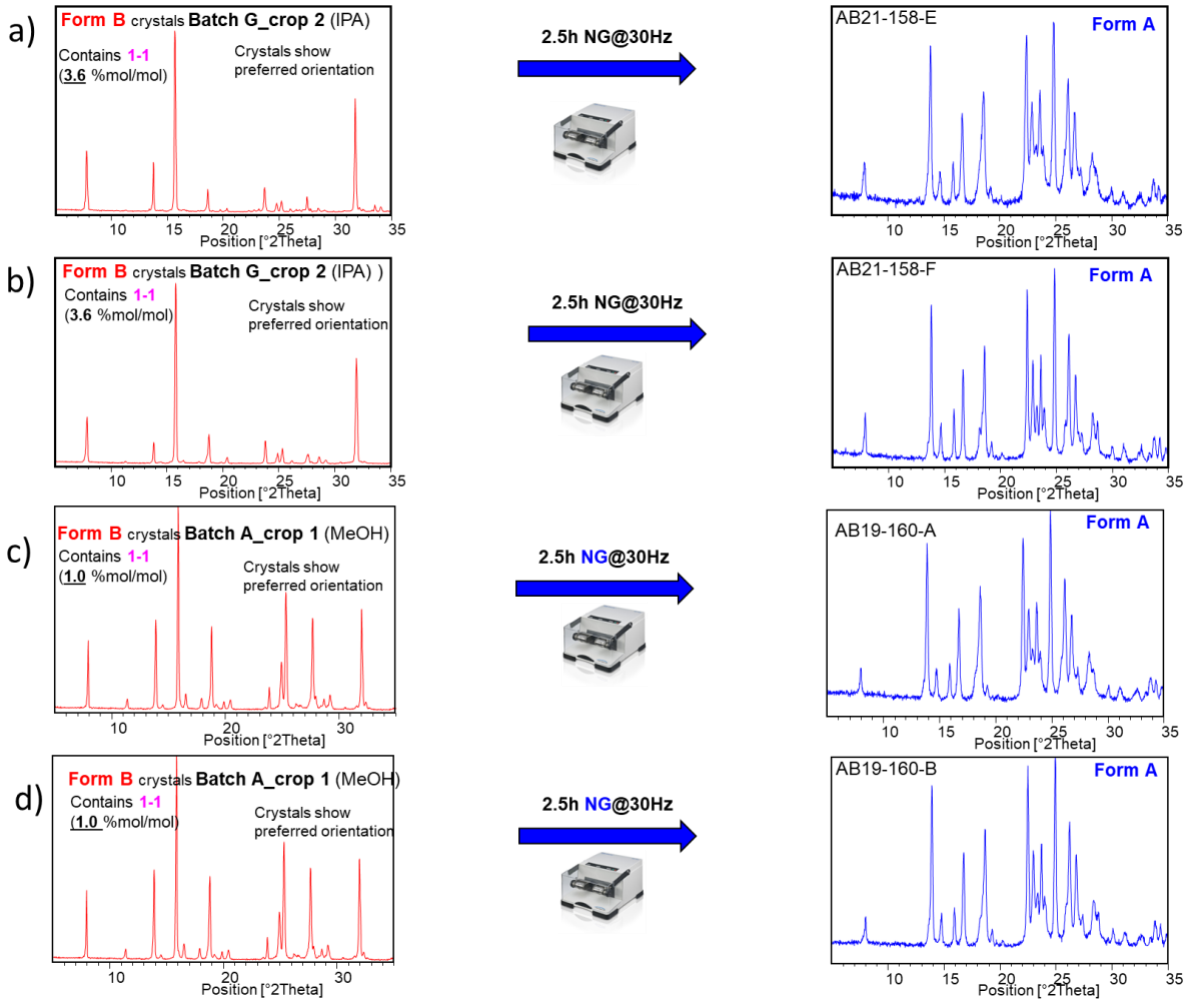

Continue on next page

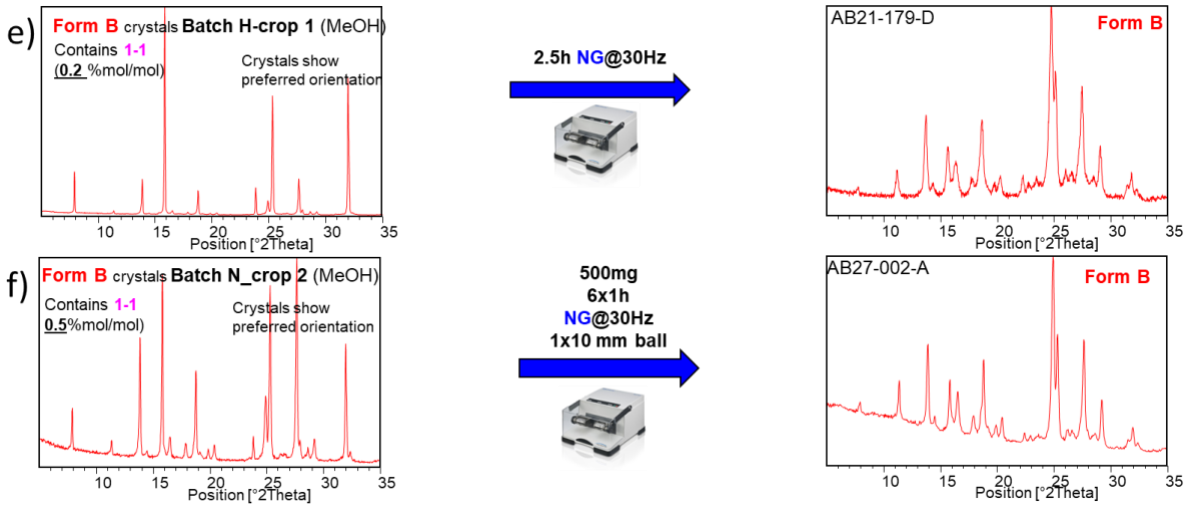

Figure S 19 Attempted transformation of analytical batches (200 mg to 500 mg) of crystals of **Form B** to **Form A** by **NG** at 30 Hz, following the procedure illustrated above in Scheme S11. The dryness, humidity or level of residual solvents of these crystals are unknown and may vary from batch to batch and from crop to crop. The % mol/mol of **1-1** has been determined by HPLC analysis; and is preserved through all manipulations and polymorph transformations. The experimental details of the batches used of **Form B** crystals are listed on **Table S6.** See explanation for the success or failure of these attempted transformations in Section 6.3.3.

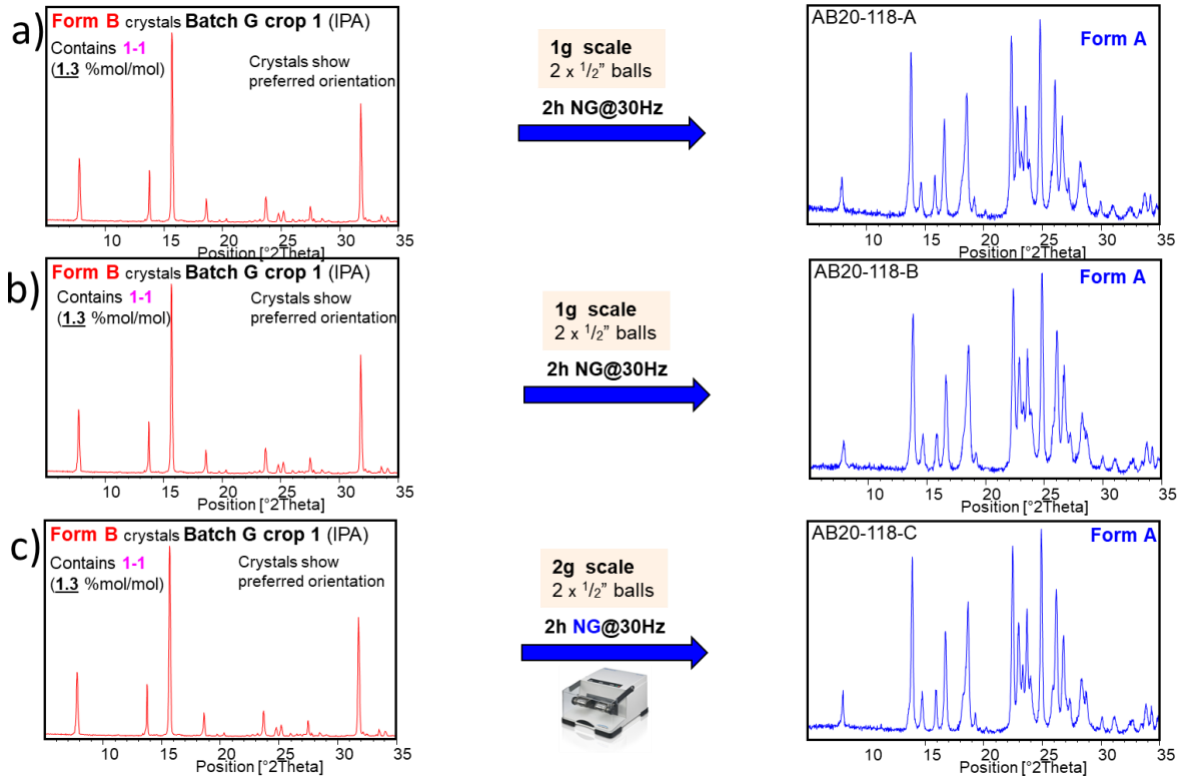

Continue on next page

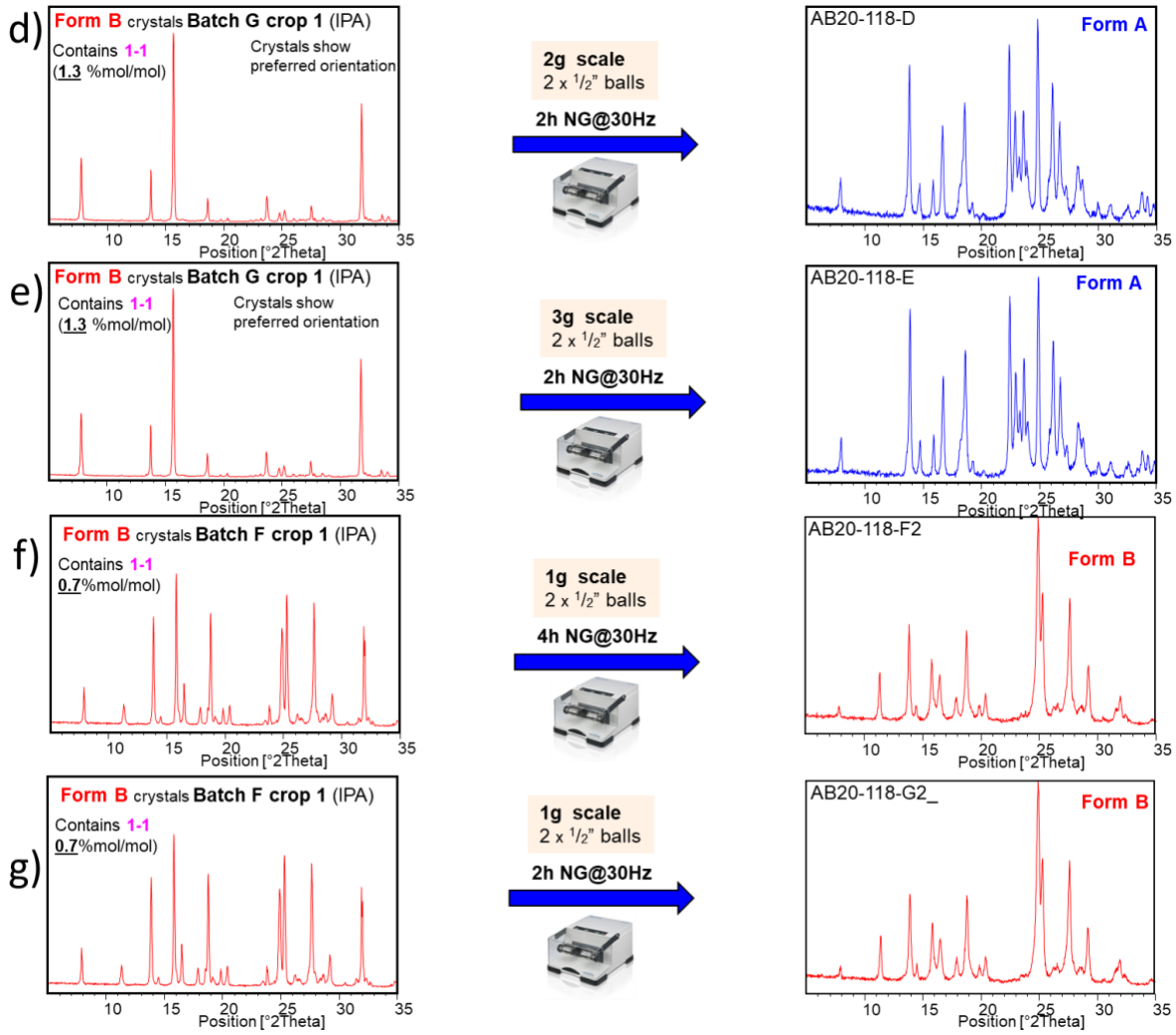

Figure S 20 Attempted direct transformation at gram scale of crystals of **Form B** to **Form A** by 2-4 h ball mill **NG** at 30 Hz, following the procedure illustrated above in Scheme S11. The dryness, humidity or level of residual solvents of those crystals are unknow and may vary from batch to batch and from crop to crop. PXRD scans of the crystals of **Form B** show preferred orientation. The % mol/mol of **1-1** has been determined by HPLC analysis; and is preserved through all manipulations and polymorph transformations. The experimental details of the **Form B** crystals batches used are listed on **Table S6.** See explanation for the success or failure of these attempted transformations in Section 6.3.3.

We postulated that if the grinding jar were to be heated while grinding, the polymorph transformation would be enabled. The outcome of Figure S 21, appears not to support this hypothesis, despite finally grinding at 60ºC for 4 hours.

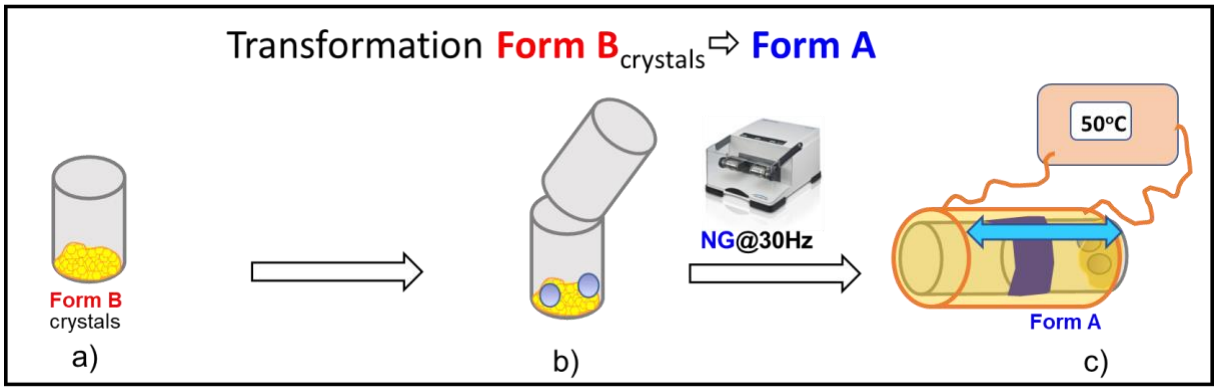

Scheme S 12; Schematic diagram of the **NG** procedure with heating mantle used heated up to 60ºC, to transform crystals of **Form B** to **Form A** as used for the experiment in Fig. S21. The heating mantle is discussed in Section 1.2.3. Step a) add crystals of **Form B** to jar. b) add 2x 7 mm ball bearings. Close jar and seal. c) install the heating jacket around the jar and connect it to the controller. Set the controller at 40ºC. Immediately, **NG** at 30 Hz with the objective to transform crystals of **Form B** to **Form A**. The increase the heating to 50ºC and finally to 60ºC.

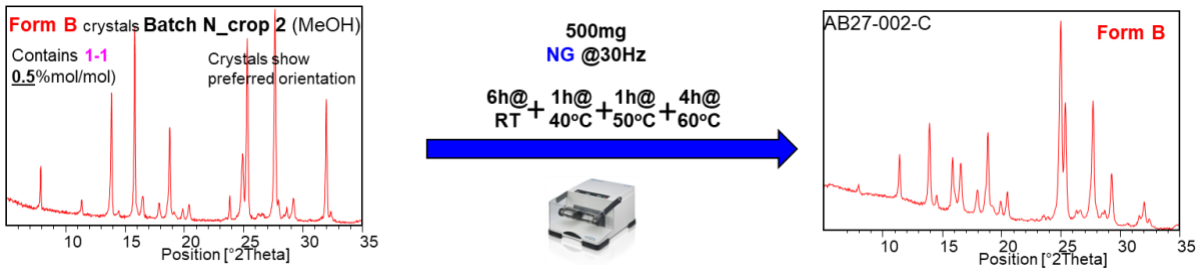

Figure S 21 Attempted transformation as in Scheme 12 of crystals of **Form B** to **Form A** by extensive ball mill **NG** with heated jars. Despite the long grinding at ambient and later at 40ºC, 50ºC and even 60ºC, no transformation occurred. PXRD scans of the crystals of **Form B** show preferred orientation. The % mol/mol of **1-1** has been determined by HPLC analysis; and is preserved through all manipulations and polymorph transformations. The experimental details of the **Form B** crystal Batch N crop 2 are listed on **Table S6.** See explanation for the failure of this attempted transformation in Section 6.3.3.

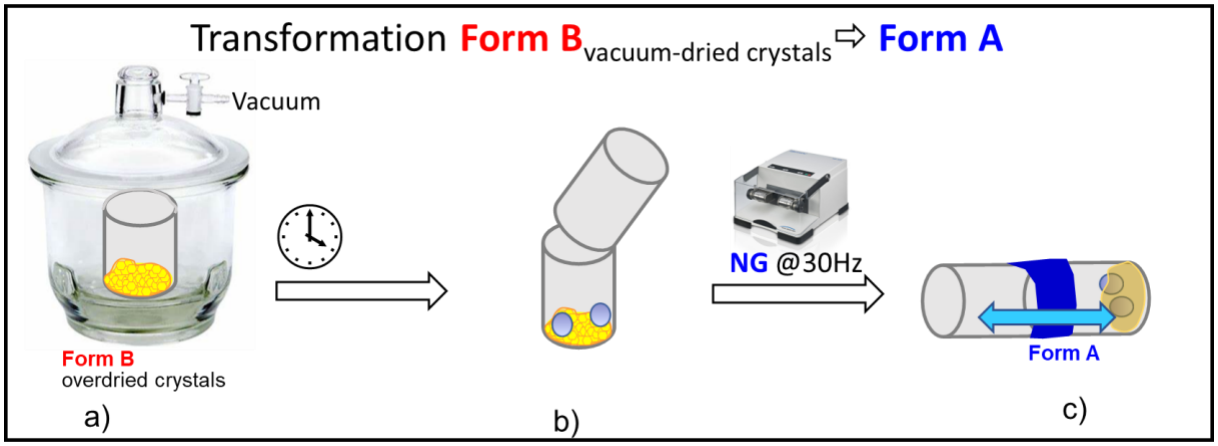

Scheme S 13: Schematic diagram of the procedure proposed to transform crystals of **Form B** to **Form A**. We hypothesise here that crystals of **Form B** subjected to extensive vacuum may be more reactive to undergo polymorph transformation to **Form A** on **NG**. Step a) dry crystals under vacuum to remove residual solvents from crystallisation procedure; b) add 2x 7mm ball bearings to jar, close and seal jar. c) **NG** at 30 Hz for long enough with the objective to transform crystals of **Form B** to **Form A**.

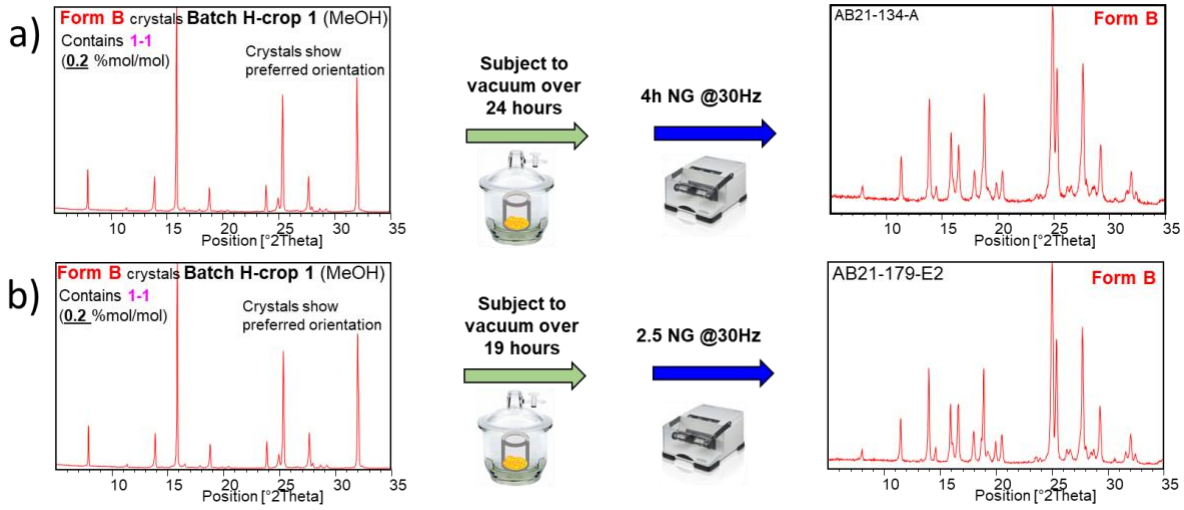

Figure S 22 Attempted transformation of crystals of **Form B** to **Form A** by 1st subjecting those crystals to severe vacuum followed by ball mill **NG**. No polymorph transformation took place. PXRD scans of the crystals of **Form B** show preferred orientation. The % mol/mol of **1-1** has been determined by HPLC analysis; and is preserved through all manipulations and polymorph transformations. The experimental details of the **Form B** crystals Batch H crop 1 are listed on **Table S6.** See explanation for the failure of these attempted transformations in Section 6.3.3.

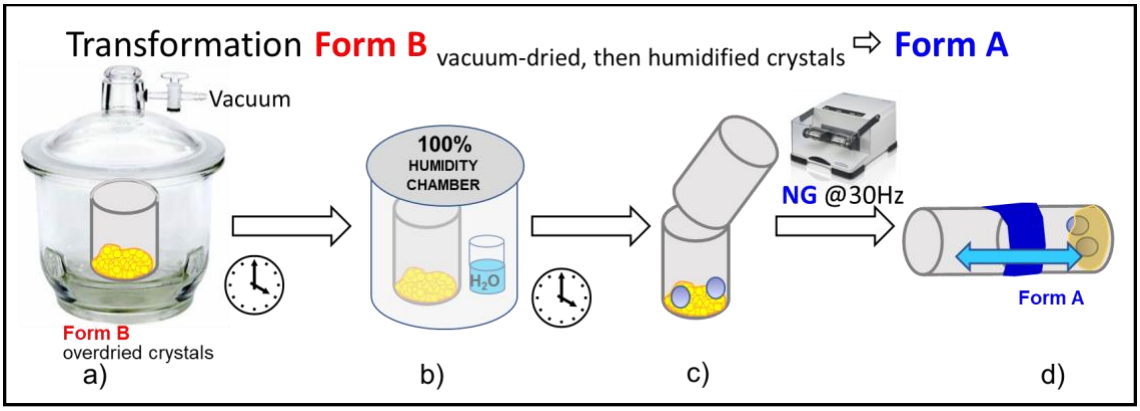

Scheme S 14 : Schematic diagram of the procedure proposed to transform crystals of **Form B** to **Form A**. a) the crystals of **Form B** are dried under vacuum. b) These crystals are subjected to 100% high humidity; c) add 2x 7mm ball bearings to jar, close and seal jar. d) **NG** at 30 Hz for long enough with the objective to transform crystals of **Form B** to **Form A**

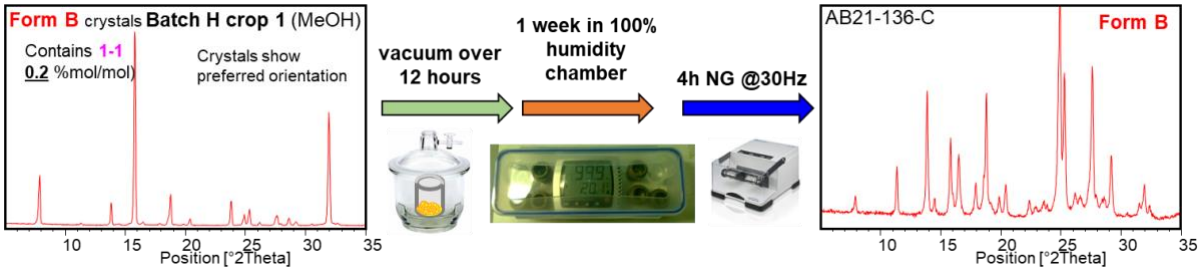

Figure S 23 Following procedure outline in Scheme S14, overdried crystals of **Form B** are subject to 100% high humidity before performing NG at 30 Hz with the objective to transform them to **Form A**. PXRD scans of the crystals of **Form B** show preferred orientation. The % mol/mol of **1-1** has been determined by HPLC analysis; and is preserved through all manipulations and polymorph transformations. The experimental details of the **Form B** crystals batch H crop 1 used are listed on **Table S6.** See explanation for the failure of this attempted transformation in Section 6.3.3.

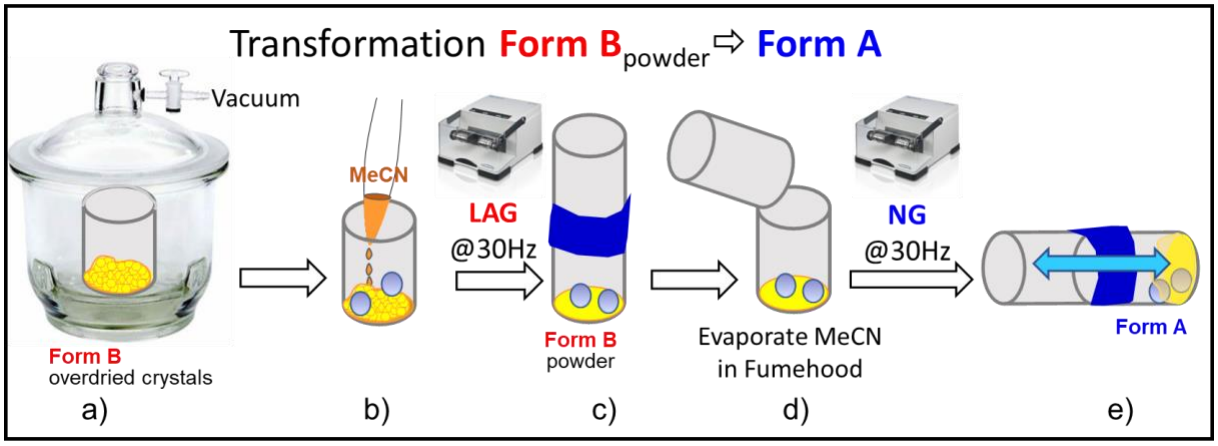

Scheme S 15 Schematic illustration of the steps proposed to transform crystals of **Form B** to **Form A**. The purpose here is to transform the crystals of **Form B** first to powder of **Form B**, before performing **NG**. Step a) dry crystals under vacuum to remove residual solvents from crystallization procedure; b) add 2x 7mm ball bearings to jar; and 50 μL acetonitrile to the over-dried crystals. Acetonitrile is rapidly absorbed by the crystals; c) close jar and grind the crystals into powder of **Form B**. d) Open the jar and allow MeCN to evaporate in the fumehood; Step e) close jar containing dried **Form B** powder and **NG** at 30 Hz for long enough with the objective to transform powder of **Form B** to **Form A**.

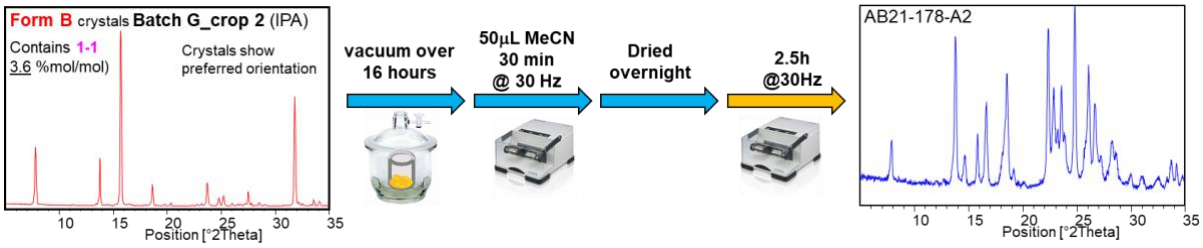

Figure S 24 The strategy of this attempted polymorph transformation is to first transform the crystals of Form B to powder by **LAG** with MeCN, in the hope that the dried powder of **Form B** with more surface area will be more likely to transform to **Form A** on **NG**. PXRD scans of the crystals of **Form B** show preferred orientation. The % mol/mol of **1-1** has been determined by HPLC analysis; and is preserved through all manipulations and polymorph transformations. The experimental details of the **Form B** crystals batch G crop 2 used are listed on **Table S6.** See explanation for the success of this attempted transformation in Section 6.3.3.

What next:

Appreciating that subjecting **Form B** crystals to high vacuum (Scheme S13 to S15) did not result in a significant improvement of the reactivity of **Form B** to polymorph transformation to **Form A**, we decided to subject **Form B** crystals directly to a high humidity environment before performing **NG**, so as to transform it to **Form A**.

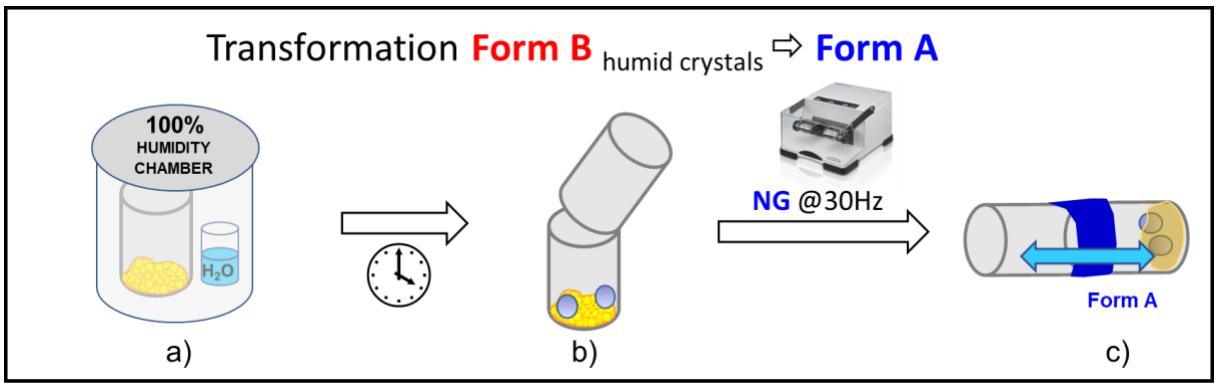

Scheme S 16 Schematic diagram of the steps recommended to transform crystals of **Form B** to **Form A**. In an attempt to make the surface of the crystals more reactive, the crystals are stored in a 100% RH chamber for days or weeks (Step a). b) add 2x 7mm ball bearings to jar with humid crystals of **Form B**. Close and seal jar. c) **NG** at 30 Hz for long enough with the objective to transform humid crystals of **Form B** to **Form A**.

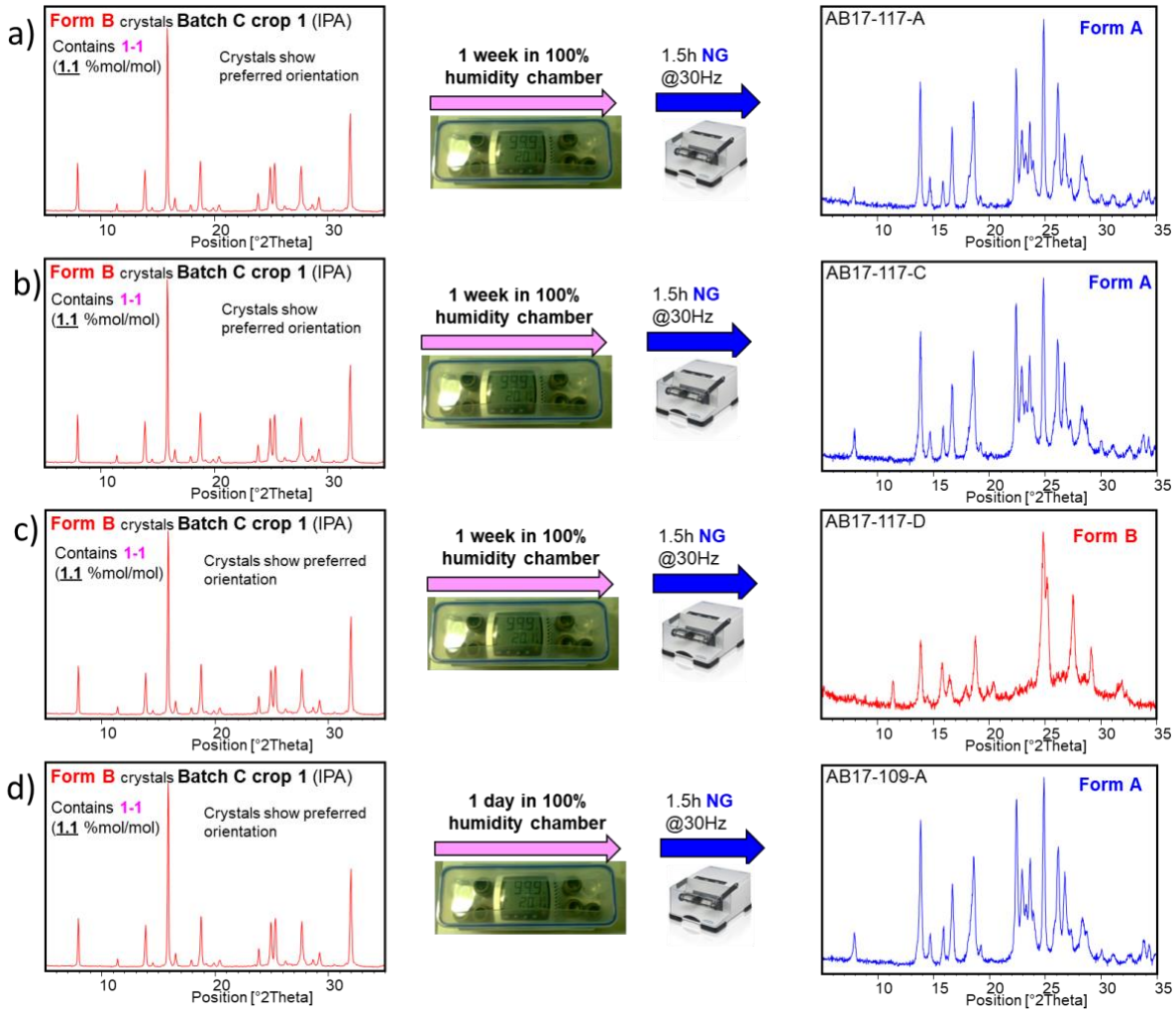

Continue on next page

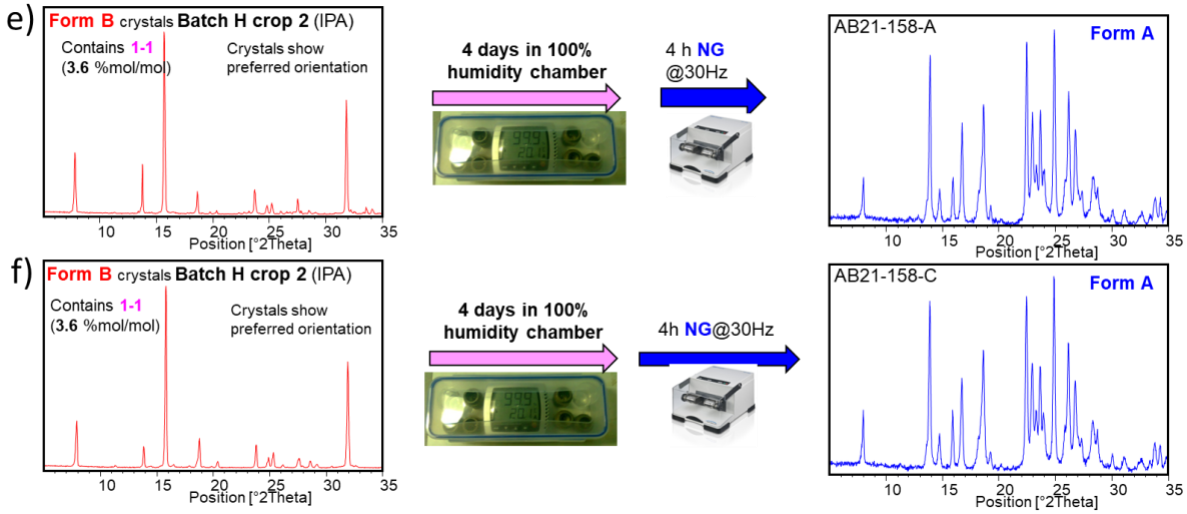

Figure S 25 Transformation of crystals of **Form B** on storage at 100% RH for a period of time to be followed by **NG** at 30Hz with the objective to obtain **Form A**. PXRD scans of the crystals of **Form B** show preferred orientation. The % mol/mol of **1-1** has been determined by HPLC analysis; and is preserved through all manipulations and polymorph transformations. The experimental details of the **Form B** crystal batches used are listed on Table S6**.** See explanation for the success and failures of these attempted transformations in Section 6.3.3.

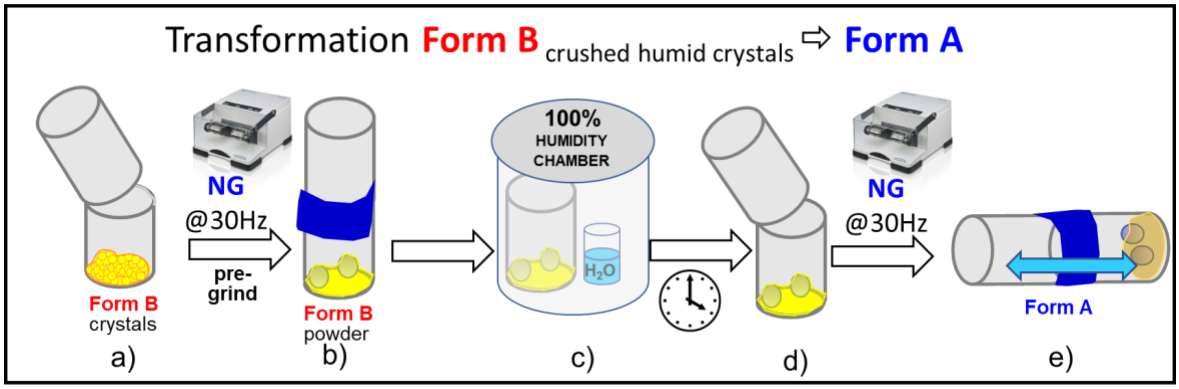

Scheme S 17 Schematic diagram of the steps recommended to transform crystals of **Form B** to **Form A**. Step b) pre-grind crystals of **Form B** to increase surface area. Step c) expose crushed crystals to high humidity (100% RH chamber) for days or weeks. Step e) **NG** for long enough with the objective to transform humid crushed crystals of **Form B** to **Form A**.

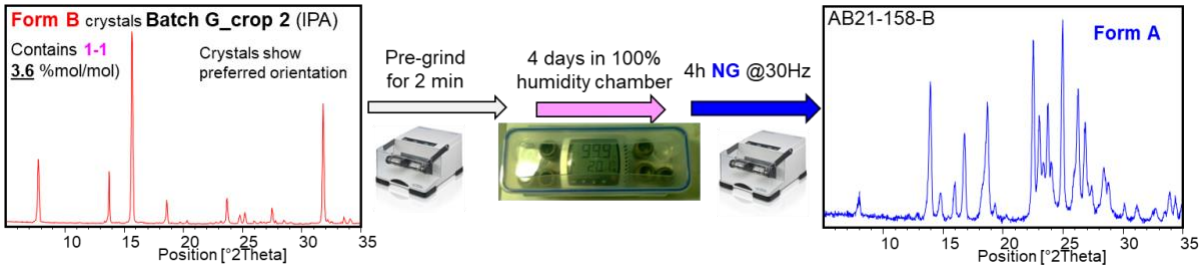

Figure S 26 Transformation of pre-crushed crystals of **Form B** to **Form A** on storage at 100% RH for a period of time to be followed by **NG** at 30Hz as depicted in Scheme S17. PXRD scans of the crystals of **Form B** show preferred orientation. The % mol/mol of **1-1** has been determined by HPLC analysis; and is preserved through all manipulations and polymorph transformations. The experimental details of the **Form B** crystals batches used are listed on Table S6. See explanation for the success of this attempted transformation in Section 6.3.3.

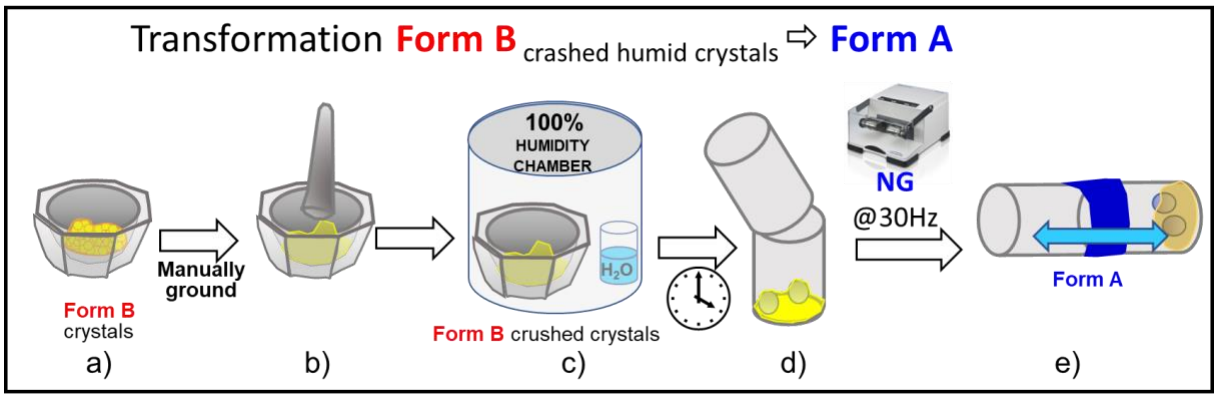

Scheme S 18 Schematic diagram of the steps recommended to transform crystals of **Form B** to **Form A**. Step b) crush crystals of **Form B** with a mortar and pestle; Step c) expose crushed crystals to high humidity (100% RH chamber) for days or weeks. Step e) **NG** for long enough with the objective to transform humid crushed crystals of **Form B** to **Form A**.

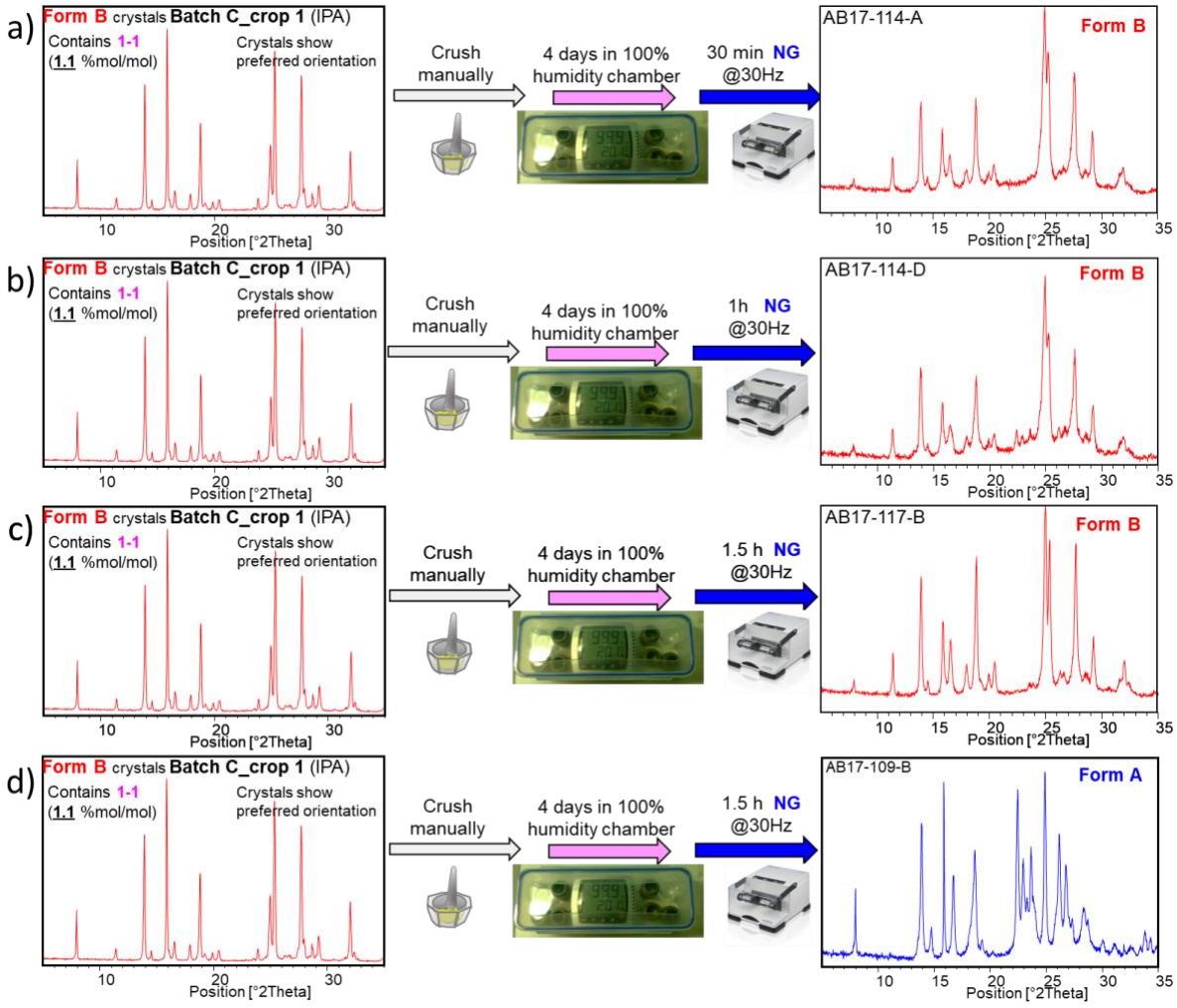

Continue on next page

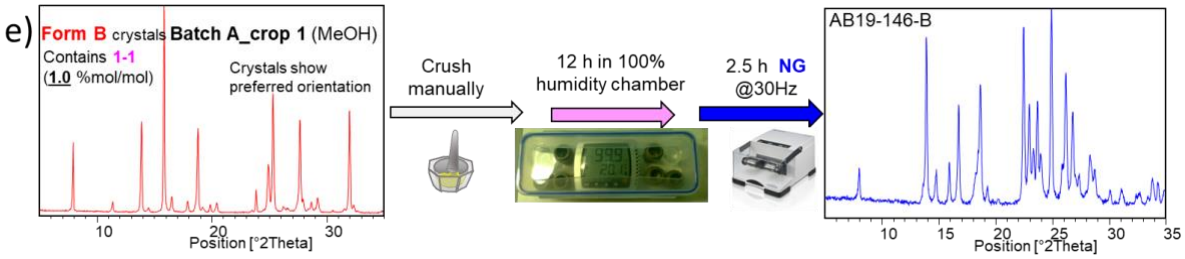

Figure S 27 Attempted transformation of manually crushed crystals of **Form B** subjected to 12-24 h of high humidity, followed by **NG** to transform them to **Form A** as schematically illustrated in Scheme S 18. PXRD scans of the crystals of **Form B** show preferred orientation. The % mol/mol of **1-1** has been determined by HPLC analysis; and is preserved through all manipulations and polymorph transformations. The experimental details of the **Form B** crystals batches used are listed on Table S6. See explanation for the success and failures of these attempted transformations in Section 6.3.3.

What next:

None of procedures tried in 6.3.1 succeeded in reproducibly and consistently transforming crystals of **Form B** to **Form A**. In previously published solid-state DCC experiments, we demonstrated that **LAG** with very few μL of MeCN, not sufficient to solvate **Form B**, can lead to the reproducible formation of **Form A**.[6]

6.3.2 Transformation of crystals of Form B to Form A by LAG with MeCN

This strategy (Scheme S19) only obtained partial success. Figure S24 shows that only1 in 8 experiments were transformed to **Form A**.

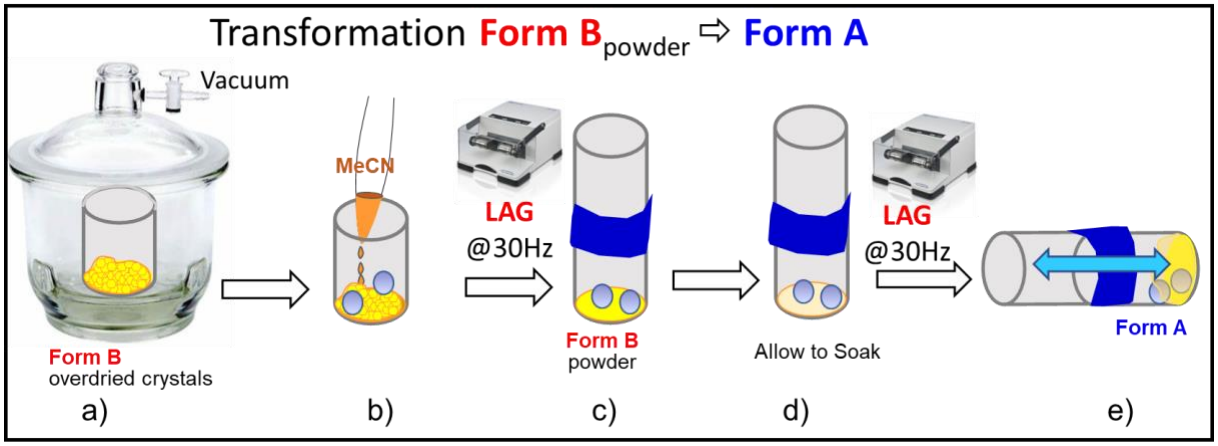

Scheme S 19: Schematic illustration of the steps proposed to transform crystals of **Form B** to **Form A by LAG**. We investigate here if it is more effective to add smaller than larger volumes of MeCN (e.g. < 10μL) to transform by **LAG, Form B** to **Form A**. Step a) dry crystals under vacuum to remove residual solvents from crystallization procedure; b) add 2x 7mm ball bearings to jar and <10 μL acetonitrile to crystals of **Form B**. Acetonitrile is rapidly absorbed by the crystals; c) close jar and grind the crystals (< 30 min at 30 Hz) into powder of **Form B**. Step d) allow MeCN to soak further overnight into the crashed crystals of **Form B**. Step e) **LAG** for long enough with the objective to transform powder of **Form B** to **Form A**.

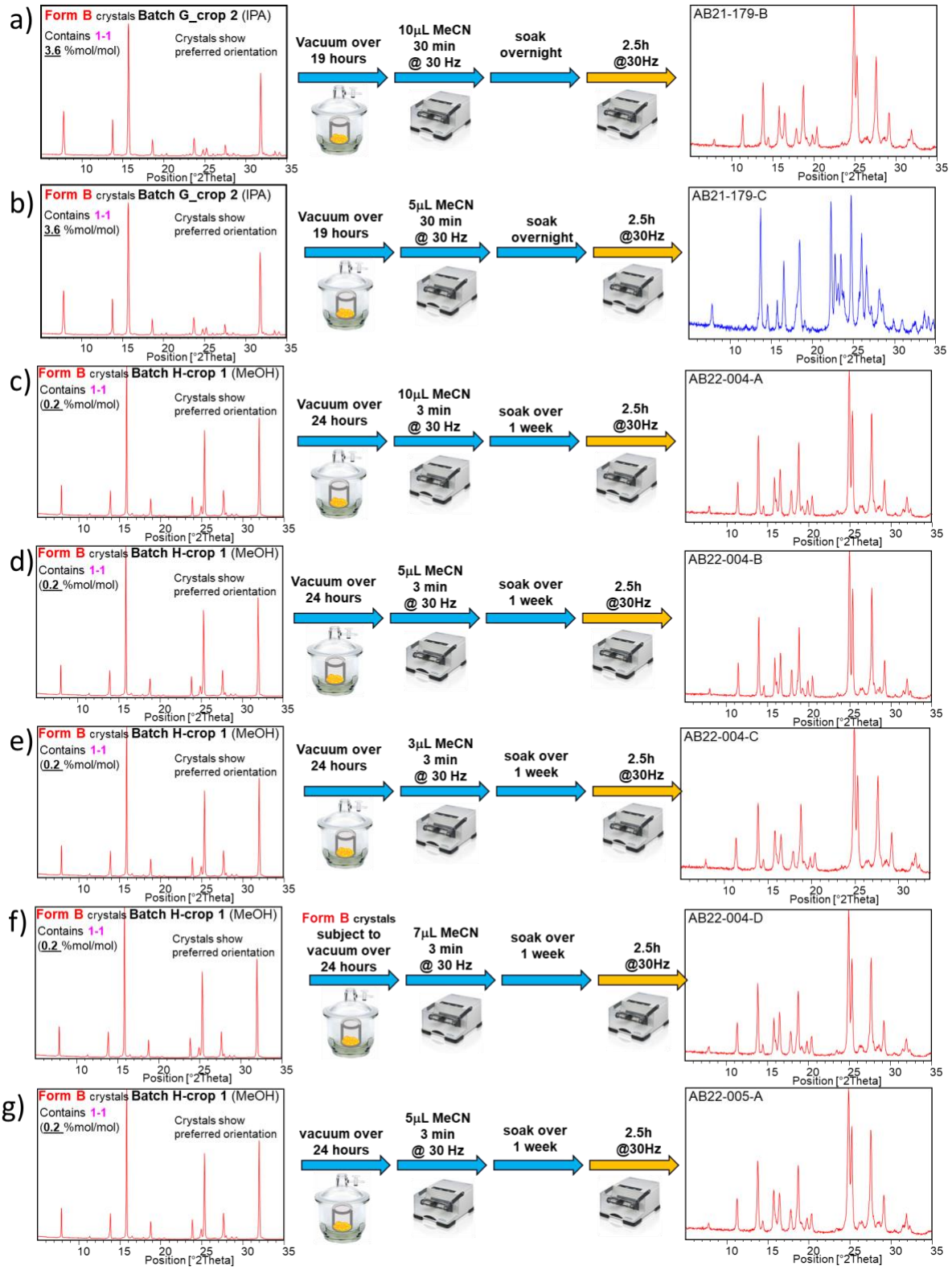

Continue on next page

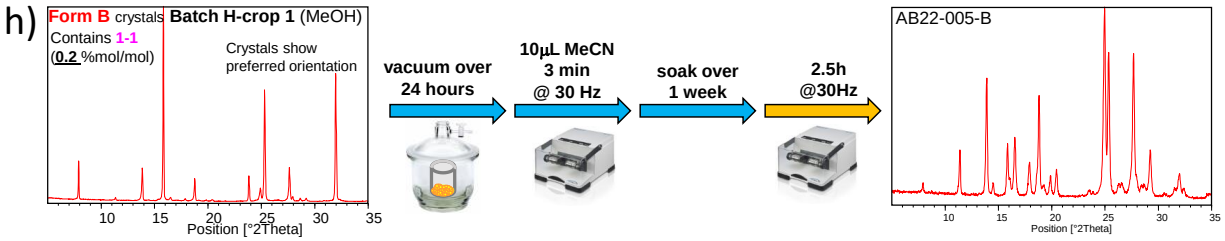

Figure S 28 Polymorphic transformation of vacuum dried crystals of **Form B** allowed to soak in ≤ 10 µL MeCN before performing **LAG** at 30 Hz with the objective to obtain **Form A.** PXRD scans of the crystals of **Form B** show preferred orientation. The % mol/mol of **1-1** has been determined by HPLC analysis; and is preserved through all manipulations and polymorph transformations. The experimental details of the **Form B** crystals batches used are listed on Table S6. See explanation for the success and failure of these attempted transformations in Section 6.3.3.

6.3.3 Unexpected trend

By carefully looking at the levels of **1-1** in all the experiments run in Section 6.3, we appreciate that many of those experiments where **Form B** crystals did not transform to **Form A**, happen to contain < 0.9% mol/mol of **1-1** as in:

Figure S.19. e) Batch H crop 1 with 0.2%, f) Batch N crop 2 with 0.5%

Figure S.20. f) & g) Batch F crop 1 with 0.7 %,

Figure S.21 Batch N crop 2 with 0.5 %

Figure S.22 a) & b) Batch H crop 1 with 0.2 %,

Figure S.23 Batch H crop 1 with 0.2%

Figure S.24 e) to h) Batch H crop 1 with 0.2%.

For these cases, the experimental conditions could not affect the outcome, as without enough **1-1**, the polymorphic transformation of **Form B** to **Form A** was not enabled.

Similarly, the successful transformation from **Form B** to **Form A** happen to contain > 0.9% mol/mol of **1-1** as in:

Figure S.19. a) & b) Batch G crop 2 with 3.6%; c) & d) Batch A crop 1 with 1.0%;

Figure S.20. a) to e) Batch G crop 1 with 1.3%

Figure S.24. Batch G crop 2 with 3.6%

Figure S.25. a), b), d) Batch C crop 1 with 1.1%; e)& f) Batch H crop 2 with 3.6%.

Figure S.26. Batch G crop 2 with 3.6%

Figure S.27 d) Batch C crop 1 with 1.1%; e) Batch A crop 1 with 1.0%

Figure S.24 b) Batch G crop 2 with 3.6%

There are a few experiments, where the content of **1-1** is ≥ 0.9%, but no transformation took place. A plausible explanation is that the grinding conditions were not met as in:

Figure S.25 c) Batch C crop 1 with 1.1%; the explanation here is not obvious, as a) b) & d) are prepared also with Batch C crop 1 with 1.1%, with 1.5 h **NG** at 30 Hz are successfully transformed to **Form A** while c) is not under the same grinding conditions. Maybe, the surface of the crystals of **Form B** in c) are not as humid as in as a) b) & d.

Figure S.27 a); b) & c) Batch C crop 1 with 1.1%; the explanation may be that 0.5h, 1h & 1.5 h, i.e. < 2.5h NG grinding at 30 Hz is not sufficient to transform to **Form A**, as it successfully happens with e). The explanation why d) does not while c) does transform, could be that 1.5 h NG is at the threshold of transforming.

Figure S.28 a) Batch G crop 2 with 3.6%. Could be explained by the addition of 10 μL MeCN may have been sufficient to solvate the surface of the crystals and therefore make **Form B** more stable than **Form A**.

6.4 Transformation of crystals of Form B to Form C

6.4.1 Transformation of premilled Form B crystals subject to LAG with water to Form C (elaborate procedure)

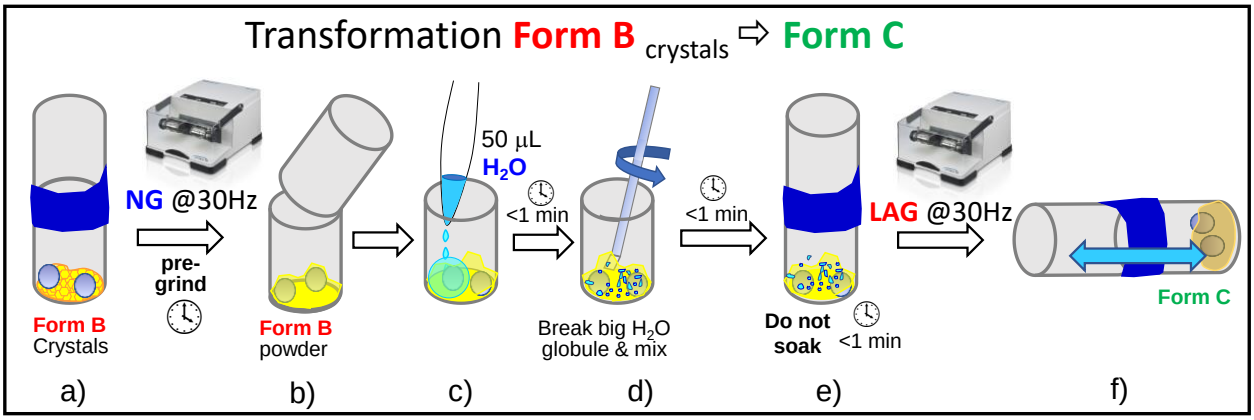

Scheme S 20 Step a) add 2x 7mm ball bearings to jar containing crystals of **Form B**, close and seal jar; b) Pre-NG **Form B** crystals for a few minutes at 30 Hz to increase surface area; c) Add 50 μL water to the powder; a large globule of water will form; typically engulfing a ball; d) break water into droplets with a micro-spatula; do not take long; e) close and seal jar; do not allow water to soaks into powder; f) **LAG** at 30 Hz with the objective to transform powder of **Form B** to **Form C**.

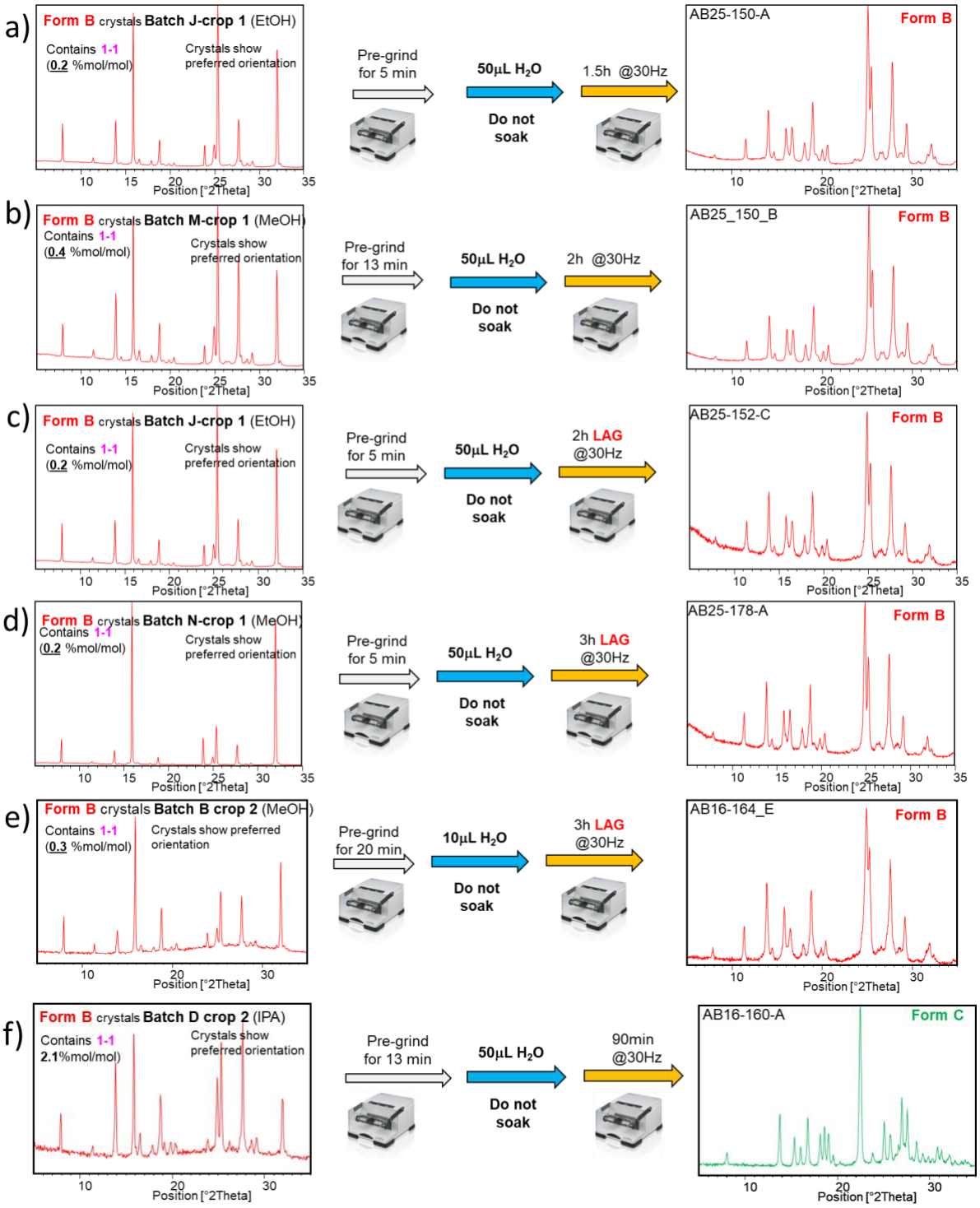

Continue on next page

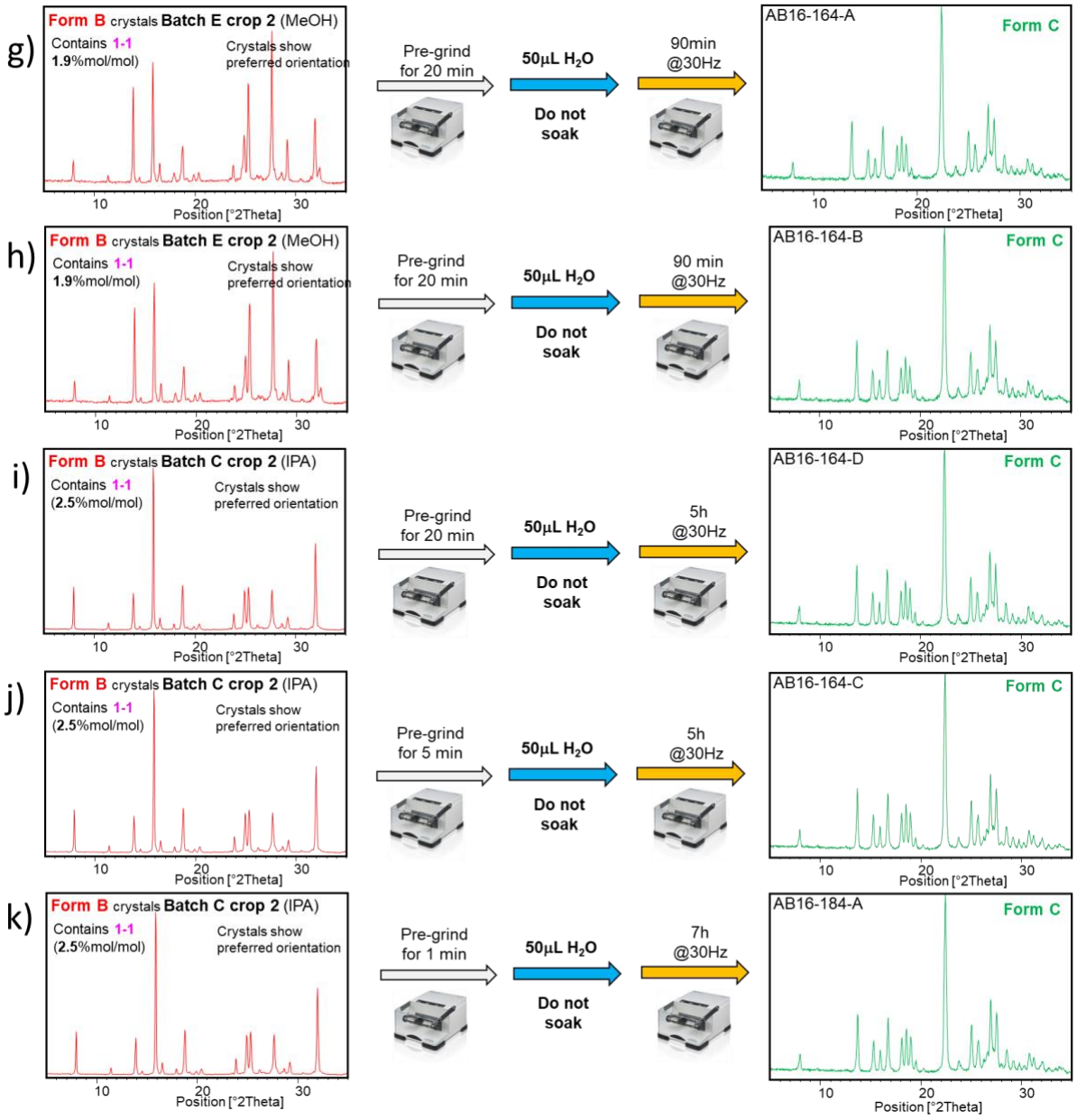

Figure S 29 Attempted transformation of pre-ground crystals of **Form B** to **Form C,** on addition of 50 µL water and **LAG** at 30Hz as in Scheme S20. PXRD scans of the crystals of **Form B** show preferred orientation. The % mol/mol of **1-1** has been determined by HPLC analysis; and is preserved through all manipulations and polymorph transformations. The experimental details of the **Form B** crystal batches used are listed on Table S6. See explanation for the success and failures of these attempted transformations in Section 6.4.2.

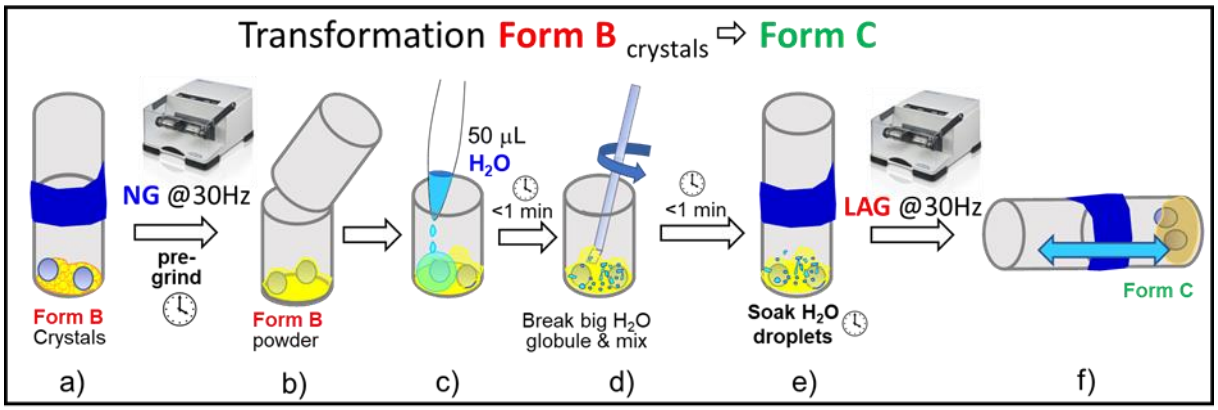

Scheme S 21 . Step a) add 2x 7mm ball bearings to jar containing crystals of **Form B**, close and seal jar; b) Pre- NG **Form B** crystals for a few minutes at 30 Hz to increase surface area; c) Add 50 µL water to the powder; a large globule of water will form; typically engulfing a ball; d) break water into droplets with a micro-spatula; do not take long; e) close and seal jar; allow water to soaks into powder for < 15 min; f) LAG at 30 Hz with the objective to transform powder of **Form B** to **Form C**.

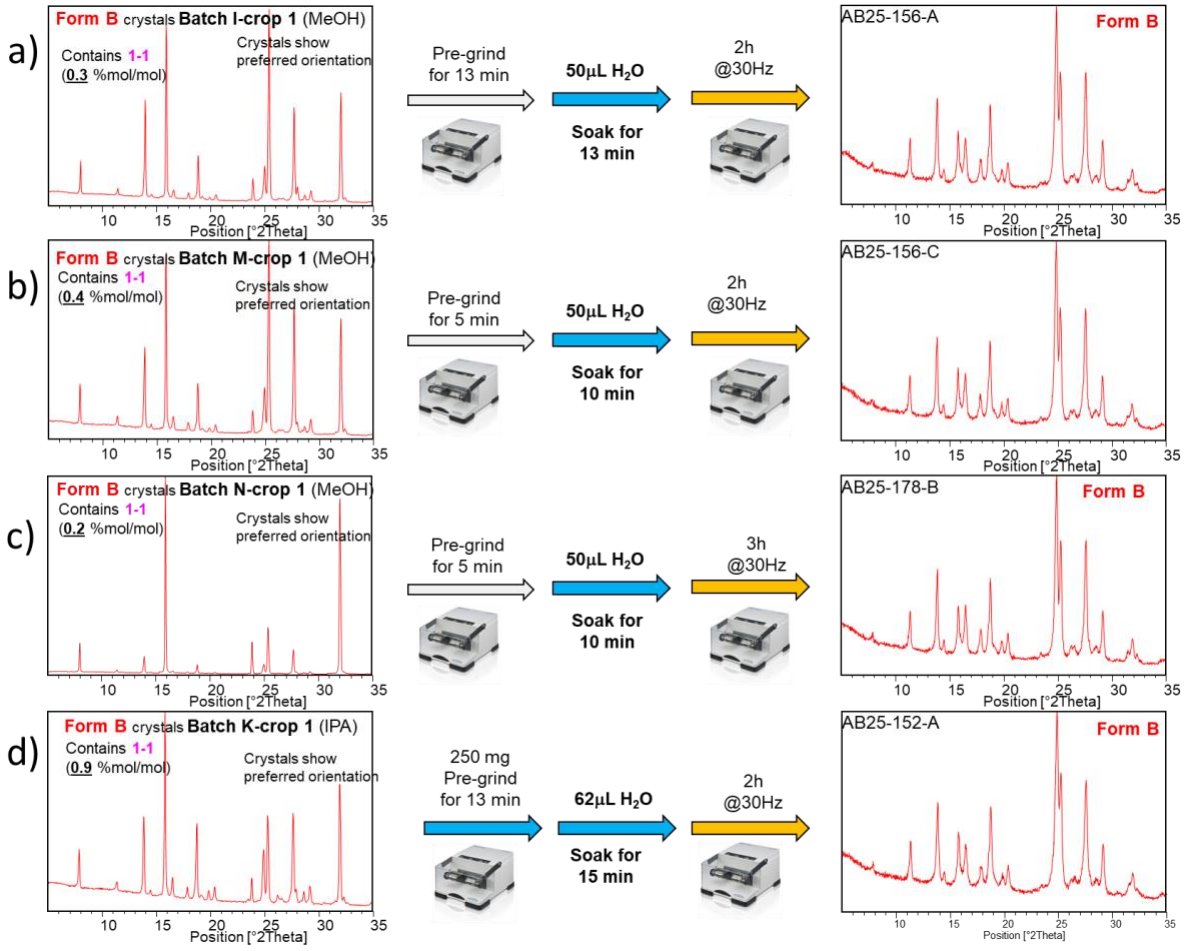

Continue on next page

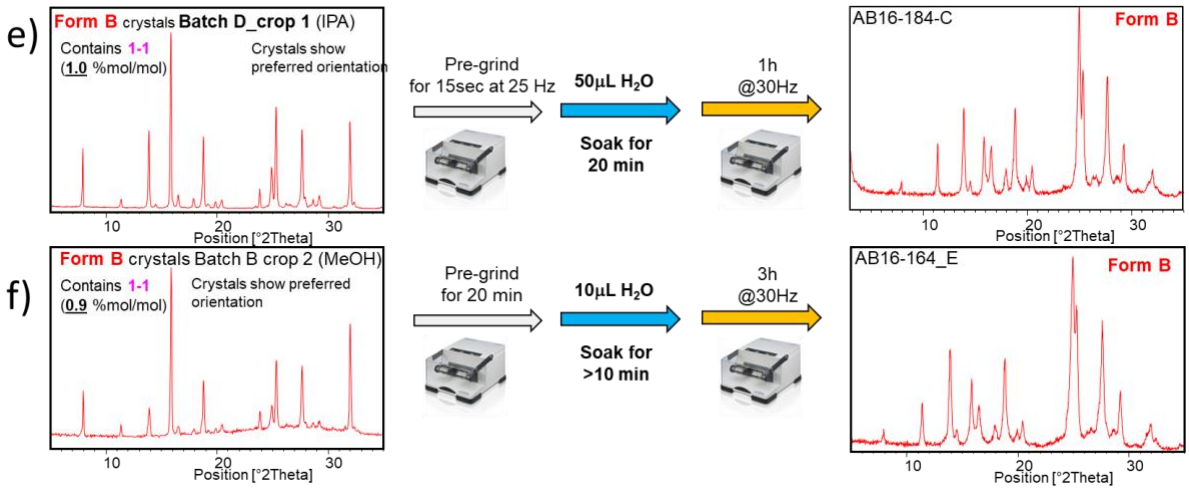

Figure S 30 Attempted transformation of pre-ground crystals of **Form B** to **Form C,** on addition of 10 to 62 µL water and **LAG** at 30Hz, allowing the water to soak over 10 minutes. PXRD scans of the crystals of **Form B** show preferred orientation. The % mol/mol of **1-1** has been determined by HPLC analysis; and is preserved through all manipulations and polymorph transformations. The experimental details of the **Form B** crystal batches used are listed on Table S6. See explanation for the failures of these attempted transformations in Section 6.4.2.

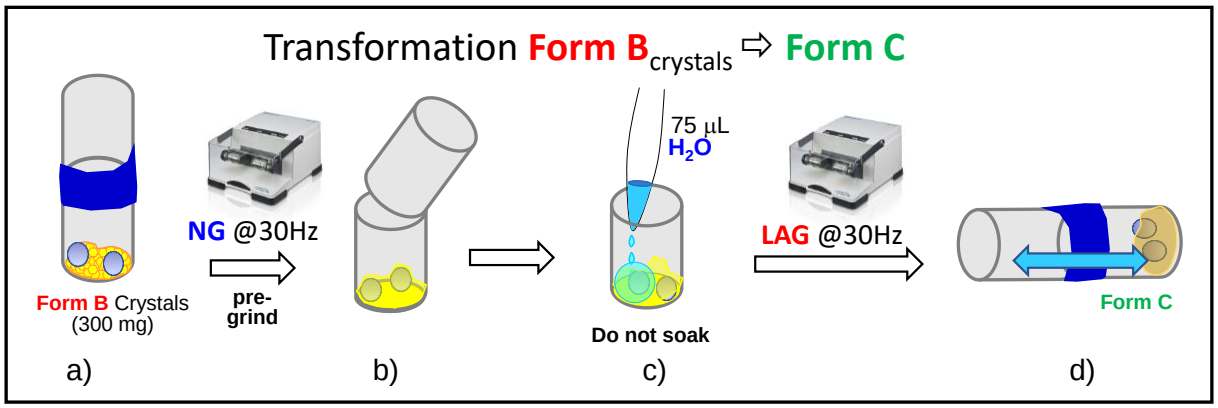

Scheme S 22 Step a) add 2x 7mm ball bearings to jar containing crystals of **Form B**, close and seal jar; b) Pre-NG **Form B** crystals for a few minutes at 30 Hz to increase surface area; c) Add 50 µL water to the powder; a large globule of water will form, typically engulfing a ball; do not allow the liquid to soak into the powder. d) close and seal jar; immediately LAG at 30 Hz with the objective to transform powder of **Form B** to **Form C**.

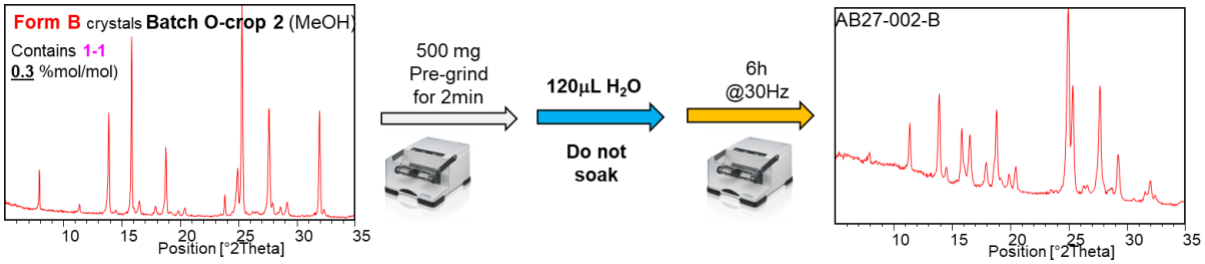

Figure S 31 Attempted transformation of pre-ground crystals of **Form B** to **Form C,** on addition of 120 µL water and **LAG** at 30Hz, avoiding water from soaking.. PXRD scans of the crystals of **Form B** show preferred orientation. The % mol/mol of **1-1** has been determined by HPLC analysis; and is preserved through all manipulations and polymorph transformations. The experimental details of the **Form B** crystal batches used are listed on Table S6. See explanation for the failure of this attempted transformation in Section 6.4.2.

6.4.2 Unexpected trend

By carefully looking at the levels of **1-1** in all the experiments run in Section 6.4, we appreciate that those experiments where **Form B** crystals did not transform to **Form C**, happen to contain < 1.5% mol/mol of **1-1** as in:

Figure S29	a) & c) Batch J crop 1 with 0.2%; b) Batch M crop 1 with 0.4%; d) Batch N crop 1 with 0.2%; e) Batch B crop 2 with 0.3%;
Figure S30	a) Batch I crop 1 with 0.3%; b) Batch M crop 1 with 0.4%; c) Batch N crop 1 with 0.2%; d) Batch K crop 1 with 0.9%; e) Batch D crop 1 with 1.0%; f) Batch B crop 2 with 0.9%
Figure S31	a) Batch O crop 2 with 0.3%;

Similarly, the successful transformation from **Form B** to **Form C** happen to contain > 1.5% mol/mol of **1-1** as in:

Figure S25	g) Batch D crop 2 with 2.1%; h) & i) Batch E crop 2 with 1.9%; j) & k) Batch C crop 2 with 2.5%

6.5 Reversible polymorph transformation: Form A to Form C and vice versa

As **Form A** samples can only be prepared by polymorph transformation from crystal from **Form B**, if they contain **1-1** at a level of > 0.9% mol/mol, all available sample of **Form A** must contain **1-1** at a level of > 0.9% mol/mol.

Similarly, sample of **Form C** obtained from crystals of **Form B**; they must contain **1-1** at a level of > 1.5% mol/mol.

6.5.1 Polymorph transformation: Form A to Form C

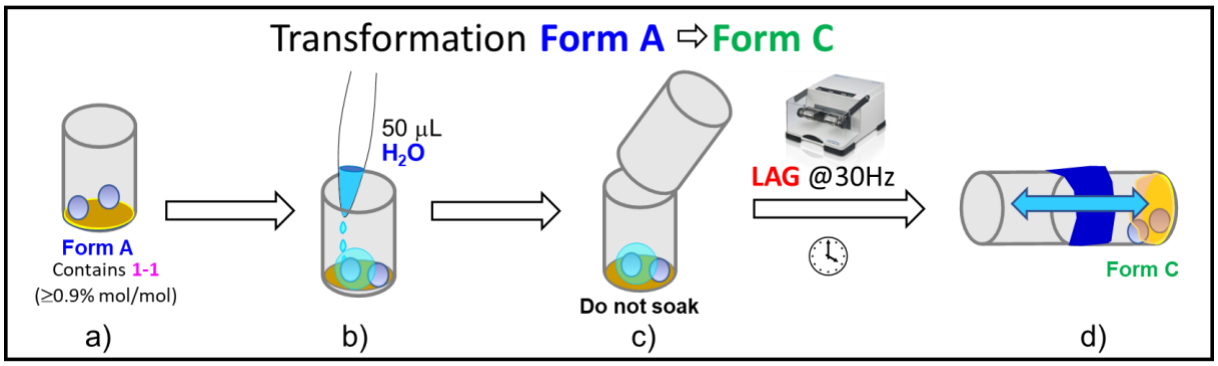

Scheme S 23 Step a) add 2x 7mm ball bearings to jar containing powder of **Form A** including **1-1** at levels > 0.9% mol/mol. Close and seal jar; b) Add 50 µL water to the powder; a large globule of water will form, typically engulfing a ball; c) do not allow the liquid to soak into the powder. Close and seal jar; d) immediately LAG at 30 Hz with the objective to transform powder of **Form A** to **Form C**.

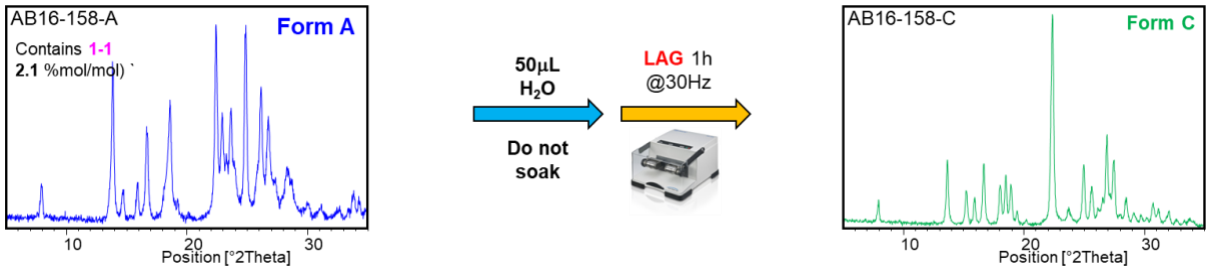

Figure S 32 Transformation of **Form A** to **Form C** by 1h **LAG** at 30 Hz with water, this should not be allowed to soak into the powder. Procedure depicted in Scheme S23 is used. This scheme is very similar to Scheme S8 used for the anticlockwise polymorph transformation turnover experiments. As far as we know, **Form A** has to contain > 0.9% mol/mol of **1-1** for this polymorph transformation to be enabled.

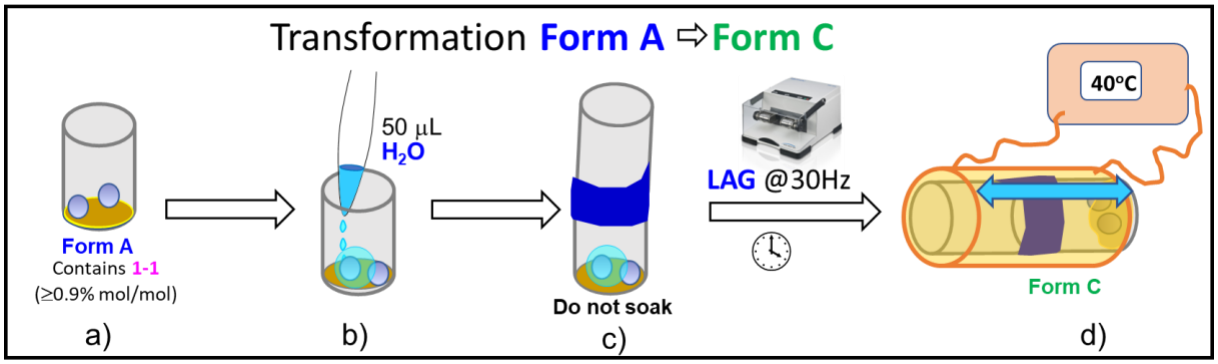

Scheme S 24 Step a) add 2x 7mm ball bearings to jar containing powder of **Form A** including **1-1** at levels > 0.9% mol/mol. Close and seal jar; b) Add 50 µL water to the powder; a large globule of water will form, typically engulfing a ball; c) do not allow the liquid to soak into the powder. Close and seal jar; d) install the heating jacket around the jar and connect to the controller. Set the controller at 40ºC. Immediately LAG at 30 Hz with the objective to transform powder of **Form A** to **Form C**.

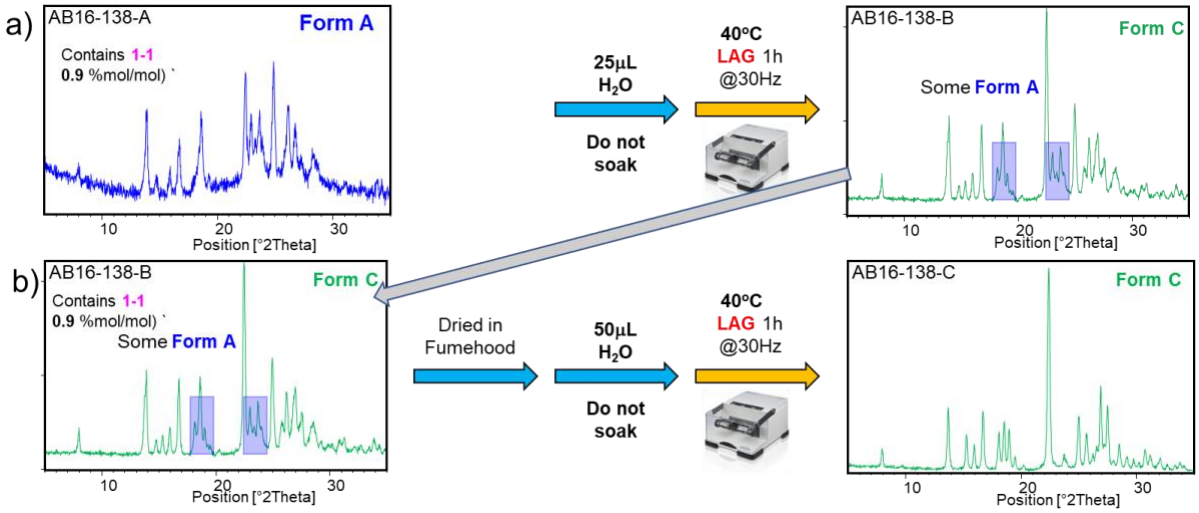

Figure S 33 Transformation of **Form A** to **Form C** by 2 sets a) and b) of 1h LAG at 30 Hz with water, the jar being heated at 40ºC while grinding as illustrated in Scheme S 24. Water should not be allowed to soak into the powder. What is interesting here is that **Form A** has **1-1** only at 0.9% mol/mol. This experiment demonstrated that the transformation from **Form A** to **Form C** is not as demanding as that from **Form B** to **Form C**, which requires a level of **1-1** ≥ 1.5% mol/mol. The jars may need to be heated, as here, to enable this polymorph transformation with such a low level of **1-1**.

6.5.2 Polymorph transformation: Form C to Form A

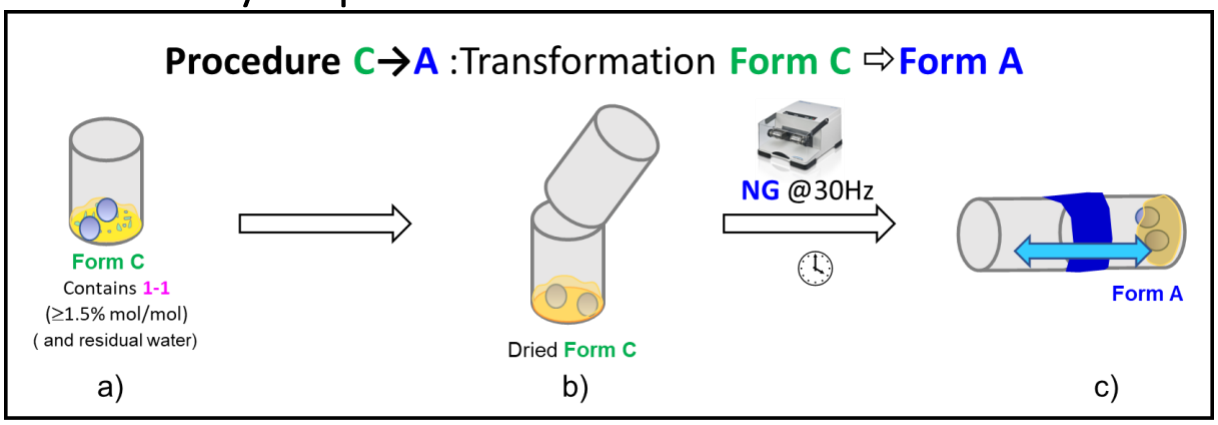

Scheme S 25 Step a) Make sure that the residual water used to prepare **Form C** has been allowed to evaporate in the fumehood. **Form C** typically includes **1-1** at levels > 1.5% mol/mol, unless it has been prepared from Form A, (See Figure S33). Add 2x 7mm ball bearings to jar; b) Close and seal jar; d) **NG** at 30 Hz with the objective to transform powder of **Form C** to **Form A**.

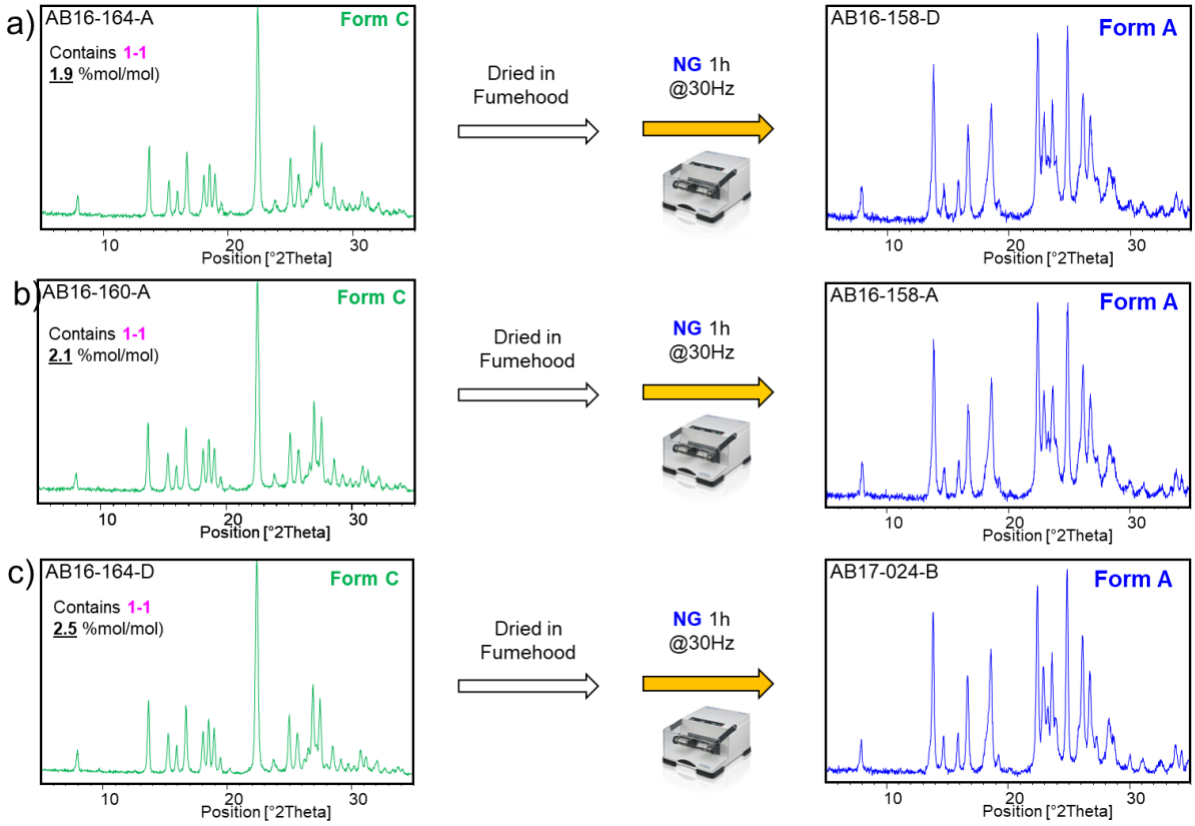

Figure S 34. Polymorph transformation from **From C** to **Form A** by 1h NG at 30 Hz following procedure depicted in Scheme S25, which is very similar to Scheme S3 used for the clockwise polymorph transformation turnover experiments. These polymorph transformation are successful as all 3 batches of **Form B** contain **1-1** at levels above > 1.5% mol/mol.

6.5.3 Conclusions

Form C can easily be transformed from **Form A** containing >1.5% mol/mol of **1-1** using protocol described in Scheme S8. It is also feasible to obtained **Form C** from **Form A** containing just 0.9 % mol/mol of **1-1**, if **NG** is performed at 40°C. It may also work at ambient temperature.

Form A can be easily obtained from **Form C** containing >1.5% mol/mol of **1-1** using protocol described in Scheme S3. We do not have data if this transformation is feasible with lower levels of **1-1**.

6.6 Reversible polymorph transformation: Form B powder to Form C powder and vice versa

6.6.1 Polymorph transformation: Form B powder to Form C

Here, we can start from **Form B** obtained either from failed polymorph transformations to **Form A** or to **Form C**, or from the reversible transformation of **Form C** or **Form A**. The history of the formation of **Form B** powder will not be considered here, but maybe relevant to the grinding time required for the polymorph transformation.

All **Form C** used in these experiments could have been obtained from direct transformation of crystals of **Form B**, therefore it will contain **1-1** at >1.5% mol/mol. However, if **Form C** was obtained from the transformation from **Form A** as is the case of Figure S33 it may contain **1-1** just >0.9% mol/mol.

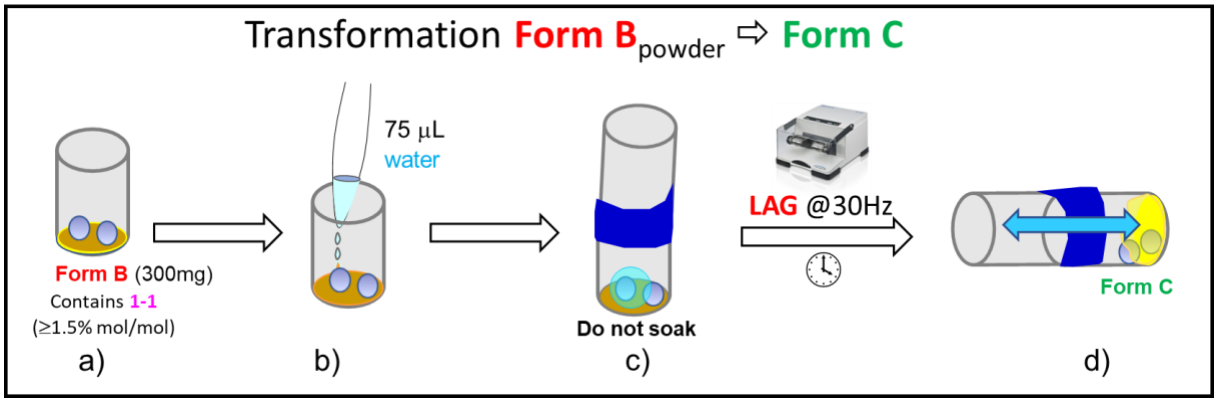

Scheme S 26 Step a) make sure that **Form B** powder does not contain residual MeCN**.** Only use **Form B** powder that contains **1-1** at levels > 1.5% mol/mol. Add 2x 7mm ball bearings to jar; b) Add 75 µL water to 300 mg powder; a large globule of water will form, typically engulfing a ball. Close and seal jar; d) Immediately, LAG at 30 Hz with the objective to transform powder of **Form B** to **Form C.**

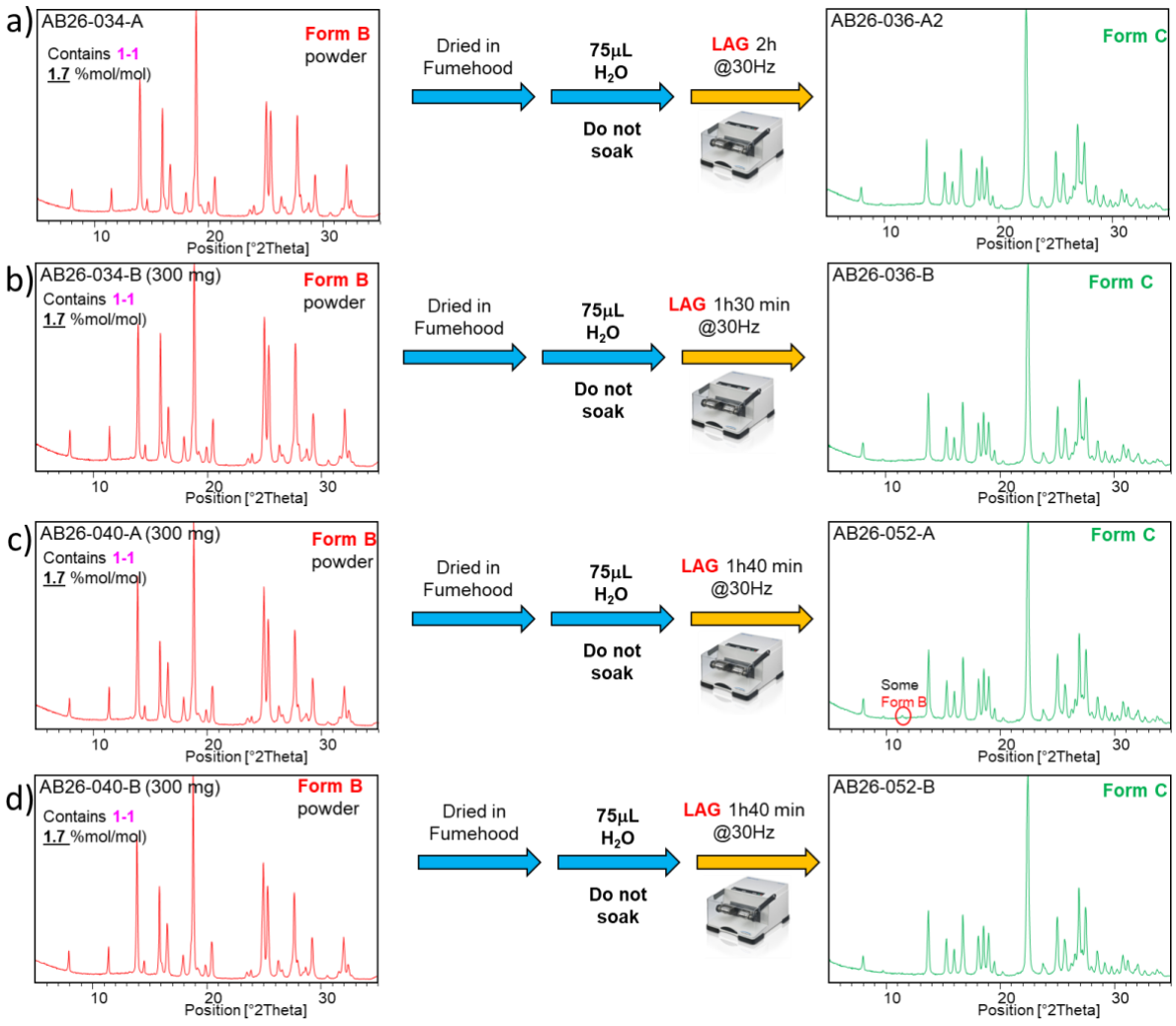

Figure S 35 Polymorph transformation of powder of **Form B** to **Form C** using procedure depicted in Scheme 26 , which is very similar to Scheme S2 used for the clockwise polymorph transformation turnover experiments.All samples of **Form B** contain **1-1** at levels above > 1.5% mol/mol, supporting that 90 min **LAG** at 30 Hz should suffice to achieve a reproducible and quantitative transformation. This may depend on the grinding history of **Form B** powder.

6.6.2 Polymorph transformation: Form C to Form B

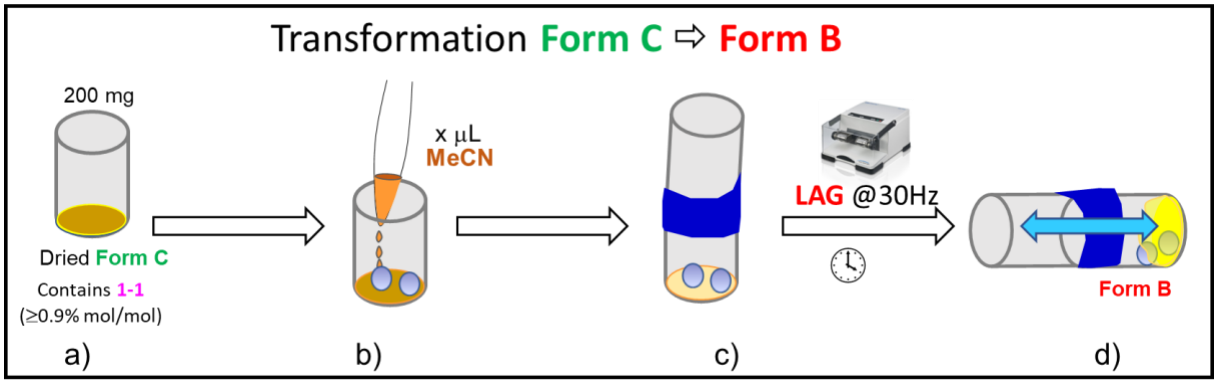

Scheme S 27 Step a) Make sure that **Form C** powder does not contain residual water**. Form C** powder typically contains **1-1** at levels > 1.5% mol/mol, however the levels of **1-1** can be as low as 0.9%w/w if **Form C** was formed from **Form A** using procedure depicted in Scheme S24. b) Add 2x 7mm ball bearings to jar; Add 50 µL MeCN, which quickly soaks into the powder; c) Close and seal jar; d) Immediately**, LAG** at 30 Hz with the objective to transform powder of **Form C** to **Form B.**

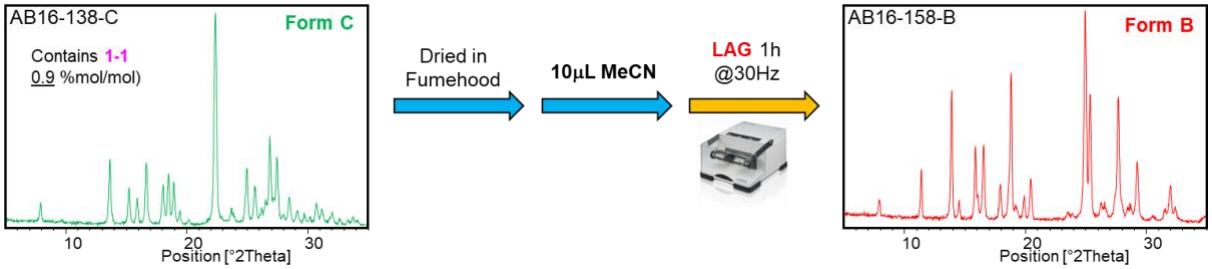

Figure S 36 Polymorph transformation of **Form C** to **Form B** using procedure depicted in Scheme S27, which is very similar to Scheme S9 used for the anti-clockwise polymorph transformation turnover experiments, but here using only 10 µL MeCN. This volumen of MeCN appears to suffice for the polymorph transformation. What is interesting here is that **Form C** contains **1-1** at 0.9% mol/mol, very low to be originally formed from **Form B**, but not impossible if it was formed from **Form A** as in Figure S33. It is clear that the polymorph transformation of **Form C** to **Form B** by **LAG** with MeCN, does not required either high levels of **1-1**, large volume or MeCN (just 10 µL) or long grinding time (just 1h).

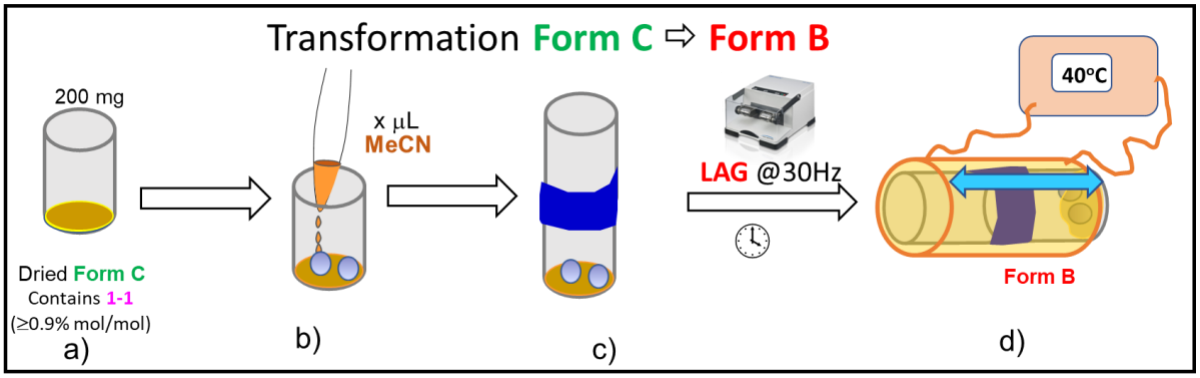

Scheme S 28 Step a) Make sure that **Form C** powder does not contain residual water**. Form C** powder typically contains **1-1** at levels > 1.5% mol/mol. b) Add 2x 7mm ball bearings to jar; Add 20 µL MeCN, which quickly soaks into the powder; c) Close and seal jar; d) install the heating jacket around the jar and connect to the controller. Set the controller at 40ºC. Immediately **LAG** at 30 Hz with the objective to transform powder of **Form C** to **Form B**.

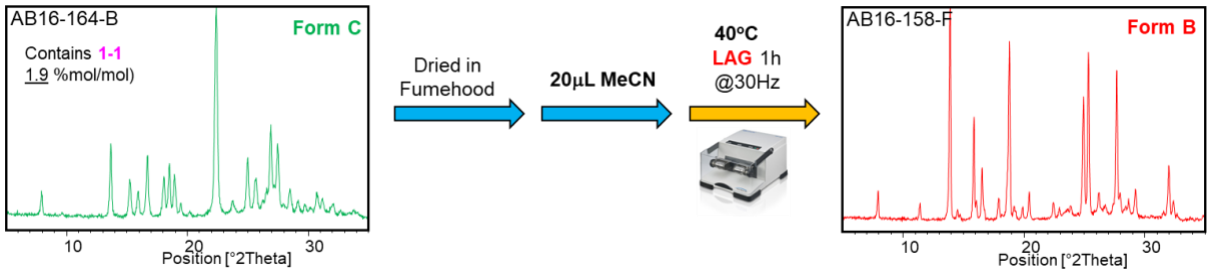

Figure S 37 Polymorph transformation of **Form C** to **Form B** using procedure depicted in Scheme S28, similar to Scheme S27 but the jar is heated to 40ºC while grinding. The polymorph transformation is not a challenge, as it has 1.9% mol/mol of **1-1**. 20µL of MeCN was added which is a higher volume of MeCN than needed as learned from Figure S36 and milled for 1h at 30 Hz. Probably 30 min or less would have sufficed.

6.6.3 Conclusions

Form C can be reproducible be transformed from **Form B as far as it contains** >1.5% mol/mol of **1-1** using protocol described in Scheme S5. This transformation requires the highest content of **1-1** from all the other polymorph transformation investigated.

Form B can be easily obtained from **Form C** with just 10 µL MeCN, using protocol described in Scheme S9. We suspect that this transformation does not require a high level of **1-1** as 0.9% mol/mol of **1-1** resulted in a transformation. Maybe this transformation could take place with even < 0.9% mol/mol of **1-1** , but we have no data to support this hypothesis.

6.7 Reversible polymorph transformation: Form B powder to Form A and viceversa

6.7.1 Polymorph transformation: Form B powder to Form A

6.7.1.1 Transformation of Form B powder to Form A: by NG

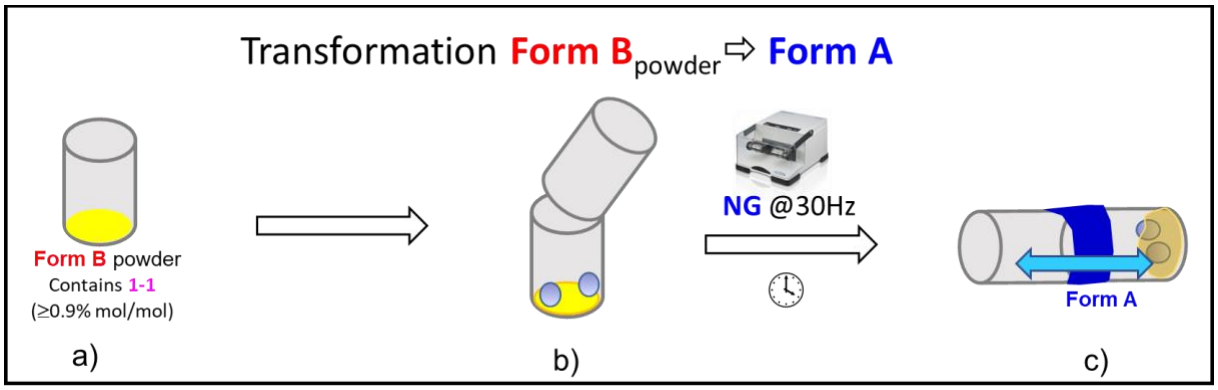

Scheme S 29 Step a) Make sure that **Form B** powder does not contain residual MeCN**.** Only use **Form B** powder that contains **1-1** at levels > 0.9% mol/mol. b) Add 2x 7mm ball bearings to jar Close and seal jar; c) NG at 30 Hz with the objective to transform powder of **Form B** to **Form A.**

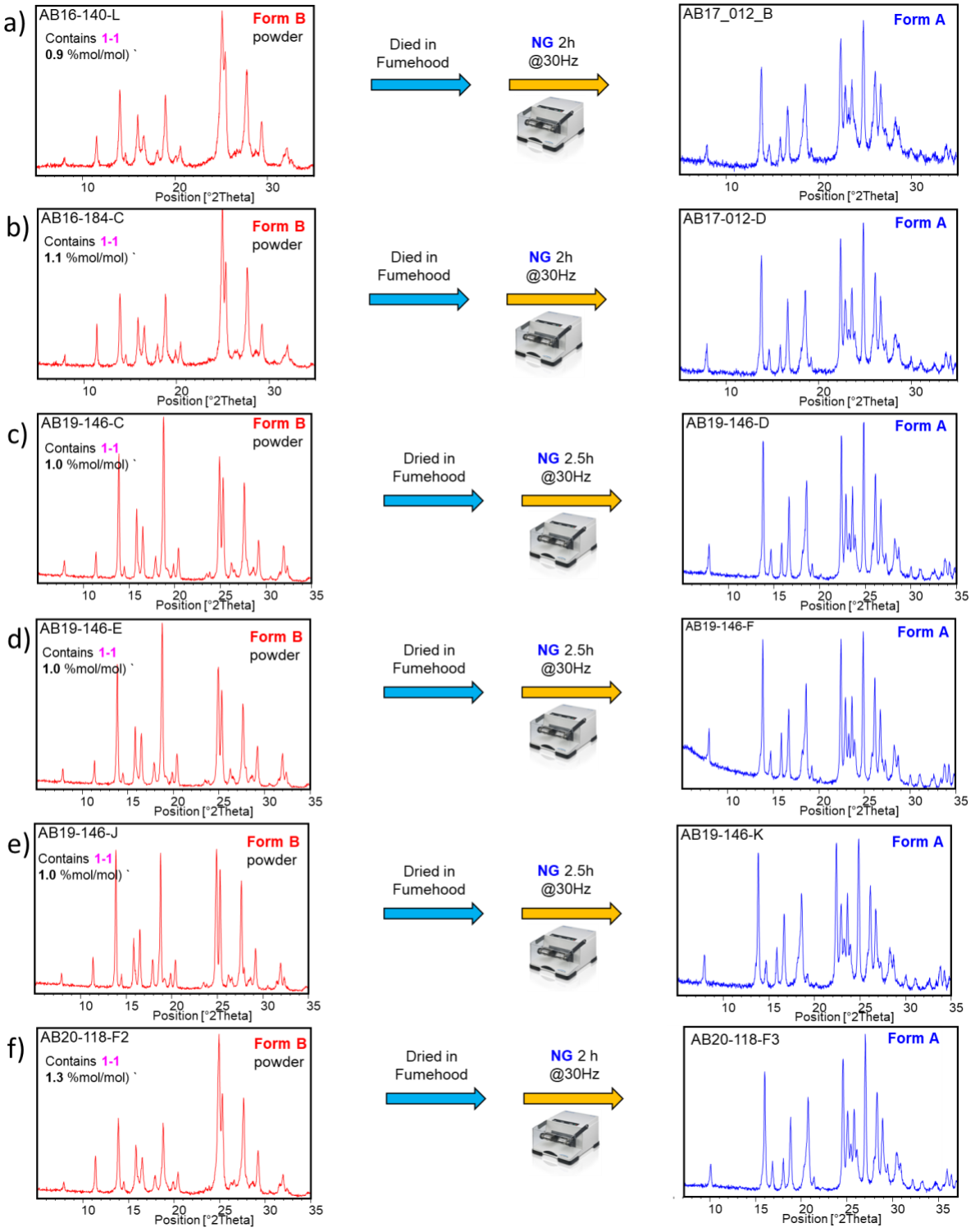

Continue on next page

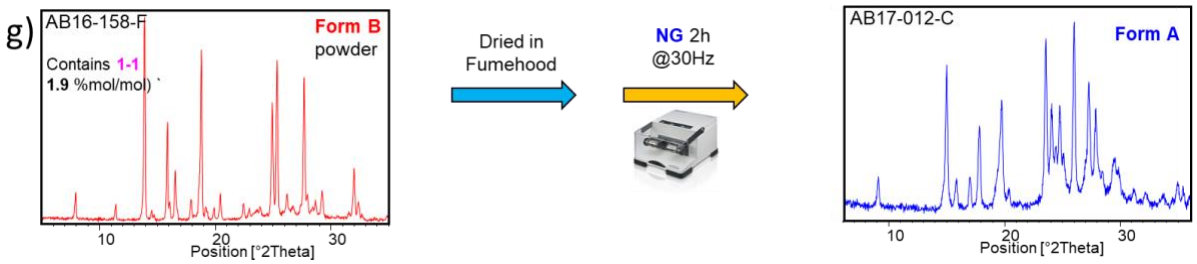

Figure S 38 Polymorph transformation of **Form B** powder to **Form A** by **NG** using procedure depicted in Scheme S29, which is very similar to Scheme S10, used for the anti-clockwise polymorph transformation turnover experiments These polymorph transformations are not a challenge, as they have ≥ 0.9% mol/mol of **1-1**,

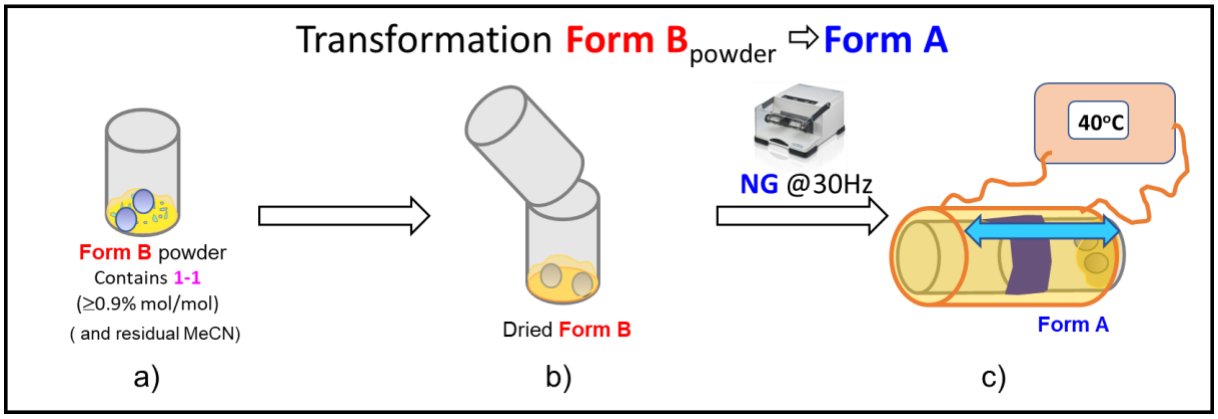

Scheme S 30 Step a) make sure that **Form B** powder does not contain residual MeCN**.** Only use **Form B** powder that contains **1-1** at levels > 0.9% mol/mol. b) Add 2x 7mm ball bearings to jar. Close and seal jar; c) install the heating jacket around the jar and connect to the controller. Set the controller at 40ºC. NG at 30 Hz with the objective to transform powder of **Form B** to **Form A**.

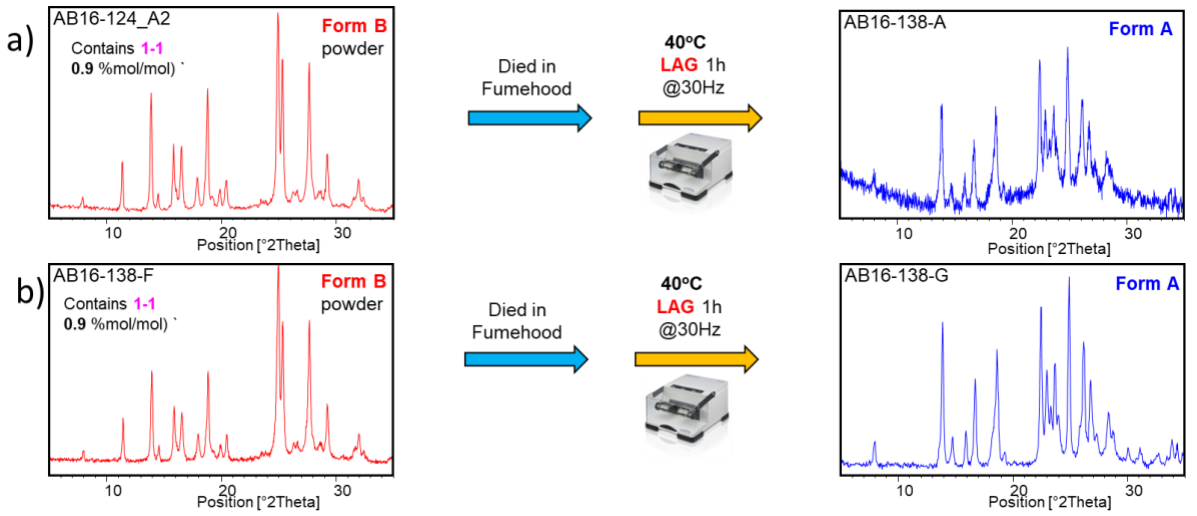

Figure S 39 Polymorph transformation of **Form B** powder to **Form A** by **NG** using procedure depicted in Scheme S30, which is very similar to Scheme S29, the difference is that here the jars are being heated to 40ºC. These polymorph transformations are not a challenge, as they have ≥ 0.9% mol/mol of **1-1**.

6.7.1.2 *Transformation of Form B powder to Form A: by LAG*

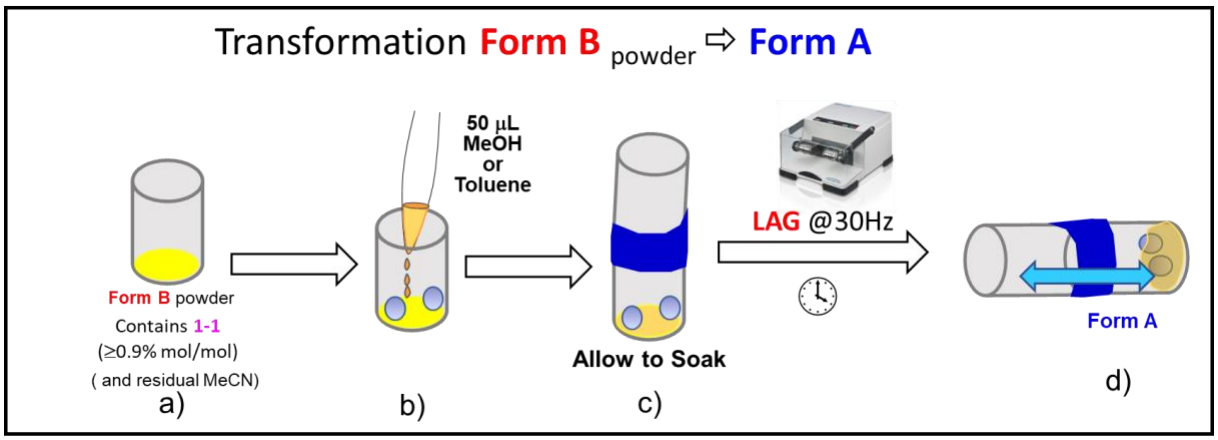

Scheme S 31 Step a) make sure that **Form B** powder does not contain residual MeCN**.** Only use **Form B** powder that contains **1-1** at levels > 0.9% mol/mol. b) Add 2x 7mm ball bearings to jar. Add 50µL of MeOH or toluene. These solvents are reluctant to soak into powder. Allow time for the solvent to soak into powder. Close and seal jar. d) LAG at 30 Hz with the objective to transform powder of **Form B** to **Form A**.

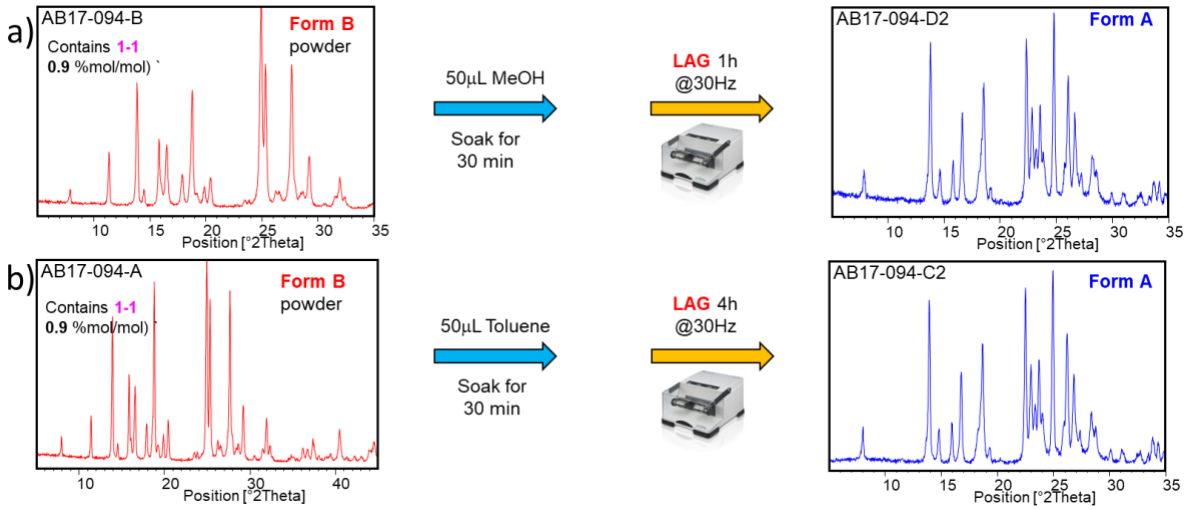

Figure S 40 Polymorph transformation of **Form B** powder to **Form A** by **LAG** using procedure depicted in Scheme S31, for a) using 50µL of MeOH while for b) using 50µL of Toluene. These polymorph transformations are not a challenge, as they have ≥ 0.9% mol/mol of **1-1**.

6.7.2 Polymorph transformation: Form A to Form B

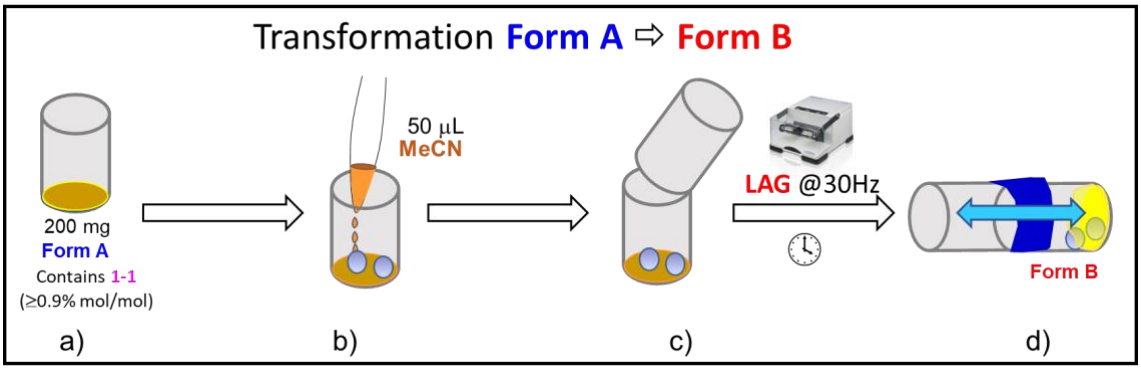

Scheme S 32 Step a) Add **Form A**. This powder typically contains **1-1** at levels > 0.9% mol/mol, otherwise it would not have been formed: b) Add 2x 7mm ball bearings to jar; Add 50 µL MeCN, which quickly soaks into the powder; c) Close and seal jar; d), LAG at 30 Hz with the objective to transform powder of **Form A** to **Form B**.

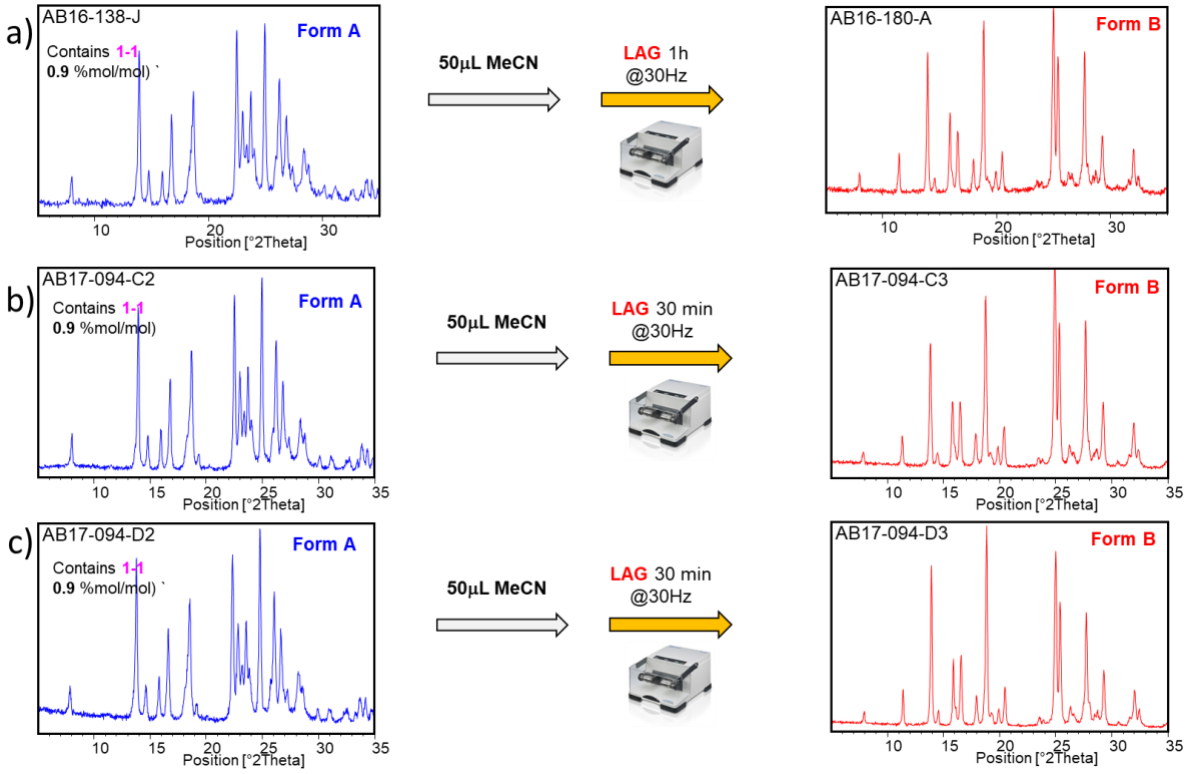

Figure S 41 Polymorph transformation of **Form A** to **Form B** by **LAG** with MeCN using the procedure depicted in Scheme S32. This procedure is very similar to Scheme S 4 used for the clockwise polymorph transformation turnover experiments. These polymorph transformations are not a challenge, as they have ≥ 0.9% mol/mol of **1-1**.

6.7.3 Conclusions

Form A can be reproducible transformed from **Form B** by **NG** as far as it contains >0.9% mol/mol of **1-1** using protocol described in Scheme S10.

Form B can be easily obtained from **Form A** by **LAG** with 50 µL MeCN, using protocol described in Scheme S9. We suspect that this transformation does not require higher levels than 0.9% mol/mol of **1-1**, but we have no data to support this hypothesis.

7 COMPUTATIONAL DETAILS

7.1 Computational Methods

Crystal geometries were taken from experimentally determined structures: Form A (FUQLIM01), Form B (FUQLIM02), and Form C (see section 2.2.2). All simulations were performed within the framework of plane wave Density Functional Theory (DFT), as implemented in CASTEP v20.[20] The wavefunction was expanded in plane waves to a kinetic energy cutoff of 900 eV, with ion-nuclear interactions approximated through norm-conserving pseudopotentials as generated on-the-fly in CASTEP. The exchange-correlation functional of Perdew-Burke-Ernzerhof (PBE)[21] was used throughout, with the semi-empirical dispersion correction of Tkatchenko-Scheffler (TS).[22] The electronic structure was sampled on a Monkhorst-Pack[23] grid with spacing no greater than 0.5 A^{-1} for each system. The structures were fully relaxed with convergence criteria of 10^{-10} eV/atom for the energy, 2 x 10^{-3} eV.$Å^{-1}$ for residual atomic forces, and 10^{-4} Å on atomic displacements. Subsequent phonon calculations were performed within the linear response framework as implemented in CASTEP[24] using a fine grid G_{max}=61.478 $Å^{-1}$.

7.1.1 Optimisation of Crystal Structures

To validate our theoretical models, the optimized crystal geometries were compared against experimental unit cell geometries, Table S 11. In all cases the experimental values are reproduced to within 2% of the unit cell volume, suggesting overall good performance of the selected model.

Table S 11 Comparison of optimized (PBE-TS) crystal geometries against experimental data. Values for Δ are calculated as $\Delta = 100(\text{comp} - \text{exp})/\text{exp}$

	Form A	Form B	Form C
a (exp)	13.4561	7.1338	11.1691
a (calc)	13.4529	6.9981	11.1971
Δa /%	-0.02	-0.27	+0.25
b (exp)	7.1030	7.8770	15.9311
b (calc)	7.0649	7.8373	15.8115
Δb /%	-0.54	-0.50	-0.75
c (exp)	13.8346	11.372	7.15033
c (calc)	14.1614	11.5755	7.04287
Δc /%	+2.36	+1.79	-1.50
α (exp)	90	83.189	90
α (calc)	90	81.5305	90
$\Delta\alpha$ /%	--	-1.99	--
β (exp)	109.73	80.954	94.6882
β (calc)	110.6281	80.6599	93.7325
$\Delta\beta$ /%	+0.82	-0.36	-1.01
γ (exp)	90	82.910	90
γ (calc)	90	84.9270	90
$\Delta\gamma$ /%	--	+2.43	--
V (exp)	1244.67	623.037	1268.04
V (calc)	1259.6512	618.2644	1244.2387
ΔV /%	+1.20	-0.77	-1.88

7.2 Simulated Vibrational Spectra

The phonon spectra were calculated for each polymorph at the Γ point, Figure S42. Further *k* points could not be obtained owing to the significant computational costs of the simulations on the large unit cells. For all three forms, no imaginary frequencies were obtained, confirming that the structures correspond to a minimum on the respective potential energy surfaces. With 104 atoms in the primitive cells of **Forms A** and **C**, and 52 in the primitive cell of Form B, there are 312 (**Forms A** and **C**) and 156 (**Form B**) normal modes of vibration for each cell.

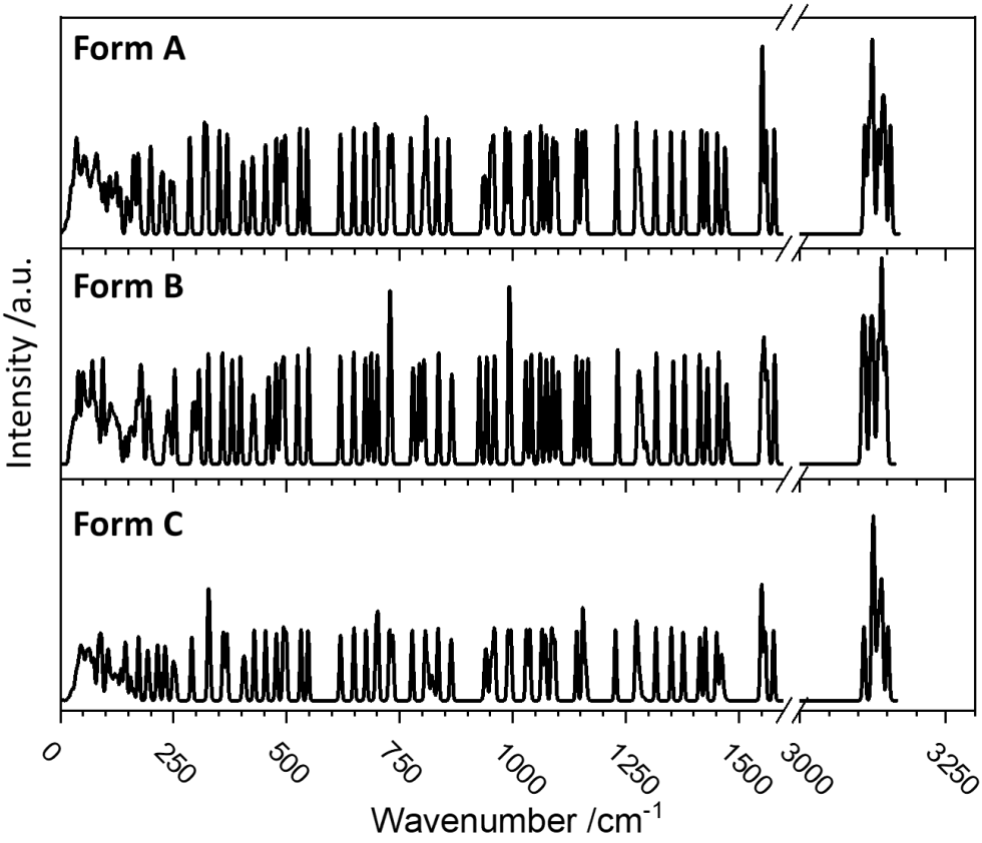

Figure S 42 Vibrational density of states for the three polymorphic forms of (**1-2**), simulated at k=Γ

7.3 Thermodynamic Stability

In its first approximation the relative stability of polymorphic forms can be taken as the lattice energy,

$$U_{latt} = \frac{E_{crystal}}{Z} - E_{molec} \qquad \textbf{Eqn 1}$$

where $E_{crystal}$ is the total energy of the crystal that comprises *Z* molecules, each with internal energy E_{molec}. To assess the relative stability of the three polymorphs, $E_{molec}$the asymmetric unit (1 molecule) was optimized in cubic cell of *a*=25Å to eliminate interactions between periodic images. Moreover, by allowing the isolated molecule to relax, we account also for configurational energy when including E_{molec}. Consistent with earlier reports,[6] our PBE-TS simulations do suggest that **Form B** is more stable as a bulk polymorph as compared with **Form A**, Table S12.

However, we note that the relative lattice energy of **Form C** is essentially identical to that of **Form B**, at least from a purely static perspective.

Table S 12 Energetic contributions to the lattice energy for the three polymorphs of **1-2**, as obtained at PBE-TS level of theory. Energies are provided in eV and given per unit cell.

	Form A /eV	**Form B /eV**	**Form C /eV**
$E_{crystal}$	-17061.10402744	-8530.610768490	-17061.228599
Z	4	2	4
E_{molec}	-4264.101550410		
U_{latt}	-1.17446	-1.20383	-1.2056

As is commonly the case, and observed here, the free energy differences between polymorphic phases is small, and can therefore depend strongly on vibration contributions to the free energy, Table S13 and Figure S43. Owing to the size of the unit cells only the phonon frequencies at the Γ-point could be calculated, providing an approximate vibrational correction. We note also that our simulations do not account for thermal expansion of the systems, although we expect similar degrees of thermal expansion in all three polymorphic forms.

The Helmholtz-free energy can be written with vibrational contributions as

$$F_{tot} = E_{pot} + F_{vib} \qquad \textbf{Eqn 2}$$

Where F_{vib} is the vibrational free energy and E_{pot} is the internal energy of the system.

Table S 13 Vibrationally corrected energies for the three polymorphic forms. The vibrational zero point energy (ZPE) is given alongside the total free energy (F_{tot}) at both 0 K and 290 K.

	Form A	**Form B**	**Form C**
ZPE /eV.molec^{-1}	4.705	4.706	4.716
ΔF_{tot} 0K /eV.molec^{-1}	2.047	0	0.510
ΔF_{tot} 290K /eV.molec^{-1}	-40.388	-45.082	-40.136

When an approximation for the vibrational contribution to the free energy is included, no immediate reordering of the bulk stabilities is observed at 0 K, Table S13. Moreover, with increasing temperature **Form B** remains the bulk stable form. However, we note that as the temperatures approach room temperature, the free energy of **Forms A** and **C** converge, with the forms predicted to be within 0.3 kJ.mol^{-1} of each other by room temperature. This energetic similarity may explain the difficulty in isolating the two LAG polymorphs during mechanochemical reactions, but the relative ease of obtaining **Form B** from either phase. This energetic difference highlights the impressive ability of ball milling grinding to selectively produce polymorphs that are exceptionally close in energy, provided the right ball milling conditions are correctly identified.

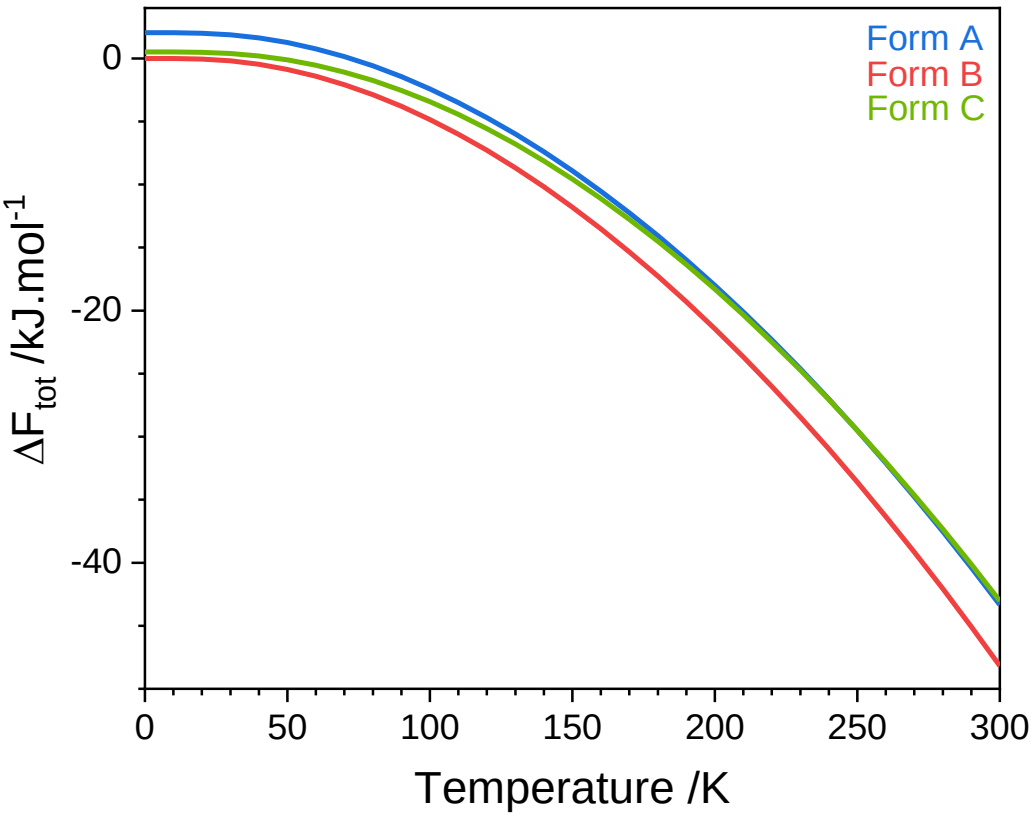

Figure S 43 The Helmholtz free energy for the three polymorphic forms of (1-2) as a function of temperature. Simulations were performed at PBE-TS level of theory using the fully optimized geometry.

8 Conclusions

Form A, **Form B** and **Form C** from **1-2**, can be easily and reproducibly interconverted as far as they comply with the necessary grinding conditions and have enough impurity (1-1) required for the polymorph transformation as explain below.

Form C can be reproducible be transformed from **Form B** as far as it contains >1.5% mol/mol of **1-1** using protocol described in Scheme S3 and S5. This transformation requires the highest content of **1-1** from all the other ones.

Form C can be reproducible be obtained from **Form A** as far as it contains >0.9% mol/mol of **1-1** using protocol described in Scheme S8.

Form B can be easily obtained from **Form C** with just 10 μL MeCN, using protocol described in Scheme S9, though this uses 50 μL MeCN. We suspect that this transformation does require level of ≤0.9% mol/mol of **1-1**, but we have no data to support this hypothesis.

Form B can be obtained from **Form A** by LAG with MeCN using protocol described in Scheme S4 requiring level of **1-1** ≤0.9% mol/mol.

Form A can be reproducible obtained from **Form B** as far as it contains >0.9% mol/mol of **1-1** using protocol described in Scheme S7 and S10.

Form A can be reproducible obtained from **Form C** as far as it contains >0.9% mol/mol of **1-1** using protocol described in Scheme S3.

9 Literature

1. Belenguer, A. M.; Friscic, T.; Day, G. M.; Sanders, J. K. M., Solid-state dynamic combinatorial chemistry: reversibility and thermodynamic product selection in covalent mechanosynthesis. *Chem. Sci.* **2011,** *2* (4), 696-700.
2. Belenguer, A. M.; Lampronti, G. I.; Wales, D. J.; Sanders, J. K. M., Direct Observation of Intermediates in a Thermodynamically Controlled Solid-State Dynamic Covalent Reaction. *Journal of the American Chemical Society* **2014,** *136* (46), 16156-16166.
3. Ana M. Belenguer; Michalchuk, A. A. L.; Lampronti, G. I.; Sanders, J. K. M., Understanding the unexpected effect of frequency on the kinetics of a covalent reaction under ball-milling conditions. *Beilstein J. Org. Chem.* **2019,** *15*, 1226–1235.
4. Belenguer, A. M.; Lampronti, G. I.; Sanders, J. K. M., Implications of Thermodynamic Control: Dynamic Equilibrium Under Ball Mill Grinding Conditions. *Israel Journal of Chemistry n/a* (n/a).
5. Belenguer, A. M.; Michalchuk, A. A. L.; Lampronti, G. I.; Sanders, J. K. M., Using Solid Catalysts in Disulfide-Based Dynamic Combinatorial Solution- and Mechanochemistry. *ChemSusChem n/a* (n/a), e202102416.
6. Belenguer, A. M.; Lampronti, G. I.; Cruz-Cabeza, A. J.; Hunter, C. A.; Sanders, J. K. M., Solvation and surface effects on polymorph stabilities at the nanoscale. *Chem. Sci.* **2016,** *7* (11), 6617-6627.
7. Belenguer, A. M.; Lampronti, G. I.; De Mitri, N.; Driver, M.; Hunter, C. A.; Sanders, J. K. M., Understanding the Influence of Surface Solvation and Structure on Polymorph Stability: A Combined Mechanochemical and Theoretical Approach. *Journal of the American Chemical Society* **2018,** *140* (49), 17051-17059.
8. Belenguer, A. M.; Lampronti, G. I.; Sanders, J. K. M., Reliable Mechanochemistry: Protocols for Reproducible Outcomes of Neat and Liquid Assisted Ball-mill Grinding Experiments. *JoVE* **2018,** (131), e56824.
9. Belenguer, A. M.; Cruz-Cabeza, A. J.; Lampronti, G. I.; Sanders, J. K. M., On the prevalence of smooth polymorphs at the nanoscale: implications for pharmaceuticals. *CrystEngComm* **2019,** *21* (13), 2203-2211.
10. Lampronti, G. I.; Michalchuk, A. A. L.; Mazzeo, P. P.; Belenguer, A. M.; Sanders, J. K. M.; Bacchi, A.; Emmerling, F., Changing the game of time resolved X-ray diffraction on the mechanochemistry playground by downsizing. *Nature Communications* **2021,** *12* (1), 6134.
11. David, W. I. F.; Shankland, K.; van de Streek, J.; Pidcock, E.; Motherwell, W. D. S.; Cole, J. C., DASH: a program for crystal structure determination from powder diffraction data. *Journal of Applied Crystallography* **2006,** *39* (6), 910-915.
12. Boultif, A.; Louër, D., Indexing of powder diffraction patterns for low-symmetry lattices by the successive dichotomy method. *J. Appl. Cryst.* **1991,** *24*, 987-993.
13. Coelho, A. A., TOPAS and TOPAS‐Academic: an optimization program integrating computer algebra and crystallographic objects written in C++. *Journal of Applied Crystallography* **2018,** *51* (1), 210-218.
14. Dollase, W., Correction of intensities for preferred orientation in powder diffractometry: application of the March model. *Journal of Applied Crystallography* **1986,** *19* (4), 267-272.
15. R. W. Cheary, A. A. C., J. P. Cline, Fundamental Parameters Line Profile Fitting in Laboratory Diffractometers. *J Res Natl Inst Stand Technol* **2004,** *109* (1), 1–25.
16. Black, D. R., Windover, D., Henins, A., Filliben, J., and Cline, J. P, Certification of standard reference material 660B. *Powder Diffraction* **2011,** *26* (02), 155-158.
17. Coelho, A. A., *TOPAS-Academic - Technical Reference Version 7* Bruker-axs: http://www.topas-academic.net/, 2020.

18. Garnier, E., Powder Diffraction. Theory and Practice. Edited by R. E. Dinnebier and S. J. L. Billinge. Cambridge: RSC Publishing, 2008. Pp. xxi + 582. Price (hardcover): GBP 59.00. ISBN (online): 978-1-84755-823-7; ISBN (print): 978-0-85404-231-9. *Acta Crystallographica Section A* **2009,** *65* (1), 51.
19. Payzant, E. A., Other Topics. In *Principles and Applications of Powder Diffraction*, 2009; pp 365-380.
20. Clark, S. J.; Segall, M. D.; Pickard, C. J.; Hasnip, P. J.; Probert, M. I. J.; Refson, K.; Payne, M. C., First principles methods using CASTEP. *Zeitschrift für Kristallographie - Crystalline Materials* **2005,** *220* (5-6), 567-570.
21. Perdew, J. P.; Burke, K.; Ernzerhof, M., Generalized Gradient Approximation Made Simple. *Physical Review Letters* **1996,** *77* (18), 3865-3868.
22. Tkatchenko, A.; Scheffler, M., Accurate Molecular Van Der Waals Interactions from Ground-State Electron Density and Free-Atom Reference Data. *Physical Review Letters* **2009,** *102* (7), 073005.
23. Monkhorst, H. J.; Pack, J. D., Special points for Brillouin-zone integrations. *Physical Review B* **1976,** *13* (12), 5188-5192.
24. Refson, K.; Tulip, P. R.; Clark, S. J., Variational density-functional perturbation theory for dielectrics and lattice dynamics. *Physical Review B* **2006,** *73* (15), 155114.